CHONDROCYTIC ACETYLCHOLINESTERASE/ALPHA7 NACHR SIGNALING IN CARTILAGE HOMEOSTASIS AND OSTEOARTHRITIS

LIU JUN

PhD

The Hong Kong Polytechnic University

2026

The Hong Kong Polytechnic University

Department of Biomedical Engineering

Chondrocytic Acetylcholinesterase/alpha7 nAChR signaling in Cartilage Homeostasis and Osteoarthritis

LIU Jun

A thesis submitted in partial fulfillment of the requirements for the degree of Doctor of Philosophy

August 2025

CERTIFICATE OF ORIGINALITY

I hereby declare that this thesis is my own work and that, to the best of my knowledge and belief, it reproduces no material previously published or written, nor material that has been accepted for the award of any other degree or diploma, except where due acknowledgement has been made in the text.

_____ (Signed)

LIU Jun 劉珺_____（Name of student）

Membership of the Panel for the Oral Examination

LIU Jun (BME), PhD candidate

Prof. Sharon RUAN (BoE Chair)
Department of Biomedical Engineering
The Hong Kong Polytechnic University

Prof. Danny CHAN
School of Biomedical Sciences
The University of Hong Kong

Prof. Yu HUANG
Department of Biomedical Sciences
City University of Hong Kong

Prof. Chunyi WEN (Internal Member)
Department of Biomedical Engineering
The Hong Kong Polytechnic University

Graphic abstract

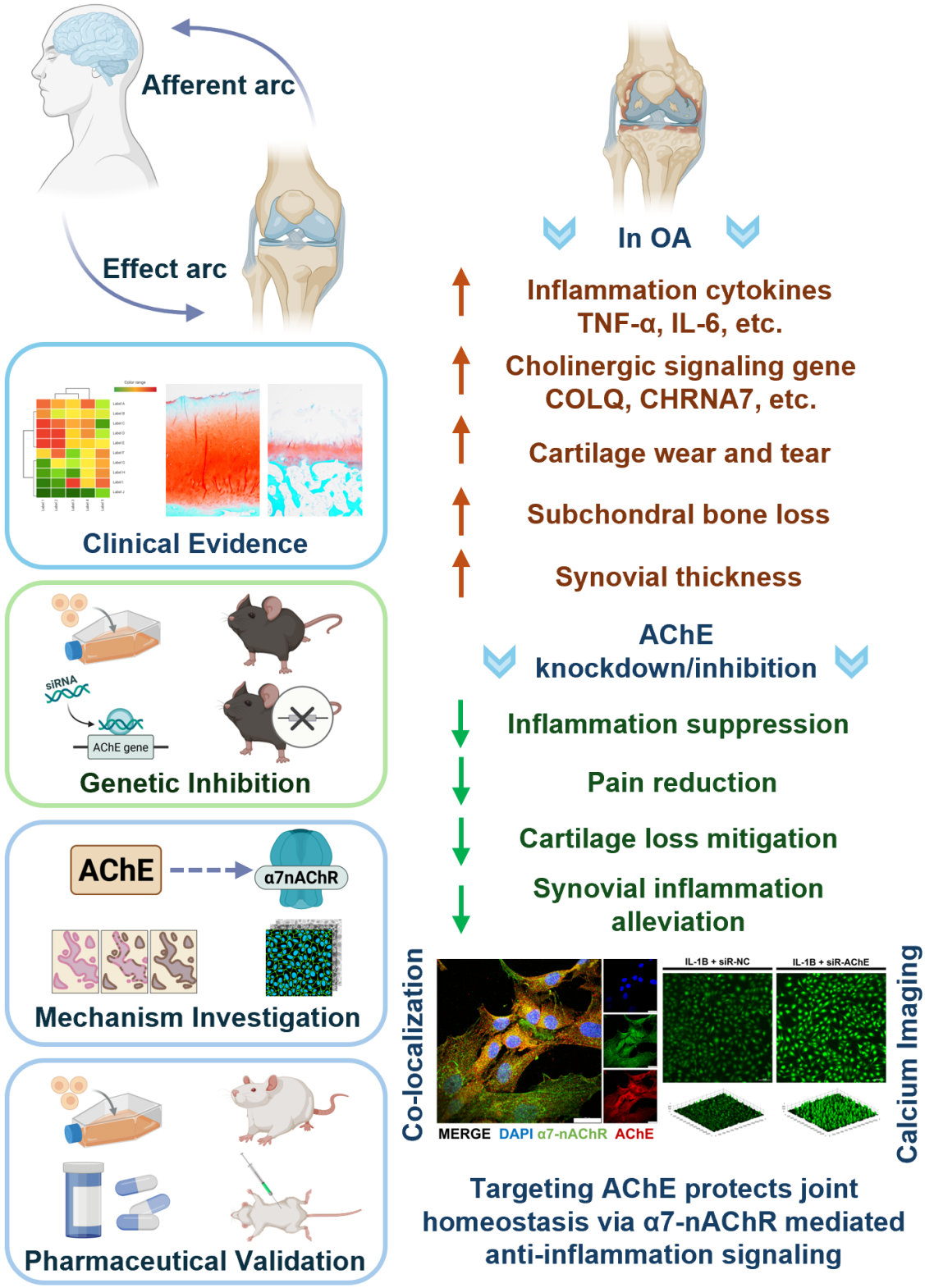

Schematic overview of the study. Targeting AChE/α7nAChR in osteoarthritis.

Abstract

Background

Emerging evidence indicates a bidirectional link between neurodegenerative and skeletal disorders, positioning osteoarthritis (OA) within a systemic "brain–joint axis" regulated by cholinergic signaling. Central to this axis, dysregulation of acetylcholinesterase (AChE), acetylcholine (ACh) and the α7 nicotinic acetylcholine receptor (α7nAChR) perturbs cholinergic homeostasis and promotes inflammation and tissue catabolism. We hypothesized that AChE/ACh/α7nAChR dysregulation in bone and cartilage accelerates OA progression by disrupting cholinergic signaling, and that targeting AChE/ACh/α7nAChR signaling restores joint protection. We aimed to define cholinergic signaling in cartilage homeostasis and OA, test the chondroprotective effects of AChE modulation *in vitro* and *in vivo*, and delineate mechanisms involving ACh and α7nAChR mediated anti-inflammatory pathways.

Hypothesis

We hypothesized that dysregulated AChE/ACh/α7nAChR signaling in joint tissues promotes OA progression by disrupting cholinergic homeostasis, and that targeting AChE would restore ACh/α7nAChR mediated joint protection.

Objectives

This study aims to elucidate cholinergic signaling in cartilage homeostasis and OA, determine the chondroprotective effects of AChE modulation *in vitro* and *in vivo*, and clarify its mechanisms via ACh/α7nAChR mediated anti-inflammatory pathways.

Key Findings

Analysis of public RNA-sequencing datasets implicated the involvement of cholinergic signaling, and inflammatory cascades in OA pathogenesis. OA cartilage showed increased expression of cholinergic components (e.g., CHRNA7, CHRNA10 and COLQ) and inflammatory mediators (e.g., MMP-13 and TNFAIP1), underscoring pathway dysregulation in disease. *In vitro*, siRNA knockdown of AChE in IL-1β stimulated chondrocytes reduced inflammatory cytokines, including TNF-α and IL-6. *In vivo*, genetic AChE deletion in chondrocytes or osteoblasts mitigated cartilage deterioration, synovial degeneration, preserved subchondral bone, and improved pain-related or locomotor outcomes after surgically induced OA, accompanied by lower AChE, Nf-kB, and TNF-α expression. In a collagenase induced inflammatory OA model, chondrocyte-specific AChE deletion similarly reduced subchondral bone loss. Pharmacological treatment with AChE inhibitor donepezil decreased inflammatory cytokine TNF-α expression and increased ACh at serum level, which attenuated cartilage degeneration, synovial inflammation and subchondral bone loss in a hypertensive rat OA model. Mechanistically, immunofluorescence demonstrated co-localization of AChE and α7nAChR in human OA chondrocytes and cartilage, suggesting functional proximity. Functional assays indicated that AChE inhibition exerts anti-inflammatory effects via α7nAChR activation and the cholinergic anti-inflammatory pathway; under inflammatory conditions, an α7nAChR antagonist (α-bungarotoxin) reversed these effects. Ion channel imaging indicated both ACh-

treated and AChE-knockdown chondrocytes displayed increased ion channel activation relative to untreated cells. Electrophysiological recordings further supported that AChE knockdown can partially counteract the inhibitory effects of α7nAChR antagonism on cholinergic signaling.

Conclusion

This thesis demonstrates AChE contributes to OA pathogenesis by modulating joint inflammation and cartilage degradation. Genetic and pharmacological AChE inhibition confer chondroprotection across models, with effects mediated through AChE/ACh/α7nAChR signaling and local cholinergic anti-inflammation pathways. The AChE/α7nAChR axis therefore represents a promising therapeutic target for disease modification in OA.

List of Publications

Journal articles arising from the study

Liu, J., Zhao, F., Zhang, T., Dai, B., Wang, Y., Wang, H., Zhang, Y., Au, M., Courties, A., Cao, H., Pan, F., Sellam, J., Wang, X., Wen, C. Chondrocytic Acetylcholinesterase–Alpha7 nAChR Signaling Orchestrate Cartilage Degradation and Osteoarthritis. (Under preparation)

Luo, x., Zhao, F., **Liu, J.,** Lauwers, M., Au, M., Cao, H., Qin, L., Wang, X., Wen, C. Non-Enzymatic Function of Acetylcholinesterase in Aged and Osteoporotic Bone remodeling in mice. (Under preparation)

Other journal articles

NI, J., Au, M., Tang, K, Zhao, F., Wang, W., Zhang, L., Zhou, B., Zhu, L.,, Lau, L., Toh, Y., Wang, X., Tang, X., Wang, H., **Liu, J.**, Zhang, C., Lauwers, M., Luo, C., Chan, J., Dong, C., Yuan, S., Wen, C. Pulmonary endothelin-1 triggers iron overload and skeletal injury in post-COVID-19. Cell Reports. (Under revision)

Wang, H., Zhang, L., Zhang, Y., Wang, W., Ni, J., **Liu, J.**, Gong, W., Au, M. T., Yeung, M. H. Y., Cao, H., & Wen, C. (2025). Spatially resolved single-cell-based histocytomorphometry for growth plate analysis across multiple species. Journal of Orthopaedic Translation, Article 101015. https://doi.org/10.1016/j.jot.2025.10.007.

Zhu, Y., Dai, B., Zhang, S., **Liu, J.**, Xu, S., Liu, W., Chen, X., Zhang, H., Li, Q., Pang, F. O., Li, W., Wen, C., Qin, L., Xu, J., & Ngai, T. (2025). Tissue Mimetic Membranes for Healing Augmentation of Tendon–Bone Interface in Rotator Cuff Repair. *Advanced Materials (Weinheim)*, 37(10), Article 2407358. https://doi.org/10.1002/adma.202407358.

Wang, W., Jiang, T., Zhang, J., **Liu, J.**, Chan, L. C., Lin, M., Li, J., Ding, C., Chiu, K. Y., Fu, H., Chan, P. K., & Wen, C. (2024). Subchondral bone expansion in advanced knee osteoarthritis: Relation with radiographic severity and role in surgical decision-making. *Osteoarthritis and Cartilage Open*, 6(2), Article 100461. https://doi.org/10.1016/j.ocarto.2024.100461.

Conference papers

LIU, J., Wang, Y., Zhao, F., & Wen, C. (2025). ROLE OF ACETYLCHOLINESTERASE IN CARTILAGE HOMEOSTASIS AND OSTEOARTHRITIS DEVELOPMENT. *Osteoarthritis and Cartilage*, 33, S78–S78. https://doi.org/10.1016/j.joca.2025.02.108. (**Podium presentation**)

NI, J., Au, M. T., Tang, K., **LIU, J.**, Zhao, F., Yuan, S., & Wen, C. (2025). ENDOTHELIN RECEPTOR BLOCKADE ATTENUATES SARS-COV-2-INDUCED GROWTH PLATE INJURY BY REDUCING CHONDROCYTE CIRCADIAN GENE REGULATED-VIRUS UPTAKE. *Osteoarthritis and Cartilage*, 33, S340 – S341.

https://doi.org/10.1016/j.joca.2025.02.483 (Poster presentation)

Liu, J., Wang, H., Zhang, Y., & Wen, C. (2024). THE RESTORATIVE AND PROTECTIVE EFFECT OF DONEPEZIL IN OSTEOARTHRITIS. *Osteoarthritis and Cartilage*, 32, S588–S589. https://doi.org/10.1016/j.joca.2024.02.869. (Poster presentation)

Conference activities

First runner-up in 2025 OARSI China Night 3MT Competition, “Role of Acetylcholinesterase in Cartilage Homeostasis and Osteoarthritis Development”.

Booth presentation in Asia Summit on Global Health (ASGH) 2023, “Chinese Herb Huperzine A-derived Dimers for Osteochondral Repair”.

Secretary of the 2025 OARSI China-Germany Night.

Secretary of the 2024 OARSI China-Germany Night.

Acknowledgment

“Cast into desperate situations, one finds survival; thrust into certain peril, one finds life.” This enduring wisdom has been the compass guiding my academic journey over the past four unforgettable years, years marked by trials that sometimes felt overwhelming, but always revealed new strength and clarity. Confronted with challenges and uncertainty, I learned to adapt, persist, and ultimately prevail.

I am profoundly grateful to Prof. WEN Chunyi, who has not only guided my research with wisdom and patience but has also shown me, by example, what resilience and dedication look like. To the incredible members of the WEN Lab, thank you for every shared experiment, late-night discussion, and moments of encouragement that made the tough journey lighter. To Prof. WANG Xinluan, Prof. SELLAM Jérémie, Prof. PAN Feng, Dr. CAO Huijuan and Dr. DAI Bingyang, for their valuable expertise and constructive discussions, which significantly enhanced the depth and scope of my research.

Lastly, to my parents and my girlfriend, your love, faith, and support have been my anchor through every storm and my light in every uncertain moment.

Additionally, portions of this manuscript underwent language refinement with the assistance of the artificial intelligence tool GPT-4.1, and schematic figures were prepared using BioRender.com.

Table of Contents:

Graphic abstract III

Abstract IV

List of Publications VII

Acknowledgment X

Table of Contents: XI

List of Abbreviations XIII

List of Figures XIV

Chapter 1 Introduction 1

1.1 Introduction 1

Chapter 2 Literature Review 5

2.1 Osteoarthritis 5

2.2 Association between skeletal diseases and dementia: Brain-joint axis 7

2.3 Cholinergic signaling in joint homeostasis and osteoarthritis 10

2.4 Nicotinic acetylcholine receptors and inflammation 13

2.5 Clinical evidence of cholinergic anti-inflammatory pathway 16

2.6 Pre-clinical evidence of cholinergic anti-inflammatory pathway 18

2.7 Acetylcholinesterase in anti-inflammation signaling 19

2.8 Protective effects of acetylcholinesterase inhibitor 21

2.9 Research Gaps 23

2.10 Research Hypothesis 25

2.11 Research Objectives 26

Chapter 3 Materials and Methods 28

2.1 Materials 28

2.2 Methods 30

Chapter 4 Results 47

4.1 The involvement of cholinergic system in OA pathogenesis 47

4.2 Genetical knockdown of Acetylcholinesterase 50

4.3 Pharmaceutical inhibition of Acetylcholinesterase 62

4.4 Exploration of the mechanisms of acetylcholinesterase and alpha7 acetylcholine receptor signaling in inflammation regulation 65

Chapter 5 Discussion and Conclusion 72

5.1 Discussion 72

5.2 Conclusion 78

Chapter 6 Limitations and future Plan 83

Reference 86

List of Abbreviations

ACh	Acetylcholine
AChE	Acetylcholinesterase
AChR	Acetylcholine receptor
ACLT	Anterior Cruciate Ligament Reconstruction Surgery
AD	Alzheimer's disease
α7nAChR	Alpha 7 nicotinic acetylcholine receptor
BChE	Butyrylcholinesterase
COLQ	Collagen like tail subunit of asymmetric acetylcholinesterase
CHRNA7	Alpha 7 nicotinic acetylcholine receptor encoding gene
ChAT	Choline acetyltransferase
COL2A1	Collagen type II alpha 1 chain
ECM	Extracellular matrix
IL-1B/IL-1β	Interleukin 1 beta
IL-6	Interleukin 6
MMP-13	Matrix metallopeptidase 13
MSC	Mesenchymal stem cell
NF-κB	Nuclear factor kappa B
NNCS	Non-neuronal cholinergic system
OA	Osteoarthritis
OB	Osteoblast
OC-Cre	Osteocalcin cre
OPG	Osteoprotegerin
OVX	Ovariectomy
RANK	Receptor activator of NF-κB
RANKL	RANK ligand
RT-PCR	Transcription-polymerase chain reaction
RunX2	Runt-related transcription factor 2
TGF-β	Transforming growth factor-β
TNF-A/TNF-α	Tumor necrosis factor alpha
TRAP	Tartrate resistance acid phosphatase
VNS	Vagus nerve stimulation
VAChT	Vesicular acetylcholine transporter

List of Figures

Figure 2-1 Safranin O/Fast Green and Hematoxylin/Eosin staining of human tibial plateau sections. Showing progressive cartilage degeneration, from thick, intact cartilage in mild osteoarthritis to nearly complete loss in severe osteoarthritis. Scale bar, 500 μm. 5

Figure 2-2 Incidence rates (/1000 person-years) of knee OA (black), hip OA (red), and hand OA (green). Suggesting the increasing prevalence of OA. Solid, all population; short dash line, women; long dash line, men (Prieto-Alhambra et al., 2014). 7

Figure 2-3 Schematic of the "brain–joint axis" and clinical trials: NCT05387135 (Elsehrawy et al., 2025), NCT05625178 (Aoyagi et al., 2025), NCT04520516 (Courties, Deprouw, Rousseau, et al., 2022), NCT03919279 (Courties, Deprouw, Maheu, et al., 2022)) investigating vagus nerve stimulation in osteoarthritis through modulation of the cholinergic anti-inflammatory reflex. By increasing acetylcholine production, vagus nerve stimulation could activate nicotinic receptors, dampen inflammation, and potentially prevent cartilage degradation. This brain–joint link underscores the role of neural modulation in peripheral inflammation. The diagram was redrawn and modified based on published literature (Berenbaum & Meng, 2016). 9

Figure 2-4 Schematic of the cholinergic anti-inflammatory pathway (Kelly et al., 2022). The central nervous system releases acetylcholine via pathways such as the vagus nerve to suppress macrophage driven inflammation. The cholinergic anti-inflammatory pathway is a neural circuit through which the central nerve system regulates peripheral immunity. Through the vagus and splenic nerves, acetylcholine produced by cells downregulates the inflammatory functions of macrophages expressing α7 nicotinic acetylcholine receptors. The central nervous system releases acetylcholine via pathways such as the vagus nerve to suppress macrophage driven inflammation. 16

Figure 2-5 The visible portion above the waterline illustrates research topics with abundant published literature, submerged layers indicate less explored research topics with fewer existing literature. AChE and α7nAChR are co-localized in osteoblasts, but their interactions in chondrocytes is uncharted. The impact of AChE dysregulation on OA pathogenesis and cartilage homeostasis, and its potential as a therapeutic target for inflammation management, remains to be elucidated. The precise role of AChE with the "brain–joint axis", especially in the peripheral branch, remains unknown. 23

Figure 2-6 Schematic of research hypothesis. We aim to examine how acetylcholinesterase (AChE) influences osteoarthritis (OA) progression.

Acetylcholine (ACh) activates anti-inflammatory signaling via the α7 nicotinic acetylcholine receptor (α7nAChR). We propose that inhibiting AChE will potentiate this pathway, reduce inflammatory cytokines, and investigate potential interactions between AChE and α7nAChR. 25
Figure 2-7 Workflow of the study, progressing from objective 1 (human sequencing database and clinical knee specimen analysis) to objective 2 (in vitro and in vivo genetic knockdown and pharmacological inhibition), and objective 3 (mechanistic investigation of AChE and α7nAChR in OA). 26
Figure 3-1 Workflow of human OA specimens' collection and primary cultured chondrocytes......33
Figure 3-2 Schematic of Research of Interests (ROI) in micro-CT analysis. Medial compartment of the subchondral bone was analysis as it is more closely related to the OA development (red shaded area).....41
Figure 4-1 Analysis of publicly available RNA sequencing datasets. A. Heatmap showing the expression profiles of selected cholinergic signaling-related genes in bulk RNA-seq dataset (GSE114007). **B.** Individual expression plots of selected genes in bulk RNA-seq dataset (GSE114007). **C.** Individual expression plots of selected genes in single-cell RNA-seq dataset (GSE255460). Unpaired two-tailed Student's t-test were performed. * $p<0.05$; ** $p<0.005$; *** $p<0.001$; **** $p<0.0001$.....47
Figure 4-2 Characterization of clinical human OA specimens. A. Representative histochemical staining image of human osteoarthritic tibial plateau specimens. Scale bars = 100 μm. **B.** ELISA quantification of TNF-A and AChE protein levels in lysates from human OA chondrocytes (n=3). **C.** Western blot analysis of AChE concentration in human OA chondrocyte lysates from three different human donors. **D.** Heatmap showing the relative AChE expression value of western blot image, normalized by GAPDH (n=3). All data are expressed as means ± SEM. Paired two-tailed Student's t-test were performed. * $p<0.05$. 49
Figure 4-3 The anti-inflammation and chondral protective effects of knockdown in vitro. A. Schematic diagram of the *in vitro* experiments. **B.** KEGG pathway analysis of the inflammatory cell culture model. **C.** Heatmap showing the expression of selected inflammatory genes in bulk RNA-sequencing data. **D.** Characterization of interleukin-1β (IL-1β) stimulation in vitro. **E**. AChE enhances interleukin-6 (IL-6) expression in the presence of IL-1β. **F.** PCR validation of the anti-inflammatory effects following siRNA-mediated AChE knockdown. One-way ANOVA with Post-hoc tests were performed. * $p<0.05$; ** $p<0.005$; *** $p<0.001$; **** $p<0.0001$.....51
Figure 4-4 Osteoblast-specific AChE knockout mice in posttraumatic OA – bone volume analysis and behavioral tests. A. Schematic diagram of animal experiments and the body size of animals. **B.** Representative micro-

CT images of medial subchondral bone. **C.** Quantitative analysis of BV/TV differences between ACLT and SHAM legs in each group (n=8). **D.** Quantitative analysis of BV/TV, Tb. N and structure model index in each group (n=8). **E.** Behavioral assessments of animals using the Rotarod and von Frey tests (n=8). All data are expressed as means ± SEM. One-way ANOVA with Post-hoc tests or unpaired two-tailed Student's t-test were performed. * p<0.05; ** p<0.005; *** p<0.001; **** p<0.0001. 53

Figure 4-5 Osteochondral-specific AChE knockout mice in posttraumatic OA – histological staining and analysis of cartilage and synovium. A. Representative histological images of tibial articular cartilage with OARSI scoring in joint morphology and cartilage integrity (n=8). Scale bars = 50 μm. **B.** Representative images and quantitative analysis of synovial lining thickness using an arbitrary scoring system ranging from 0-3 (n=8). Scale bars = 100 μm & 500 μm. **C.** Serum AChE, ACh, choline, TNF-α, and IL-1β were measured at the end point. All data are expressed as means ± SEM. One-way ANOVA with Post-hoc tests or unpaired two-tailed Student's t-test were performed. * p<0.05; ** p<0.005. 55

Figure 4-6 Chondrocyte-specific AChE knockout mice in posttraumatic OA – bone volume analysis and behavioral tests. A. Schematic diagram of animal experiments and the body size of animals. **B.** Representative micro-CT images of medial subchondral bone. **C.** Quantitative analysis of BV/TV differences between ACLT and SHAM legs in each group (n=8). **D.** Quantitative analysis of BV/TV, Tb. N and structure model index in each group (n=8). **E.** Behavioral assessments of animals using the Rotarod and von Frey tests (n=8). All data are expressed as means ± SEM. One-way ANOVA with Post-hoc tests or unpaired two-tailed Student's t-test were performed. * p<0.05; ** p<0.005; *** p<0.001; **** p<0.0001. 56

Figure 4-7 Chondrocyte-specific AChE knockout mice in posttraumatic OA – histological staining and analysis of cartilage and synovium. A. Representative histological images of tibial articular cartilage with OARSI scoring in joint morphology and cartilage integrity (n=8). Scale bars = 50 μm. **B.** Representative images and quantitative analysis of synovial lining thickness using an arbitrary scoring system ranging from 0-3 (n=8). Scale bars = 100 μm & 500 μm. **C.** Serum AChE, ACh, choline, TNF-α, and IL-1β were measured at the end point. All data are expressed as means ± SEM. One-way ANOVA with Post-hoc tests or unpaired two-tailed Student's t-test were performed. * p<0.05; ** p<0.005. 58

Figure 4-8 Chondrocyte-specific AChE knockout mice in inflammatory OA. A. Schematic diagram of animal experiments and the body size of animals. **B.** Representative micro-CT images of medial subchondral bone. **C.** Quantitative analysis of BV/TV differences between ACLT and SHAM legs in each group (n=8). **D.** Quantitative analysis of BV/TV, Tb. N and structure

model index in each group (n=8). **E.** Behavioral assessments of animals using the Rotarod and von Frey tests (n=8). **F.** Representative histological images of subchondral bone and quantitative analysis of newly formed osteoid (n=8). Scale bars = 100 μm. All data are expressed as means ± SEM. One-way ANOVA with Post-hoc tests or unpaired two-tailed Student's t-test were performed. * p<0.05; ** p<0.005. 60

Figure 4-9 Histological staining of chondrocyte-specific AChE knockout mice in inflammatory. A. Representative histological images of tibial articular cartilage with OARSI scoring in joint morphology and cartilage integrity (n=8). Scale bars = 50 μm. **B.** Representative images and quantitative analysis of synovial lining thickness using an arbitrary scoring system ranging from 0-3 (n=8). Scale bars = 100 μm & 500 μm. All data are expressed as means ± SEM. One-way ANOVA with Post-hoc tests or unpaired two-tailed Student's t-test were performed. **** p<0.0001. 61

Figure 4-10 The anti-inflammation and chondral protective effects of donepezil *in vitro*. A. Schematic diagram of the experimental design for C28/I2 cell culture assays. **B.** Schematic diagram of the MSC-derived chondrocytic cell pellet model experiments. **C.** Cell viability analysis under increasing concentrations of donepezil. **D.** Representative histological images of chondrocytic cell pellets. Scale bars = 500 μm. **E.** Quantitative analysis of cell pellet morphology and size. **F.** Transcriptional expression levels of inflammatory cytokines. **G.** Protein levels of AChE and TNF-α. All data are expressed as means ± SEM. One-way ANOVA with Post-hoc tests or unpaired two-tailed Student's t-test were performed. * p<0.05; ** p<0.005; *** p<0.001; **** p<0.0001. 62

Figure 4-11 The anti-inflammation and chondral protective effects of donepezil *in vivo*. A. Schematic diagram of the animal experiments. **B.** Representative micro-CT images of medial subchondral bone, with quantitative analysis of BV/TV, Tb. N and structural model index. **D.** Serum levels of TNF-A, AChE, ACh and Choline measured at the end point. **E.** Representative histological images of rat articular cartilage. Scale bars = 100 μm. **F.** Representative histological images of rat articular cartilage. Scale bars = 100 μm or 500μm. All data are expressed as means ± SEM. One-way ANOVA with Post-hoc tests were performed. * p<0.05; ** p<0.005; *** p<0.001; **** p<0.0001. 64

Figure 4-12 Immunohistochemical staining of mouse joints showed that AChE knockout reduced inflammatory cytokine expression in cartilage, without significant altering α7nAChR expression. Representative histological images of mice joint with quantitively analysis (n=8). Scale bars = 50 μm. All data are expressed as means ± SEM. One-way ANOVA with Post-hoc tests were performed. * p<0.05; ** p<0.005; *** p<0.001. 67

Figure 4-13 Investigation the regulation of AChE/α7nAChR in inflammation.

A. Immunofluorescent co-localization staining of AChE and α7nAChR in human OA cartilage sections and the mapping of fluorescence intensity. Scale bars = 20 μm. **B.** Immunofluorescent co-localization staining of AChE and α7nAChR in cultured human OA chondrocytes and the mapping of fluorescence intensity. Scale bars = 20 μm. **C.** PCR validation of AChE/α7nAChR signaling with AChE knockdown and α7nAChR antagonist (n=5). **D. C.** PCR validation of AChE/α7nAChR signaling with α7nAChR agonist and antagonist (n=4). All data are expressed as means ± SEM. One-way ANOVA with Post-hoc tests. * p<0.05; ** p<0.005.....68

Figure 4-14 Investigation of AChE/α7nAChR signaling. A. Calcium imaging of cultured chondrocyte cells, with visualization and quantitively analysis of mean fluorescence intensity (n=8). Scale bar = 100 μm. **B.** Cell membrane current changes under voltage steps in negative control siRNA groups (n=4). **C.** Cell membrane current changes under voltage steps in AChE knockdown groups (n=4). **D.** Current difference at -100mV between AChE knockdown and negative control, with or without ACh added (n=4)**. E.** Real image of needle attached to the cell membrane. **F.** Experimental design of voltage steps. All data are expressed as means ± SEM. One-way ANOVA with Post-hoc tests or unpaired two-tailed Student's t-test were performed. * p<0.05; ** p<0.005; *** p<0.001; **** p<0.0001.....70

Figure 5-1 Overall framework of the study. The research progresses from the analysis of human sequencing databases and clinical knee specimens to genetic knockdown and pharmacological inhibition of AChE, and ultimately to mechanistic investigations of AChE/α7nAChR signaling in osteoarthritis......72

Figure 5-2 Schematic of the AChE/α7-nAChR signaling in inflammation regulation......78

Chapter 1 Introduction

1.1 Introduction

Osteoarthritis (OA), once viewed as a mechanically driven joint disorder (Birmingham et al., 2019; Chang et al., 2019), is now recognized as being shaped by neural and immune pathways (Courties, Do, et al., 2020; Yang et al., 2025). Recent evidence shows that vagal neurons and neuroinflammation centrally regulate peripheral immune responses (Jin et al., 2024), this may contribute to OA risk and progression. This bidirectional communication between the body and brain underscores the pivotal role of nervous system in modulating systematic inflammation (Ordovas-Montanes et al., 2015). Among neural circuits, the cholinergic anti-inflammatory pathway stands out for its therapeutic potential: activating cholinergic signaling via vagus nerve stimulation consistently reduces joint inflammation and pain in rheumatoid arthritis (Drewes et al., 2021; Genovese et al., 2020; Koopman et al., 2016; Marsal et al., 2021). In addition to systemic inflammation in rheumatoid arthritis, there is a growing interest in vagus nerve stimulation for treating local low-grade inflammation in OA joints, in both preclinical (Cruz et al., 2024; Sprunks et al., 2024; Wu et al., 2023) and clinical settings (Aoyagi et al., 2025; Courties, Deprouw, Maheu, et al., 2022; Courties et al., 2024; Elsehrawy et al., 2025). Yet local cholinergic system in joint homeostasis and disease remains poorly understood (Lauwers et al., 2021).

Among the components of cholinergic signaling within the skeleton, the α7

nicotinic acetylcholine receptor (α7nAChR) stands out as a key mediator of anti-inflammatory effects (Courties, Petit, et al., 2022). Encoded by CHRNA7, α7nAChR is a ligand-gated ion channel with high Ca^{2+} permeability (Noviello et al., 2021) and is essential for suppressing inflammatory cytokine synthesis (Wang et al., 2003). α7nAChR is highly expressed in arthritic joint (Forsgren, 2012) as well as multiple joint-relevant cells, including synovial lining cells (Forsgren, 2012), chondrocytes (Liu et al., 2021) and osteoblasts (Courties, Petit, et al., 2022).

Activation of α7nAChR triggers anti-inflammatory signaling and suppresses pro-inflammatory cytokine production were validated in diverse in vivo models (Park et al., 2022; Patel et al., 2017; S. Zhu et al., 2021), and the principal neurotransmitter of the vagus nerve, acetylcholine (ACh), which can bind to the α7nAChR (Bouzat et al., 2004), triggers anti-inflammatory signaling (Lee, 2013; Rosas-Ballina et al., 2011). The presence of cholinergic nerve fibers in joint tissues further supports the importance of α7nAChR as a peripheral target for modulating inflammation and maintaining cartilage and bone homeostasis (Courties, Belle, et al., 2020; Gadomski et al., 2022; Mora-Antoinette et al., 2025).

In contrast, acetylcholinesterase (AChE) serves as the primary degradative enzyme for ACh, thereby limiting α7nAChR activation and modulating the extent of cholinergic signaling (Gnatek et al., 2012; Pavlov et al., 2009). AChE is present in osteoblasts (Inkson et al., 2004; Sato et al., 2010), osteoclasts (Sato et al., 2015) and chondrocyte (Spieker et al., 2016), and its activity counteracts the anti-inflammatory

and tissue-protective effects mediated by α7nAChR (Courties, Do, et al., 2020; Gnatek et al., 2012). Although AChE inhibitors have shown promise in restoring cholinergic balance (Bonaz et al., 2016) and reducing bone loss (Sato et al., 2015), the precise function of AChE in modulating α7nAChR-dependent signaling within cartilage, and its impact on OA progression, remains poorly understood. Elucidating the local interplay between AChE, ACh and α7nAChR in joint tissues is therefore a critical step toward translating the benefits of systemic cholinergic modulation into targeted, disease-modifying therapies for OA.

We propose that local AChE/α7nAChR signaling at the cartilage–subchondral bone interface is a key modulator of joint inflammation and osteoarthritis progression. To test this, we examined transcriptomic profiles and found that OA cartilage is marked by elevated levels of cholinergic markers (CHRNA7, CHRNA10, CHRNE & COLQ) and pro-inflammatory gene (TNFAIP1), reflecting disrupted signaling networks. Experimental reduction of AChE in inflamed chondrocytes led to decreased inflammatory cytokine release, while chondrocytes or osteoblasts targeted deletion of AChE in animal models mitigated cartilage loss, reduced bone resorption, alleviated synovial inflammation and improved pain behaviors. Treatment with the AChE inhibitor donepezil increased ACh level in serum, diminished inflammation and tissue damage in hypertensive rat OA models. Co-localization of AChE and α7nAChR in OA cartilage was confirmed by immunofluorescence, and mechanistic studies (qPCR, ion channel imaging and patch clamp) showed that the anti-inflammatory benefits of

AChE inhibition depend, at least partially, on the activation of α7nAChR. These results underscore the promise of modulating AChE/ACh/α7nAChR signaling as a promising strategy for OA intervention.

Chapter 2 Literature Review

2.1 Osteoarthritis

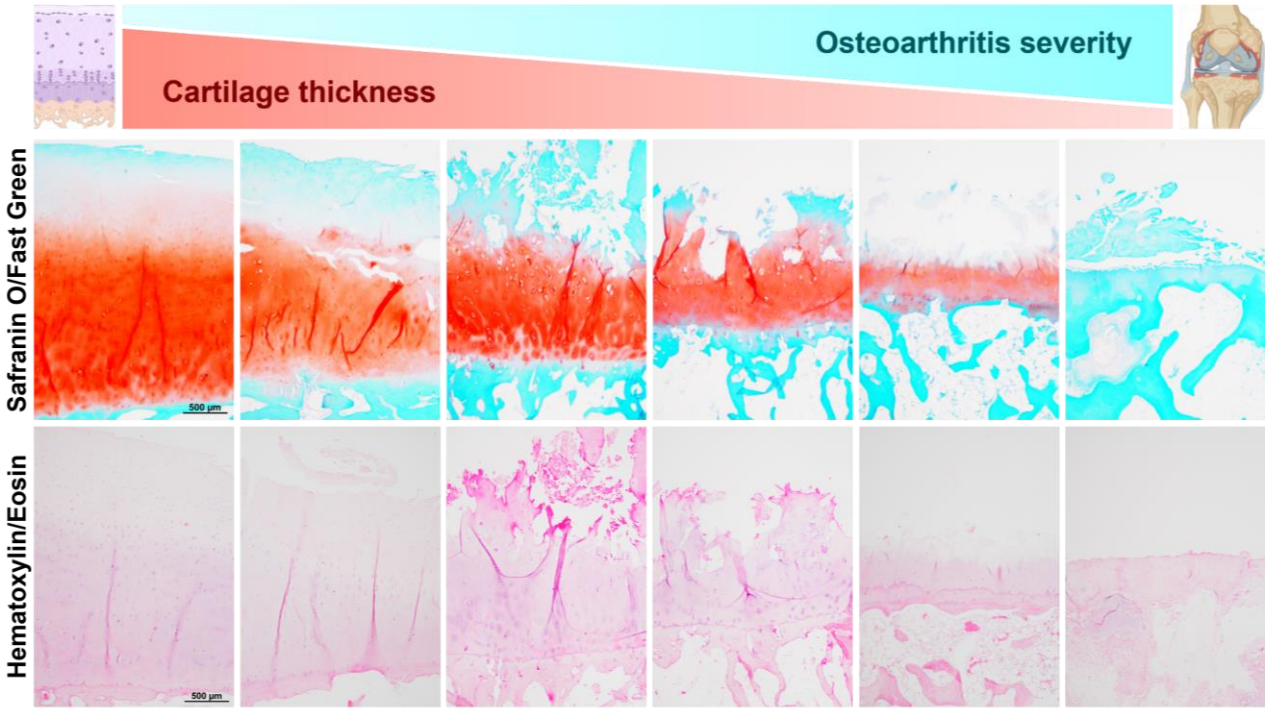

Figure 2-1 Safranin O/Fast Green and Hematoxylin/Eosin staining of human tibial plateau sections. Showing progressive cartilage degeneration, from thick, intact cartilage in mild osteoarthritis to nearly complete loss in severe osteoarthritis. Scale bar, 500 µm.

Osteoarthritis (OA) is a degenerative disease that is generally characterized by subchondral bone alteration, cartilage breakdown, and synovial inflammation (Issa & Sharma, 2006). OA is becoming more and more common worldwide, which significantly impairs quality of life for millions of individuals worldwide, yet its pathogenesis remains incompletely understood (Suri & Walsh, 2012). Over the past decades, prevalent OA cases increased by 113%, from 247.51 million in 1990 to 527.81 million in 2019, imposing a tremendous economic burden on society (Long et al., 2022). Multiple factors, including high mechanical loading (Birmingham et al.,

2019; Chang et al., 2019), traumatic injuries (Sangsuwan et al., 2022; Ziemian et al., 2021), inflammation (Neogi et al., 2016), aging (Jeon et al., 2017), genetics (Rice et al., 2019), and cholinergic system dysregulation (Courties, Do, et al., 2020), are now recognized as contributors to the complex etiology of OA. During the progression of OA, both articular cartilage and subchondral bone undergo dysregulated catabolic and anabolic remodeling processes (Loskutova et al., 2009). These pathological changes collectively contribute to joint pain, stiffness, and functional impairment, underscoring the multifactorial nature of OA.

Moreover, structural changes in cartilage, synovium, and even obesity are proven to be factors affecting OA, and the probability of OA will soar exponentially after the knee injury (Glyn-Jones et al., 2015; Hunter & Bierma-Zeinstra, 2019; Suri & Walsh, 2012). The current state of OA treatment relies heavily on symptomatic intervention, which does not cure the disease. Physical and pharmacological therapies are commonly used as non-surgical strategies to manage OA (Chen et al., 2021).

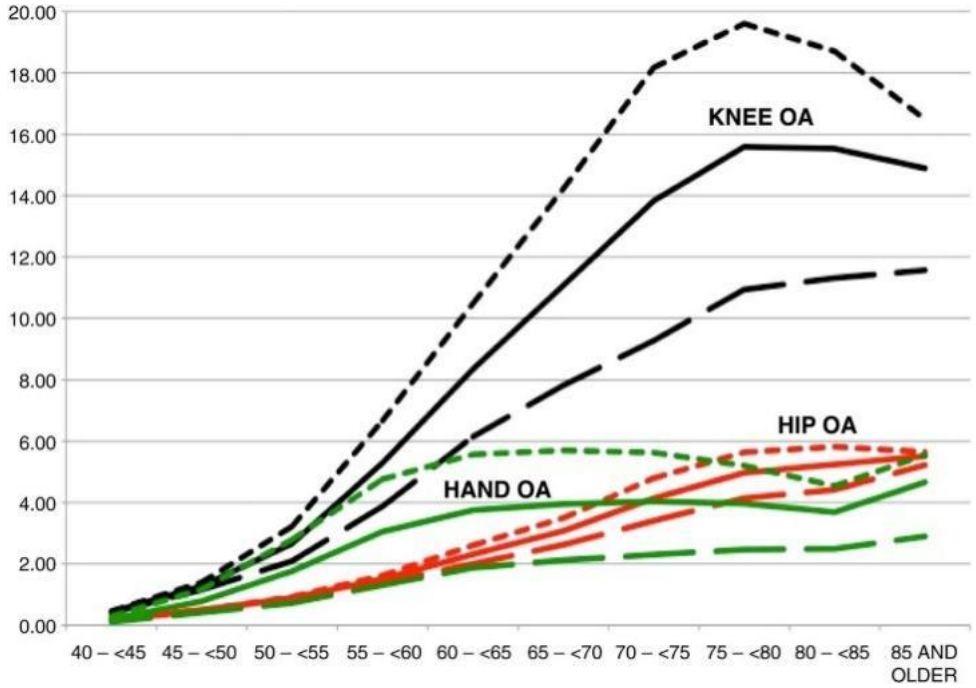

Figure 2-2 Incidence rates (/1000 person-years) of knee OA (black), hip OA (red), and hand OA (green). Suggesting the increasing prevalence of OA. Solid, all population; short dash line, women; long dash line, men (Prieto-Alhambra et al., 2014).

However, these treatments can provide only pain-relieving for most OA patients with mild or moderate OA undergoing (Ringdahl & Pandit, 2011). From the pharmacological therapy aspect, no disease-modifying drugs (DMOADs) have been approved, although some investigational drugs have shown relatively promising results (Oo & Hunter, 2022). Although paracetamol being a widespread recommendation, its benefits are often modest and its analgesic effects are generally limited under certain conditions (Abdel Shaheed et al., 2021).

2.2 Association between skeletal diseases and dementia: Brain-joint axis

A recent study revealed that distinct populations of vagal neurons mediate cytokine signaling to the brain, enabling central regulation of peripheral immune responses (Jin

et al., 2024). This bidirectional communication between the body and brain underscores the pivotal role of the nervous system in modulating systemic inflammation. Furthermore, a two-sample Mendelian randomization study identified a relationship between viral infections of the central nervous system and increased risk of knee OA, supporting the concept that neuroinflammatory processes may contribute to joint degeneration and OA pathogenesis (Yang et al., 2025). These observations reinforce the view that OA is not merely a local disorder but is also regulated by nerve systems. For instance, it was reported that OA has been linked to an increased risk of AD (Huang et al., 2015), and highly associated with its development (Weber et al., 2019). Meanwhile, multiple lines of evidence have also demonstrated a positive correlation between AD and osteoporosis (Chen & Lo, 2017), and osteoporosis patients are at increased risk of developing AD, while individuals with AD are more susceptible to osteoporotic hip fractures (Fisher et al., 2006; Zhao et al., 2012). Studies have also indicated that bone mineral density is reduced in patients with AD, suggesting that bone loss and AD may share common biological mechanisms (Loskutova et al., 2009). Collectively, the explanation for the correlation between AD and skeletal diseases is often sought in a common mechanism behind the diseases; one possibility could be a disturbance of the cholinergic system (Ogunwale et al., 2020; Tamimi et al., 2018).

In animal models, AD has been shown to exacerbate articular cartilage deterioration (Park & Shin, 2022). Similarly, knee OA can accelerate amyloid plaque deposition and induce neuroinflammation in murine models of AD (Gupta et al., 2023; Kyrkanides et

al., 2011). These findings implicated skeletal diseases, is not just local but systemic associated disease, except for non-neuronal factors, the homeostasis of the knee joint is also controlled by neuronal factors such as the cholinergic system, and this correlation is also called the "brain-joint axis" (Berenbaum & Meng, 2016).

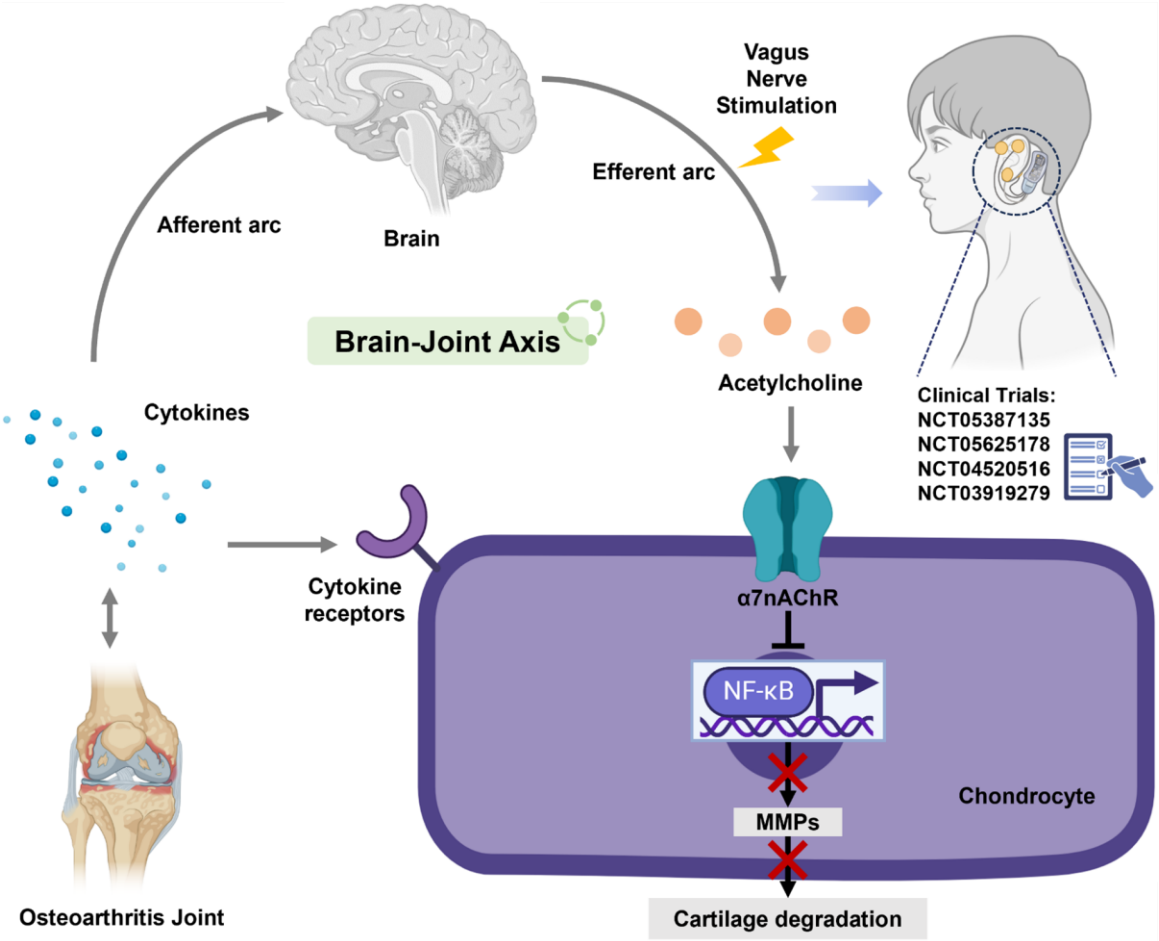

Figure 2-3 Schematic of the "brain–joint axis" and clinical trials: NCT05387135 (Elsehrawy et al., 2025), NCT05625178 (Aoyagi et al., 2025), NCT04520516 (Courties, Deprouw, Rousseau, et al., 2022), NCT03919279 (Courties, Deprouw, Maheu, et al., 2022)) investigating vagus nerve stimulation in osteoarthritis through modulation of the cholinergic anti-inflammatory reflex. By increasing acetylcholine production, vagus nerve stimulation could activate nicotinic receptors, dampen inflammation, and potentially prevent cartilage degradation. This brain–joint link underscores the role of neural modulation in peripheral inflammation. The diagram was redrawn and modified based on published literature (Berenbaum & Meng, 2016).

This concept not only highlights the strong association between OA and neuronal

disease but also suggests that these conditions may share overlapping pathological features, such as inflammation. The emerging concept of the "brain-joint axis" further underscores the bidirectional communication between the central nervous system and peripheral joints (Berenbaum & Meng, 2016). Given this intricate interplay, the role of the peripheral nervous system—especially its regulatory influence on lower limb joints—warrants further investigation. Peripheral nerves are not only essential for sensory and motor control of the joints, but also play a critical role in modulating local inflammatory responses and maintaining tissue homeostasis through various neurochemical pathways (Ordovas-Montanes et al., 2015). Among these, the cholinergic system has emerged as a key mediator of anti-inflammatory signaling in the peripheral branch (Lauwers et al., 2021). Therefore, a deeper understanding of the cholinergic system's involvement in joint may provide valuable insights into the mechanisms underlying OA and could open new avenues for therapeutic intervention targeting the brain-joint axis.

2.3 Cholinergic signaling in joint homeostasis and osteoarthritis

The complex nature of OA makes it challenging to effectively mitigate disease progression through a single therapeutic approach or target, but most drugs under development for OA have focused on single targets specific to particular phenotypes, often overlooking other potentially influential factors (Grässel & Muschter, 2020). As a multifactorial disease, OA has recently been linked to neurological disorders, particularly the association between OA and dementia, highlighting the critical

involvement of the nervous system in OA pathogenesis (Huang et al., 2015; Weber et al., 2019). Accumulating studies indicate that the nervous system not only mediates pain transmission but also regulates inflammation progression, and vagus nerve stimulation has been shown to modulate the cholinergic system and activate the cholinergic anti-inflammatory pathway, thereby suppressing inflammation (Bellocchi et al., 2023; Koopman et al., 2016; Zhiyang et al., 2023). This evidence positions the cholinergic system as a promising target for OA therapies.

Given OA's inflammatory nature, the regulatory role of the cholinergic system has become a novel therapeutic target for OA management (Luo et al., 2020). The cholinergic system may function as an endogenous modulator, wherein its activation could protect articular cartilage homeostasis and subchondral bone by dampening inflammatory cytokines, thereby mitigating OA progression (Luo et al., 2020). The cholinergic system includes acetylcholine (ACh), acetylcholinesterase (AChE), nicotinic cholinergic receptors (nAChRs), and choline acetyltransferase (ChAT), and these molecules are essential molecules in immune response (Halder & Lal, 2021). As for nicotinic acetylcholine receptors (nAChRs), these receptors are pentameric ligand-gated ion channels and mediate the synaptic transmission at the neuromuscular junction as well as cholinergic synapses (Hogg et al., 2003).

ACh is a small molecule with a positive charge, and it is the first identified neurotransmitter in the world (Meriney & Fanselow, 2019). It exhibits a diverse array of functions within the body, and these functions encompass a broad spectrum,

encompassing both motor and autonomic functions within the peripheral nervous system, as well as modulatory roles within the central nervous system (Meriney & Fanselow, 2019). ACh is also a vital neurotransmitter of the vagal nerve, which can bind to the alpha-7 nicotinic receptor (α7nAChR) and lead to activation of the anti-inflammation signaling pathway (Keever et al., 2023). The transmission of ACh in ganglionic synapses is facilitated by nicotinic receptors, which function as ligand-gated ion channels, but the postganglionic transmission is mediated through G-protein-coupled muscarinic receptors (Zaagsma & Meurs, 2006).

Cholinergic components are not only confined to neural tissues, they are also widely distributed across numerous non-neural tissues, and the cholinergic components expressed in these non-neuronal tissues are referred to as the non-neuronal cholinergic system (NNCS) (Luo et al., 2020). NNCS is also expressed in the skeletal system, and existing evidence suggests that the NNCS plays a role in the proliferation, differentiation, and death of mesenchymal stem cells, cartilage, and bone marrow cells (Guo et al., 2014; Spieker et al., 2017). Recent research using a murine model demonstrated that cholinergic nerve fibers are located in close proximity to cortical bone osteocytes in situ, and that osteocytes respond to cholinergic signaling, thereby influencing bone mechanoadaptation (Mora-Antoinette et al., 2025). These findings provide strong evidence for the involvement of the cholinergic system in joint homeostasis. Besides, NNCS also appears to be involved in endochondral and bone marrow ossification, as well as bone matrix mineralization, but further research is

required to fully understand the role of it during those processes (Guo et al., 2014).

Recently, peripheral nerves and cholinergic fibbers were found in human OA cartilage and subchondral bone samples (Courties, Belle, et al., 2020), and the NNCS are present in the synovium of OA (Schubert et al., 2012). The discovery of cholinergic fibers and non-neuronal cholinergic components in OA affected joint tissues further supports the involvement of cholinergic system in local inflammation. Moreover, the role of the cholinergic system in chondral protect was validated via the activation of α7nAChR previously (Liu et al., 2015). This finding was further proven in the α7nAChR-deficient murine OA model, resulting in disturbance of the ACh/CHRNA7 axis and aggravated cartilage degradation after the deletion of CHRNA7 (Courties, Do, et al., 2020).

Taken together, current evidence suggests that the cholinergic system may serve as a pivotal modulator of joint homeostasis and underscores the relevance of the "brain–joint axis" concept in the context of OA.

2.4 Nicotinic acetylcholine receptors and inflammation

The nicotinic acetylcholine receptors (nAChR), which are rapid-acting ionotropic receptors consist of distinct subunits: α, β, δ, ϵ, and γ (Albuquerque et al., 2009). These subunits are organized in various pentameric combinations surrounding a ligand-gated excitatory ion channel, which is permeable to sodium (Na^+), potassium (K^+), and calcium ($Ca2^+$) ions (Habibi, 2010). In mammalian sympathetic neurons, the activation of nicotinic acetylcholine receptors nAChR triggers the opening of a

nonselective cation channel, and this results in an influx of Na^+, leading to membrane depolarization and subsequent activation of voltage-gated $Ca2^+$ channels (Habibi, 2010). Among these receptors, the α7 nicotinic acetylcholine receptor (α7nAChR) plays a pivotal role in the cholinergic inflammatory pathway and is essential for suppressing inflammatory cytokine synthesis (Wang et al., 2003). This ligand-gated ion channel is assembled as a homopentamer, encoded by the CHRNA7 gene, and exhibits exceptionally high permeability to Ca^{2+} (Noviello et al., 2021). Numerous in vivo studies have demonstrated that the cholinergic system modulates peripheral immune responses, with activation of α7nAChR inhibiting inflammation and suppressing the expression of pro-inflammatory cytokines (Park et al., 2022; Patel et al., 2017; S. Zhu et al., 2021).

Given the significant role of α7nAChR in activating the cholinergic anti-inflammatory pathway, recent research interest has been directed towards maintaining agonists of α7nAChR, such as ACh (Lee, 2013) and nicotine (Liu et al., 2015; Teng et al., 2019), and modulating the inflammatory response through the inhibition of AChE (Liu et al., 2020). In human, α7nAChR is found expressed in multiple cell types relevant to OA pathophysiology, including synovial lining cells (Forsgren, 2012), chondrocytes (Liu et al., 2021) and osteoblasts (Courties, Petit, et al., 2022). Immunohistochemical analyses have revealed intense α7nAChR staining in synovial lining layers of both OA and RA patients (Forsgren, 2012), but α7nAChR and other nicotinic subunits are differentially expressed between OA and RA synovium, indicating disease specific

remodeling of the non-neuronal cholinergic system (Schubert et al., 2012). Multiple *in vivo* OA models support α7nAChR's chondroprotective role, such as agonist stimulation of α7nAChR can alleviates monosodium iodoacetate (MIA) induced cartilage degradation (Liu et al., 2021; Teng et al., 2019), reduces expression of catabolic enzymes like MMP-9 & MMP-13 (Teng et al., 2019; X. Zhu et al., 2021), and attenuates pro-inflammatory cytokines TNF-α & IL-1β (X. Zhu et al., 2021). In α7nAChR knockout mice, the absence of this regulatory mechanism correlates with accelerated cartilage lesion development during age-related OA (Courties, Petit, et al., 2022). These findings highlight a broader role of α7nAChR in cartilage homeostasis and OA development.

Given that α7nAChR activation depends on ligand availability, AChE-mediated ACh degradation emerges as a critical upstream regulator. As demonstrated in our own findings (see chapter 4 results), genetic or pharmacological AChE inhibition might activate the α7nAChR, thereby facilitating α7nAChR signaling in chondrocytes and enhancing anti-inflammatory responses in OA. This mechanistic intersection between α7nAChR and AChE positions both molecules as interdependent nodes in the "brain–joint axis" with therapeutic potential for OA.

2.5 Clinical evidence of cholinergic anti-inflammatory pathway

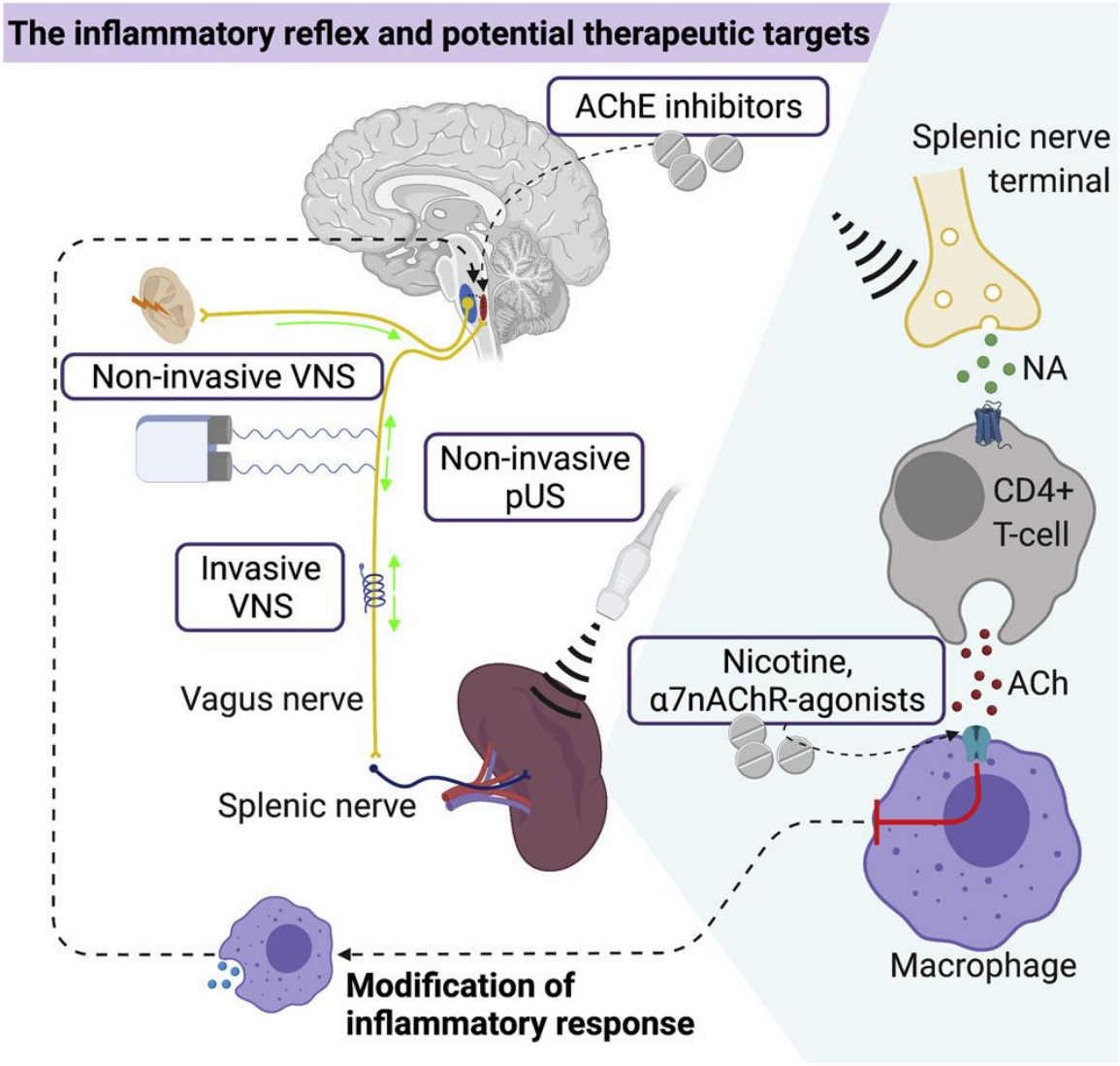

Figure 2-4 Schematic of the cholinergic anti-inflammatory pathway (Kelly et al., 2022). The central nervous system releases acetylcholine via pathways such as the vagus nerve to suppress macrophage driven inflammation. The cholinergic anti-inflammatory pathway is a neural circuit through which the central nerve system regulates peripheral immunity. Through the vagus and splenic nerves, acetylcholine produced by cells downregulates the inflammatory functions of macrophages expressing α7 nicotinic acetylcholine receptors. The central nervous system releases acetylcholine via pathways such as the vagus nerve to suppress macrophage driven inflammation.

Recent clinical and preclinical studies have provided compelling evidence supporting the pivotal role of the cholinergic anti-inflammatory pathway in

modulating joint inflammation (Courties et al., 2024; Wu et al., 2023). The vagus nerve, a key component of this pathway, has been shown to exert significant anti-inflammatory effects through nicotinic anti-inflammatory signaling, which regulates both innate and adaptive immune responses by modulating cellular and molecular inflammatory pathways (Hoover, 2017). Furthermore, the activation of cholinergic anti-inflammatory pathway has emerged as a key regulator for inflammation management and pain reduction in OA (Aoyagi et al., 2024; Aoyagi et al., 2025; Courties, Deprouw, Maheu, et al., 2022; Courties et al., 2024; Elsehrawy et al., 2025), rheumatoid arthritis (Drewes et al., 2021; Genovese et al., 2020; Koopman et al., 2016; Marsal et al., 2021), inflammatory bowel disease (D'Haens et al., 2023), chronic low back pain (Demircioğlu et al., 2024), etc. Clinical trials of vagus nerve stimulation in OA and rheumatoid arthritis demonstrate significant anti-inflammatory efficacy—providing a therapeutic paradigm transferable to skeletal disease management.

In OA, vagus nerve stimulation (VNS) has emerged as a promising neuromodulatory intervention. Multiple studies have demonstrated that electrical stimulation of the vagus nerve can activate the inflammatory reflex, resulting in reduced expression levels of pro-inflammatory cytokines, alleviation of joint pain and swelling, and overall improvement in patient-reported quality of life (Aoyagi et al., 2025; Courties, Deprouw, Maheu, et al., 2022; Courties et al., 2024). Importantly, some patients have maintained symptom improvement even after cessation of VNS treatment, indicating the potential fo

r durable anti-inflammatory effects (Elsehrawy et al., 2025). These findings highlight the therapeutic promise of neuromodulation as an adjunct to conventional pharmacological and non-pharmacological therapies for inflammatory joint diseases (Courties et al., 2024; Elsehrawy et al., 2025). Collectively, clinical evidence underscores the significance of the VNS and cholinergic anti-inflammatory pathway in the management of OA, offers a novel and potentially long-lasting approach to controlling inflammation and improving patient outcomes in these debilitating conditions.

2.6 Pre-clinical evidence of cholinergic anti-inflammatory pathway

The ability of vagus nerve stimulation (VNS) to attenuate nociception, improve joint function, and suppress inflammation underscores the therapeutic promise of engaging the cholinergic anti-inflammatory pathway in musculoskeletal disease. Pre-clinical research across multiple species has demonstrated that modulation of the vagus nerve—a central component of the cholinergic anti-inflammatory pathway—can significantly influence pain perception, inflammatory processes, and joint integrity (Cruz et al., 2024; Sprunks et al., 2024; Wu et al., 2023). In a study on mice model, percutaneous VNS prevented long-lasting surgery-induced pain, improved motor function and bone healing, and normalized satellite glial cell activity (Wu et al., 2023). A similar non-invasive approach in osteoarthritic dogs reduced discomfort and enhanced joint mobility without side effects (Sprunks et al., 2024). In contrast, vagotomy in rats

hastened gait abnormalities and joint degeneration, indicating that diminished vagal activity can exacerbate disease progression (Cruz et al., 2024). These pre-clinical data demonstrate that enhancing vagal activity—via invasive or non-invasive neuromodulation—confers analgesic, anti-inflammatory, and pro-repair effects, whereas reducing vagal tone exerts the opposite influence.

While such interventions act at the systems level, their downstream effects are potentially mediated through acetylcholine-responsive targets in peripheral tissues, including subchondral bone and articular cartilage (Courties, Belle, et al., 2020). Within chondrocytes, acetylcholine signaling via the α7nAChR might exerts anti-inflammatory and tissue-protective effects yet is counter regulated by AChE expression (Courties, Do, et al., 2020). Dysregulation of this local cholinergic balance may represent a mechanistic link between impaired vagal tone, heightened joint inflammation, and cartilage degeneration (Courties, Do, et al., 2020). Elucidating the role of AChE/ACh in modulating α7nAChR dependent signaling within cartilage therefore offers a critical step in translating the benefits of systemic vagal modulation into targeted, disease-modifying therapies for OA.

2.7 Acetylcholinesterase in anti-inflammation signaling

Acetylcholinesterase (AChE), a cholinergic enzyme catalyzing the degradation of acetylcholine, was originally identified at postsynaptic neuromuscular junctions, and together with nicotinic receptors, plays a crucial role in maintaining cholinergic system integrity (Sam & Bordoni, 2025). The presence of AChE, this ACh-

hydrolyzing enzyme, is confirmed in osteoblasts (Inkson et al., 2004; Sato et al., 2010), osteoclasts (Sato et al., 2015) and chondrocyte (Spieker et al., 2016). In addition to AChE, butyrylcholinesterase (BChE) is another cholinesterase capable of degrading acetylcholine (Johnson & Moore, 2012). However, compared with AChE, BChE has no clearly defined functions, exhibits lower catalytic efficiency for acetylcholine, and its physiological role remains unclear (Ha et al., 2020; Johnson & Moore, 2012).

Recent studies have proposed a correlation between the cholinergic system and the regulation of bone homeostasis (Luo et al., 2020). During the progression of Alzheimer's disease (AD), dysregulation of AChE can exacerbate the pathology (Subramanian et al., 2023). This can be mitigated by AChE inhibitors such as donepezil, a drug developed for AD treatment (Dong et al., 2009). AChE inhibitors can help restore the cholinergic system by increasing the amount of ACh and then initiating the anti-inflammatory response through the activation of α7nAChR (Bonaz et al., 2016). Prior studies report that donepezil reduces the risk of hip fractures in clinical cases (Tamimi et al., 2012) and rescue bone resorption in an animal model (Sato et al., 2015), and, *in vitro*, prevents type II collagen degradation and suppresses TNF-α induced MMP-13 expression (Zhang & Zhou, 2014). These findings have pointed out the importance of AChE in skeletal homeostasis and its potential to be selected as a therapeutic target in OA management.

Recent studies have revealed that AChE could contribute to inflammation progression beyond its cholinergic hydrolytic functions (Liu et al., 2020; Xia et al.,

2025; Zivkovic et al., 2023). At the cellular level, AChE was found to be co-localized with α7nAChR on macrophage surfaces, with AChE expression upregulated via NF-κB driven transcription following lipopolysaccharide (LPS) stimulation (Liu et al., 2020). This interaction between AChE and α7nAChR attenuates the cholinergic anti-inflammatory pathway by reducing ACh mediated suppression of pro-inflammatory cytokines release, thereby actively promoting pro-inflammatory signaling (Liu et al., 2020). *In vivo*, conditional overexpression of AChE in the myeloid lineage of transgenic mice exacerbates LPS induced neuroinflammation, as evidenced by upregulated transcription of pro-inflammatory cytokines and sequencing data (Xia et al., 2025). Clinically, patients with traumatic injury exhibit sustained elevation of AChE enzymatic activity, which positively correlates with injury severity, supporting its potential utility as a biomarker of sterile inflammation (Zivkovic et al., 2023).

Given the emerging evidence that AChE amplifies inflammatory process across cellular, preclinical, and clinical contexts, its dysregulation may exacerbate synovial inflammation and cartilage degeneration, contributing to the pathogenesis and progression of OA.

2.8 Protective effects of acetylcholinesterase inhibitor

Donepezil is a second-generation and commercially available acetylcholinesterase (AChE) inhibitor approved for the treatment of Alzheimer's disease, which is widely prescribed due to its high selectivity for AChE with a long half-life and markedly lower affinity for BChE (Rogers et al., 1998). Accumulating evidence indicates the

therapeutic profile of donepezil extends beyond cognitive improvement to include benefits for the skeletal system. Clinical trials demonstrated donepezil administration has been associated with a reduced risk of fracture in older adults with dementia (Matsumoto et al., 2024; Tamimi et al., 2012). Consistent with clinical observations, donepezil can inhibit osteoclast differentiation and function *in vitro* and prevent bone loss by suppressing bone resorption *in vivo* (S. Li et al., 2023; Sato et al., 2015).

Recently, the osteoprotective effects of donepezil is now being prospectively evaluated in a randomized, double-blind, placebo-controlled clinical trial (NCT06041789) in older adults with AD, assessing changes in bone mineral density, turnover markers, and bone quality over 12 months of therapy (North et al., 2025).

For chondrocyte, an *in vitro* study revealed that donepezil treatment prevented TNF-α induced loss of collagen type II in primary human chondrocytes by inhibiting the expression of MMP-13, and attenuated cartilage matrix degradation (Zhang & Zhou, 2014). The anti-inflammatory properties of donepezil have also been reported in non-articular disease models, where it reduced inflammatory cytokine production and apoptosis in both in vitro and in vivo systems (Kim et al., 2021; A. Li et al., 2023), further supporting its capacity to modulate inflammatory.

Collectively, these findings highlighted the important role of cholinergic signaling in skeletal homeostasis and suggested the potential therapeutic effects of targeting AChE in inflammation and skeletal disease management. However, despite these promising data, the role of AChE inhibition and AChE in the context of OA remains largely

unexplored. Addressing this gap will be critical for elucidating the therapeutic potential of targeting AChE in joint disease.

2.9 Research Gaps

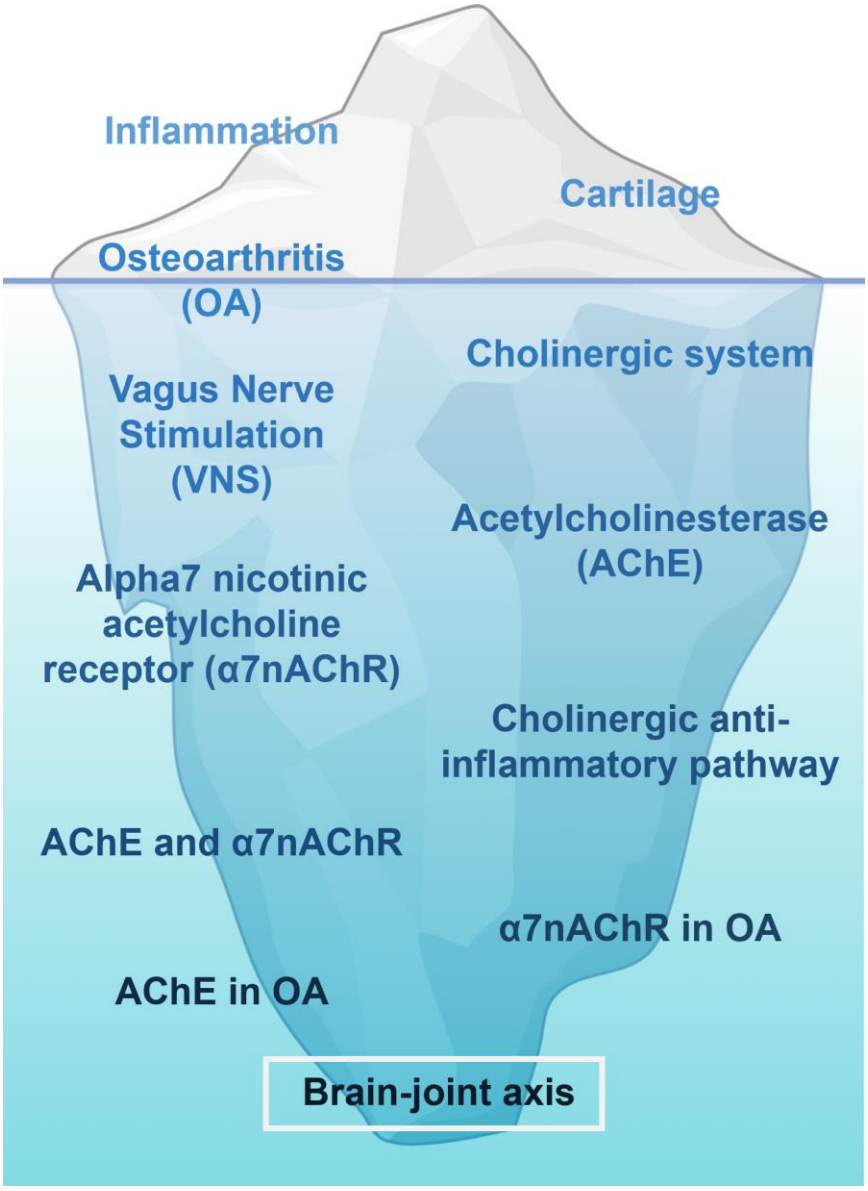

Figure 2-5 The visible portion above the waterline illustrates research topics with abundant published literature, submerged layers indicate less explored research topics with fewer existing literature. AChE and α7nAChR are co-localized in osteoblasts, but their interactions in chondrocytes is uncharted. The impact of AChE dysregulation on OA pathogenesis and cartilage homeostasis, and its potential as a therapeutic target for inflammation management, remains to be elucidated. The precise role of AChE with the "brain–joint axis", especially in the peripheral branch, remains unknown.

Although AChE modulation has demonstrated therapeutic promise in preclinical studies, including rescuing bone loss in murine models and suppressing OA-related inflammatory cytokines in cell culture, significant research gaps remain. Specifically, the precise role of AChE within the “brain-joint axis”, particularly in the peripheral branch, is not well understood. Furthermore, while co-localization and potential interaction between AChE and α7nAChR have been observed in murine osteoblasts, this relationship has yet to be explored in chondrocytes. Additionally, although elevated AChE is linked to neuronal inflammation, the impact of AChE dysregulation on OA pathogenesis and cartilage homeostasis, as well as its potential as a therapeutic target for inflammation management, remains to be elucidated.

2.10 Research Hypothesis

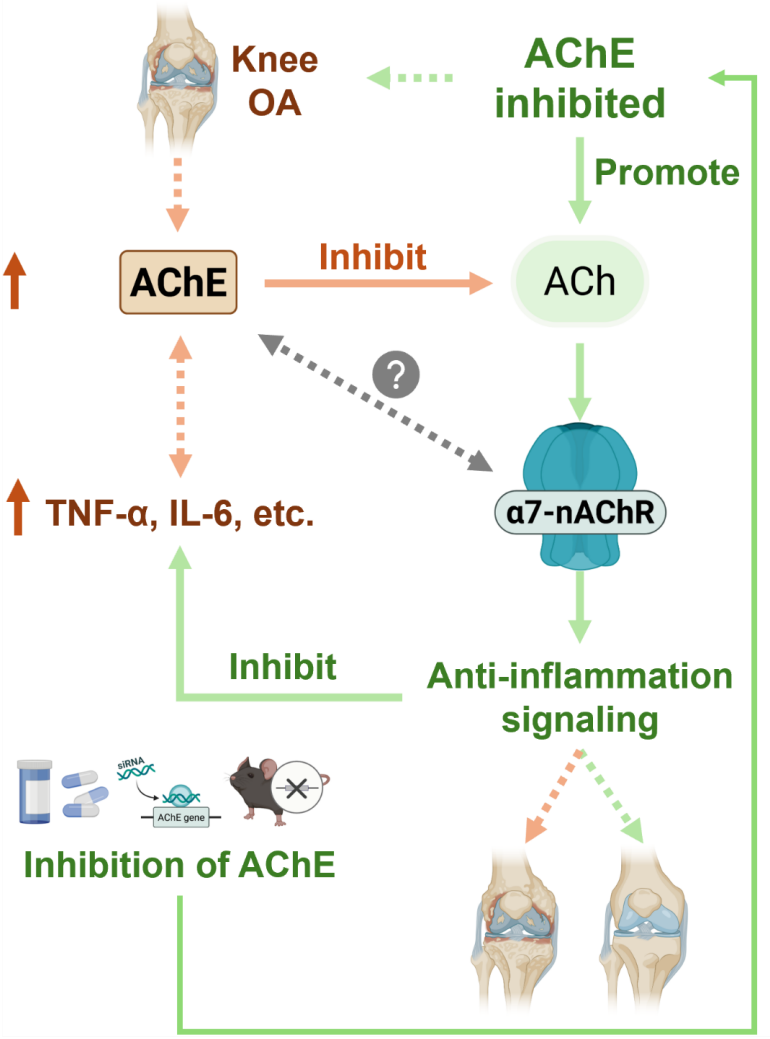

Figure 2-6 Schematic of research hypothesis. We aim to examine how acetylcholinesterase (AChE) influences osteoarthritis (OA) progression. Acetylcholine (ACh) activates anti-inflammatory signaling via the α7 nicotinic acetylcholine receptor (α7nAChR). We propose that inhibiting AChE will potentiate this pathway, reduce inflammatory cytokines, and investigate potential interactions between AChE and α7nAChR.

Although the role of α7nAChR in cartilage homeostasis and OA have been extensively studied, the contribution of AChE to cartilage homeostasis and OA development remains poorly understood. We hypothesize that dysregulation of AChE in bone and cartilage contributes to OA progression by disrupting cholinergic homeostasis, and that targeting AChE may restore cholinergic signaling mediated joint protection.

2.11 Research Objectives

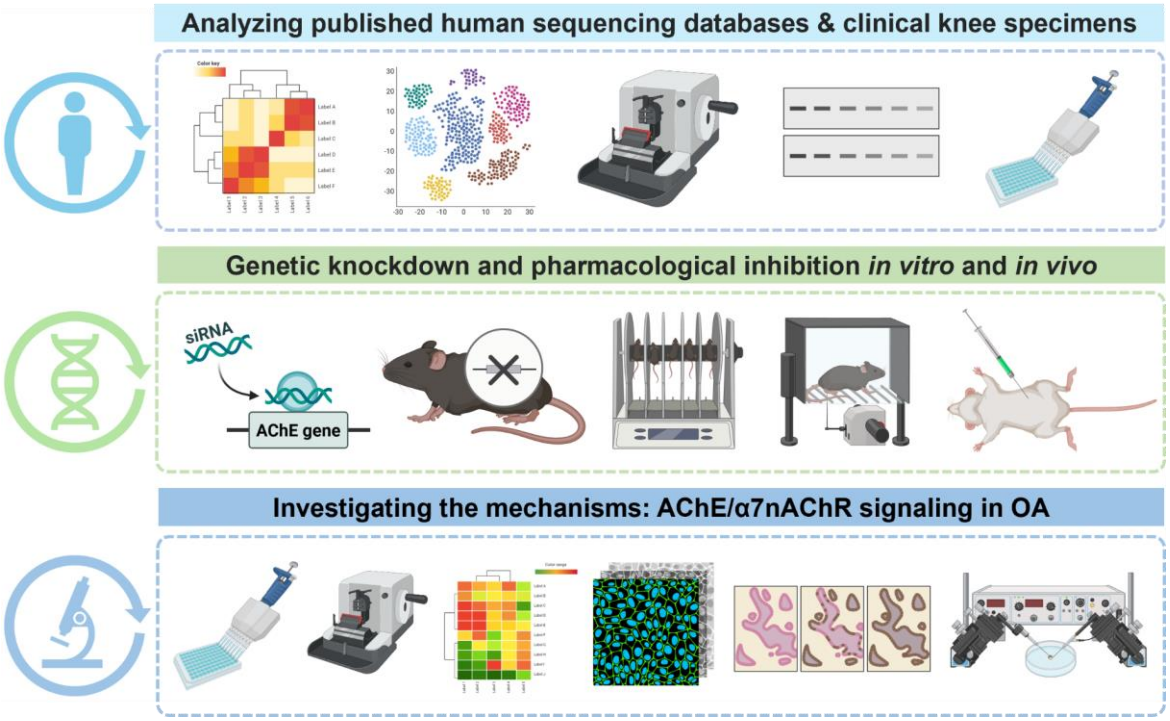

Figure 2-7 Workflow of the study, progressing from objective 1 (human sequencing database and clinical knee specimen analysis) to objective 2 (in vitro and in vivo genetic knockdown and pharmacological inhibition), and objective 3 (mechanistic investigation of AChE and α7nAChR in OA).

This study aims to elucidate the role of chondrocytic AChE in the progression of chondrocyte inflammation and OA pathogenesis. Specifically, we will:

1. Confirm the involvement of cholinergic signaling in joint cartilage homeostasis and OA progression by analyzing published human sequencing databases and characterizing differences in the expression of inflammatory cytokine and AChE in articular cartilage from clinical knee specimens.

2. Evaluate the effects of AChE modulation on inflammation and OA using both in vitro and in vivo models, employing genetic knockdown and pharmacological inhibition to verify the chondroprotective and anti-inflammatory effects.

3. Investigate the mechanisms by which AChE regulates inflammation and cartilage homeostasis, including its interaction with α7nAChR, its impact on the nicotinic anti-inflammatory signaling pathway.

Chapter 3 Materials and Methods

2.1 Materials

Reagents and materials used in this study are listed below, with respective suppliers and catalog numbers for reproducibility:

Dulbecco's Modified Eagle Medium: Nutrient Mixture F12 (DMEM-F12, Gibco™), Dulbecco's Modified Eagle Medium (high-glucose) (DMEM, Gibco™), Penicillin-Streptomycin (P/S, Gibco™), Fetal bovine serum (FBS, Gibco™), Trypsin-EDTA (0.05%) phenol red (Gibco™), DPBS no calcium, no magnesium (Gibco™), Antibiotic-Antimycotic (Gibco™), PrimeScript™ First Strand cDNA Synthesis Kit (Takara Bio), Donepezil-HCl (Aladdin, #120011-70-3), Cell Proliferation Kit I (MTT, Roche, Penzberg, Germany, #11465007001), E.Z.N.A.® Total RNA Kit I (Omega Bio-tek, Norcross, USA, #R6834-02), SYBR Green qPCR Master Mix (Universal)(MCE, #HY-K0501A), RIPA lysis buffer (Thermo Scientific, #89901), Pierce™ BCA Protein Assay Kit (Thermo Scientific, 23225), AChE Fluorescent Activity Kit (Invitrogen™, EIAACHEF), Human AChE ELISA Kit (Abclonal, RK00797), Rat AChE ELISA Kit (Abclonal, RK03461), Mouse AChE ELISA Kit (Abclonal, RK02564), Human TNF-alpha ELISA Kit (Abclonal, RK00030), Rat TNF- alpha ELISA Kit (Abclonal, RK00029), Mouse TNF- alpha ELISA Kit (Abclonal, RK04875), PVDF membranes (Millipore, USA), TRAP/ALP Stain Kit (FUJIFILM, Japan # 4987481478503), Acetylcholinesterase/ACHE Protein, Human (CHO, His) (MCE, HY-P79277) Interlukin-1 beta, Human (MCE, HY-P7028), cell permeant - Special Packaging

(Invitrogen™, X14210), Choline/Acetylcholine Assay kit (Colorimetric/Fluorometric) (Abcam, ab65345).

2.2 Methods

RNA sequencing of human chondrocyte cell line and analysis of public database

Human chondrocyte cell line C28/I2 (Merck) was treated under three conditions: negative control siRNA (NC-siRNA) alone, NC-siRNA combined with IL-1β, and AChE-siRNA combined with IL-1β. Following treatment, samples were collected and subjected to RNA sequencing, performed by Metware (Wuhan, China). Data analysis was conducted using the Metware Cloud platform (https://cloud.metware.cn), an online tool for transcriptomic analysis. In addition, RNA-seq data are available at the NCBI's Gene Expression Omnibus (GEO) data repository with the accession ID GSE114007. Meanwhile, the analysis was performed with GEO2R, which is an interactive web tool that allows users to compare two or more groups of Samples in a GEO Series in order to identify genes that are differentially expressed across experimental conditions.

Analysis of human single cell RNA sequencing database

The single-cell RNA sequencing (scRNA-seq) data used in this study were obtained from the NCBI GEO repository under accession number GSE254844. All downstream analyses were performed using the raw data from this dataset. Data preprocessing and quality control (QC) steps were adapted from the original published protocol, with modifications to address the specific objectives of this secondary analysis. Raw count matrices from 10x Genomics scRNA-seq data were imported into RStudio using the Seurat package (v5.2.0). For each sample, QC parameters were set according to sample-specific thresholds, including minimum and maximum numbers of detected genes

(nFeature_RNA), maximum UMI counts (nCount_RNA), and maximum mitochondrial gene percentage (percent.mt). These QC parameters were determined based on the original study. Cells not meeting these criteria were excluded from further analysis. To minimize the impact of doublets, DoubletFinder (v2.0.3) was applied to samples containing more than 10,000 cells, using parameter settings as described in the original protocol (pK = 0.09, nExp = 0.075 × total cell number, other parameters as default).

Cells classified as doublets were removed from the dataset. Data Integration and Normalization After QC and doublet removal, individual samples were merged into a single Seurat object. Data normalization was performed using the NormalizeData function, and highly variable genes were identified using the FindVariableFeatures function (vst method, nfeatures = 2000). The data were then scaled and subjected to principal component analysis (PCA, npcs = 30). Dimensionality reduction was performed using UMAP, and cell clustering was conducted using the Louvain algorithm with a resolution parameter of 0.8. Gene Annotation To facilitate downstream gene-level analyses, Ensembl gene IDs were converted to gene symbols using the org.Hs.eg.db annotation database. Where multiple genes shared the same symbol, unique identifiers were appended to avoid ambiguity. Visualization and Statistical Analysis A series of visualization and statistical analyses were performed to characterize gene expression patterns between OA and control groups. These included: UMAP plots colored by gene expression and sample group. Bubble plots showing normalized gene expression per 1,000 cells in each group. Violin plots and boxplots

comparing gene expression distributions between OA and control groups, with statistical significance assessed using the Wilcoxon rank-sum test. Bar plots displaying mean expression and standard error for each gene and group. Scatter plots illustrating pairwise relationships between selected genes.

All visualizations were generated using ggplot2, ggpubr, and pheatmap packages in R. Target Genes Two sets of target genes were selected for focused analysis: Group 1: ACHE, CHRNA7, COLQ, TNFAIP1, MMP13 Group 2: BMAL1, PER2 Gene names were matched to the expression matrix using exact and fuzzy matching to account for potential discrepancies in gene annotation. Group Assignment Samples were assigned to either the OA or control group according to metadata provided in the original dataset and QC parameter table.

The workflow was designed to be fully reproducible and is based on open-source R packages. Reference to Original Methods This analysis was conducted by adapting and modifying the methods described in the original publication (see GEO accession GSE254844 for raw data and detailed protocols). All major steps, including sample QC, doublet removal, data integration, normalization, clustering, and gene annotation, were performed in accordance with the referenced methodology, with minor adjustments to parameter settings and visualization approaches to address the specific aims of this secondary analysis.

Cell culture: siRNA knockdown of AChE

Human chondrocytic cell line C28/I2 (Merck) was seeded into 6-well plates 24 hours prior to treatment. Before siRNA knockdown, the culture medium was replaced with 1,500 µL antibiotic-free medium per well. For the inflammation induction group, cells were pretreated with IL-1β for 1 hour before siRNA transfection. For each well, 10 µM siRNA working stock was diluted in 250 µL Opti-MEM (Gibco™), and 10 µL Lipofectamine™ RNAiMAX Transfection Reagent (Invitrogen™) was separately diluted in 250 µL Opti-MEM. The diluted siRNA solution was transferred into RNAiMAX solution and incubated together for 5 minutes at room temperature, then gently added to the wells. Cells were harvested 24 hours post-transfection for

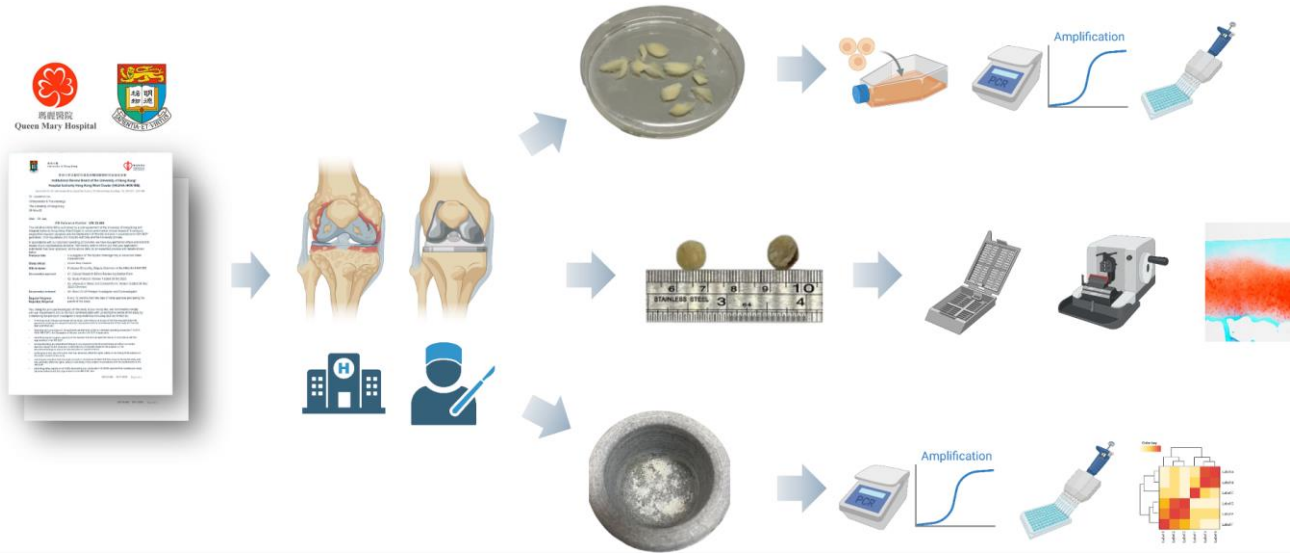

subsequent analyses.

Figure 3-1 Workflow of human OA specimens' collection and primary cultured chondrocytes.

Human OA specimens and primary cultured chondrocytes

These human OA specimens were obtained from the patients underwent total knee

replacement in Queen Mary Hospital with patients' consent. This study was approved by the Institutional Review Board of the University of Hong Kong and Hospital Authority Hong Kong West Cluster (HKU/HA HKW IRB, No.: UW23–596).

Joint specimens were collected at the hospital, rinsed with Dulbecco's phosphate-buffered saline (DPBS), and immersed in RNAlater™ Stabilization Solution (Invitrogen™, AM7021). Samples were then transported to the laboratory for further processing. Articular cartilage was dissected from the medial and lateral compartments using a surgical scalpel, and the excised cartilage pieces were placed in a mortar containing liquid nitrogen and pulverized into powder. The powdered cartilage was added 1,000 μL of RIPA lysis buffer and subjected to digestion for 30 minutes.

Human OA chondrocyte primary culturing was done according to published methods (Muhammad et al., 2021). Cartilage samples were harvested from the femoral condyles and tibial plateau of the knee joint and immediately immersed in a sterile bottle containing 1× PBS supplemented with 1% (v/v) antibiotic-antimycotic solution. The cartilage was then washed three times with PBS containing 1% (v/v) antibiotic-antimycotic to ensure sterility. Subsequently, the cartilage was minced into small pieces (approximately 2 - 3 mm) using a sterile scalpel blade in a petri dish containing DPBS. The minced tissue was digested with 0.2% (w/v) collagenase II in DMEM/F-12 medium supplemented with 5% (v/v) FBS and 1% (v/v) antibiotic-antimycotic. The cartilage fragments were incubated overnight (20 hours) at 37°C in a humidified atmosphere with 5% CO_2, using 10 mL of collagenase II solution per gram of cartilage. Following

digestion, the resulting cell suspension was filtered through a 70 μm cell strainer and centrifuged at 300 × g for 5 minutes to collect the cell pellet. The pellet was washed twice with DMEM/F-12 containing 10% (v/v) FBS. The isolated cells were then gently resuspended in culture medium and seeded into tissue culture flasks at a density of 1×10^4 cells/cm². Cells were monitored regularly under a microscope, and the culture medium was replaced every three days. For histological analysis, human OA specimens were rinsed with DPBS and fixed in 4% (w/v) paraformaldehyde (PFA) at 4 °C for 72 hours. Samples were then transferred to 70% (v/v) ethanol for storage. Using a metal coring device (diameter = 1 cm), two cylindrical cartilage–subchondral bone specimens were obtained from symmetrical regions of the medial and lateral compartments of the tibia. The specimens were decalcified in 10% (w/v) EDTA solution for 8 weeks, followed by dehydration and paraffin embedding for subsequent preparation of paraffin sections.

AChE activity

Culture medium was removed from the plates, and cells were washed three times with ice-cold DPBS. Using 200 uL RIPA lysis buffer (Thermo Scientific, 89901) per well to collect the cells, then leave at 4℃ for 30 minutes. Cell lysates were used directly, and total protein concentration was determined and normalized using the Pierce™ BCA Protein Assay Kit (Thermo Scientific, 23225). AChE activity was measured using the Ache Assay Kit (Colorimetric) (ab138871), following the manufacturer's instructions. Absorbance was measured at 405 nm using a Microplate Reader LEDETECT 96.

Choline/Acetylcholine measurement

Acetylcholine (ACh) and choline quantification in serum were performed indirectly by fluorometric determination of total and free choline using a Choline/Acetylcholine Assay kit (Abcam, ab65345) according to the manufacturer's instructions. Transgenic mice or rat serum was diluted 1:5 with the assay buffer prior to measurement. An aliquot of the diluted serum was then assayed for total and free choline as specified by the kit protocol. ACh concentration was calculated from the difference between total and free choline signals and reported as nmol per mL of serum.

Real-time quantitative PCR assay

Total RNA of the cultured cells was extracted using the E.Z.N.A.® Total RNA Kit (Omega Bio-Tek) in accordance with the manufacturer's instructions. The isolated RNA was quantified and reverse-transcribed into cDNA using the PrimeScript™ First Strand cDNA Synthesis Kit (Takara Bio). Quantitative real-time PCR was performed with SYBR® Green qPCR Master Mix (MCE) and gene-specific primers on a QuantStudio™ 3 Real-Time PCR System (Applied Biosystems™). GAPDH expression served as the internal control for normalization of target gene expression levels.

Protein extraction and western blotting

Cells or powdered human OA cartilage were lysed in RIPA buffer for 30 minutes, followed by centrifugation at 12,000 × g for 5 minutes to collect the protein-containing supernatant. Protein samples were separated by SDS-PAGE and subsequently transferred onto PVDF membranes (Millipore, USA). Membranes were blocked with

5% (w/v) non-fat milk and incubated with a primary antibody against AChE (Abcam, ab97299), followed by incubation with a secondary goat anti-rabbit IgG H&L antibody (Invitrogen, A16110). Protein bands were visualized and imaged using a Bio-Rad imaging system.

Enzyme-linked immunosorbent assay (ELISA)

Whole cell lysates and powdered human OA cartilage lysates were prepared using RIPA lysis buffer. AChE concentrations were determined by ELISA using species-specific kits: Human AChE ELISA Kit (Abclonal, RK00797), Rat AChE ELISA Kit (Abclonal, RK03461), and Mouse AChE ELISA Kit (Abclonal, RK02564), following the manufacturer's instructions. TNF-α concentrations were measured using Human TNF-α ELISA Kit (Abclonal, RK00030), Rat TNF-α ELISA Kit (Abclonal, RK00029), and Mouse TNF-α ELISA Kit (Abclonal, RK04875).

Animal experiments

Transgenic mice were procured from Cyagen Biosciences and bred under animal licenses (23-198 in DH/HT&A/8/2/4 Pt.14 and 24-181 in DH/HT&A/8/2/4 Pt.19) issued by the Hong Kong Department of Health, with ethical approval (19-20/13-BME-R-GRF and 23-24/1015-BME-R-OTHERS) from the Animal Subjects Ethics Sub-committee of the Hong Kong Polytechnic University. Mice were maintained at 25 °C on a 12-hour light/12-hour dark cycle with ad libitum access to food and water. AChEflox/flox (AChE floxed) mice were crossed with AChEflox/flox; Osteocalcin-Cre or AChEflox/flox; Col2a1-Cre mice to generate AChEflox/flox; Osteocalcin-Cre

and AChEflox/flox; Col2a1-Cre conditional knockouts (AChE-cKO; AChE−/−) and AChEflox/flox controls, all on a C57BL/6N background. Osteoarthritis (OA) was induced in the right hind limb of 3-month-old male AChE-cKO and control mice by anterior cruciate ligament transection (ACLT) or collagenase type I-A–induced OA (CIOA). Mice were euthanized two months after ACLT or one month after CIOA. Cohorts and assessments for transgenic mice were as follows: OC-cKO-ACLT and Col2-cKO-CIOA were each conducted in two cohorts (first cohort n=3; second cohort n=5), while Col2-cKO-ACLT was conducted in a single cohort (n=8). Behavioral testing was performed only in the second cohorts of OC-cKO-ACLT (n=5) and Col2-cKO-CIOA (n=5), and in all mice in the Col2-cKO-ACLT group (n=8). Serum was collected from all OC-cKO-ACLT mice (total n=8) and all Col2-cKO-ACLT mice (n=8); in the Col2-cKO-CIOA cohorts, serum was collected only from the second cohort (n=5) and not from the first cohort (n=3). All joints were harvested and fixed in 4% (w/v) neutral buffered formalin for 24 hours in 4°C and then decalcified for tissue sectioning. Safranin-O/Fast Green and H&E staining (Abcam) were performed according to the manufacturer's instructions. Bone morphology and volume of all groups was analyzed and quantified by micro-CT scanning (SkyScan 1276).

Similarly, 5-month-old male Spontaneously Hypertensive Rats (SHR) were bred under animal license (21-303 in DH/HT&A/8/2/4 Pt.8) issued by the Hong Kong Department of Health, with ethical approval (18-19/21-BME-R-HMRF) from the Animal Subjects Ethics Sub-committee of the Hong Kong Polytechnic University. Rats

were housed in a controlled clean-room environment on a standard laboratory diet and were randomly assigned to two groups: donepezil (first batch n=3; second batch n=4) and control (first batch n=2; second batch n=4). All rats underwent ACLT surgery on the right hind limb at study initiation, with the left limb serving as a sham-operated control. Postoperatively, the control group received daily intraperitoneal saline injections, and the donepezil group received donepezil (3 mg/kg/day) for eight weeks. Serum sampling was performed in the second batch only (n=4). Longitudinal micro-CT scans were acquired at baseline, 1 month, and 2 months after surgery (donepezil, n=7; control, n=6). At the end of the treatment period, rats were euthanized and bone samples were collected for subsequent analysis.

Animal OA model: surgically induced OA

Surgically induced OA mouse models were generated via anterior cruciate ligament transection (ACLT) to create mechanical instability, following previously described standard protocols (Glasson et al., 2007). Briefly, after intraperitoneal anaesthesia with 2% (v/v) isoflurane, a longitudinal cutaneous incision was made over the hind limb. In the ACLT group, the anterior cruciate ligament (ACL) was transacted under direct visualization using a microsurgical hook, taking care to avoid injury to the posterior cruciate ligament (PCL). Complete transection was verified by the presence of a positive anterior drawer sign. In the sham-operated group, only the joint capsule was opened without ligament transection.

Animal OA model: collagenase induced OA

The collagenase-induced osteoarthritis (CIOA) mouse model was established via intra-articular injection of collagenase to induce acute inflammation in the knee joint. Mice were anesthetized with 2% (v/v) isoflurane, and 10 μL of collagenase type IA solution (prepared in phosphate-buffered saline, PBS; pH 7.4) was injected through the patellar ligament into the right knee joint. The left knee served as control and received an intra-articular injection of 10 μL PBS under identical conditions.

Animal behavioural tests: von Frey and Rotarod test

Behavioral tests were carried out in the second cohort (n=5) of OC-cKO-ACLT and Col2-cKO-CIOA, and in all Col2-cKO-ACLT mice (n=8). Nociceptive tolerance in OC-Cre; AChEflox/flox and Col2-Cre; AChEflox/flox mice subjected to ACLT was assessed using an electronic von Frey apparatus (Ugo Basile) with a force range of 1–1000 g (resolution: 0.1 g). For Col2-Cre; AChEflox/flox mice subjected to collagenase-induced osteoarthritis (CIOA), nociceptive tolerance was measured using a manual von Frey filament set comprising 20 monofilaments. All measurements were performed according to a previously described simplified up–down method (Bonin et al., 2014). Animals were acclimated to the testing procedure for 7 days prior to formal assessment. Briefly, each mouse was placed on an elevated mesh grid and allowed to habituate for at least 20 minutes, or until spontaneous activity was reduced. Testing was conducted within a box to reduce stress. For the electronic von Frey assay, the probe was applied to the mid-plantar surface of the hind paw, and withdrawal thresholds were

recorded. Three measurements were taken for each paw, and the mean value was calculated. For the manual von Frey test, the 2.0 g filament was used as the start and applied to the mid-plantar surface. Upon receiving a positive paw-withdrawal response, testing was continued with progressively higher-force filaments for four additional trials. The force corresponding to the withdrawal threshold was recorded, and von Frey testing was conducted at baseline and 2 months post-ACLT, or 1 month post-CIOA induction. Changes in nociceptive tolerance were evaluated by comparing withdrawal thresholds between the sham operated and surgically treated limbs.

Motor coordination was evaluated using the rotarod test (Panlab, Harvard Apparatus). Mice were placed on rotating lanes (5 cm in diameter) and allowed to walk at a constant speed of 4 rpm for 1 minutes to acclimate. The rotation speed then accelerated from 4 to 40 rpm in 5 minutes. For each trial, the latency to fall (seconds) was recorded three times and average were taken. Assessments were conducted at baseline, 2 months post-ACLT, and 1 month post-CIOA induction to evaluate motor coordination.

Figure 3-2 Schematic of Research of Interests (ROI) in micro-CT analysis. Medial compartment of the subchondral bone was analysis as it is more closely related to the OA development (red shaded area).

Micro-computed tomography (micro-CT)

The micro-CT system (SkyScan1276, Bruker, Kontich, Belgium) was used for longitudinal monitoring of rat bone mass and microarchitecture at weeks 0, 4, and 8, and for the analysis of transgenic mice bone mass and microarchitecture. Rat and mice bone samples were fixed in 4% (w/v) paraformaldehyde for 48 hours, then transferred to 70% (v/v) ethanol for 24 hours. Specimens were scanned at a resolution of 6.0 μm (mice) and 18.0 μm (rats) per pixel, using 90 kV voltage and 200 μA current, with an Al + Cu filter. Phantoms with standard densities of 0.25 and 0.75 g/cm³ were used to calibrate bone mineral density (BMD). Three-dimensional reconstruction and analysis were performed using NRecon and CTAn 360 software (SkyScan). In the coronal plane, the medial compartment of the tibia was selected as the region of interest (ROI). The ROI was manually delineated using CTAn software (Skyscan). Quantitative analysis was conducted on the subchondral bone within the weight-bearing area of the medial compartment, assessing key parameters including bone volume fraction (BV/TV), trabecular number (Tb.N), trabecular thickness (Tb.Th), and trabecular separation (Tb.Sp). Three-dimensional reconstructions of the medial tibial subchondral bone were generated using CTvol software (Skyscan) with 21 slices of imaging files from each sample.

Multiplex immunofluorescence

After dewaxing, antigen retrieval (Proteinase K, 0.01 mg/mL at room temperature) and blocking were performed. Each primary antibody was incubated overnight at 4°C,

including anti-AChE (Abcam, ab2803, ab183591, ab97299), and anti-α7nAChR (Abcam, ab216485). Secondary antibodies and fluorophores were used according to manufacturer's instruction, included Goat anti-Mouse IgG (H+L) Cross-Adsorbed Secondary Antibody, Alexa Fluor 594 (Invitrogen), Goat anti-Rabbit IgG (H+L) Cross-Adsorbed Secondary Antibody, Alexa Fluor™ 488 (Invitrogen), and SlowFade Glass Soft-set Antifade Mountant with DAPI (Invitrogen). Staining was visualized and imaged using a Leica TCS SPE Confocal Microscope.

Cell culture: MSC pellets

Human MSC pellet cultures were established according to published protocols with minor modifications (Ziadlou et al., 2019). Cells were cultured in standard DMEM/F12 supplemented with 10% (v/v) fetal bovine serum, 10 ng/mL TGF-β1, and 1% (v/v) penicillin/streptomycin. Human mesenchymal stem cells were resuspended in complete medium. Aliquots of 1.5×10^5 cells in 150 µL were centrifuged at 400 g for 5 minutes in v-bottom non-adherent 96-well plates. Pellets were then cultured for two weeks in a humidified incubator (37°C, 5% v/v CO_2), with medium changes twice weekly.

Cell viability

The cell proliferation assay was performed using a Cell Proliferation Kit with MTT (Roche, Switzerland). Cell suspensions (100 µL, 1×10^4 cells per well) were dispensed into 96-well plates and incubated for 24 hours. The medium was then replaced with fresh media containing varying concentrations of donepezil, galantamine, or A10E, followed by an additional 24-hour incubation. Subsequently, 10 µL of MTT solution

was added to each well and incubated for 4 hours. Absorbance was measured at 570 nm using a Microplate Reader LEDETECT 96.

Histochemistry staining

After euthanasia, bone tissue was collected and immediately immersed in 4% (w/v) PFA for overnight fixation. Samples were decalcified in 10% (w/v) EDTA solution for two weeks. Following decalcification, samples were gradually dehydrated through increasing concentrations of ethanol 70% to 100% (v/v) and embedded in paraffin. Paraffin-embedded samples were sectioned at 5 μm thickness using a microtome (Leica). Sections were deparaffinized and rehydrated for standard H&E and Safranin O staining, as well as specialized procedures including multiplex immunofluorescence staining (TSA-dendron-fluorophores NEON), and Masson Trichrome staining (Abcam, ab150686).

Immunohistochemistry

After dewaxing, antigen retrieval (Proteinase K, 0.01 mg/mL at room temperature) was carried out. Endogenous peroxidase activity of the sample was quenched with 3% (v/v) hydrogen peroxide in dPBS for 10 minutes. Then, tissues sections were blocked with 10% (v/v) normal horse or goat serum for 1 hour, and incubated with primary antibodies overnight at 4°C. Primary antibodies included: anti-AChE (1:400, Abcam, ab97299), anti-NFkB p105/p50 (1:200; Abcam, ab32360), anti-TNF-α (1:200; Abcam, ab34674) and anti-α7nAChR (1:200; Abcam, ab216485). Vectastain ABC kit and DAB substrate kit (Vector Labs, USA) for peroxidase were used in DAB staining, followed by

counterstaining with Harris Hematoxylin. Negative controls were processed identically, without incubating the primary antibody. Images were acquired using a Nikon microscope.

Histological Analysis of Murine Knee Joints

Histological analysis of murine knee joints was performed according to OARSI cartilage scoring system and arbitrary synovial scoring system. Synovial lining thickness was scored on H&E-stained sections using an arbitrary scoring system ranging from 0–3 (0 being no infiltration and 3 being the highest level of infiltration) (four positions per knee joint). The score of articular cartilage degradation was evaluated based on the OARSI score system (Pritzker et al., 2006), in which the grade (severity of OA scored 1–6) is multiplied by the stage (stage of involvement scored 1–4), resulting in a score of 0–24 (three sections per knee joint). Masson's trichrome-stained sections (two sections per knee joint) to criteria samples for features of new generated osteoid in the subchondral bone area.

Patch clamp

Prior to patch-clamp experiments, C28/I2 chondrocyte cells were seeded onto 10-mm round cell-adhesive membranes and incubated at 37°C for 24 hours. Electrophysiological recordings were conducted using an Axopatch 700B amplifier connected to a Digidata 1550B interface, with data acquisition and analysis performed using pCLAMP 10 software (Molecular Devices, San Jose, CA). Glass pipettes were pulled to a resistance of 3–8 MΩ and filled with an internal solution containing 120

mM potassium gluconate, 12 mM KCl, 1 mM $MgCl_2$, 5 mM EGTA, 0.5 mM $CaCl_2$, and 10 mM HEPES, adjusted to pH 7.4. Voltage steps were applied, ranging from -100 mV to +60 mV. Spike trains were digitally recorded at a sampling rate of 10 kHz using Axoscope software (Molecular Devices), and subsequently analyzed and sorted with Offline Sorter (Plexon, Dallas, TX) and NeuroExplorer (Nex Technologies, Littleton, MA, USA) software.

Ion channel imaging

C28/I2 chondrocyte cells were seeded in 25-mm glass-bottom dishes and grown at 37 °C for overnight. Prior to ion channel imaging, culture medium was removed, and cells were washed three times with DPBS. Then DPBS was replaced with calcium-containing HEPES-buffered salt solution (HBSS), and cells were incubated with Calbryte 520 AM (4 μM) for 30 minutes at 37°C. After incubation, cells were washed three times with DPBS, replaced with HBSS, and incubated for an additional 30 minutes prior to imaging. Ion channel signaling was assessed using the Nikon Eclipse Ti2-E Live-cell Fluorescence Imaging System at 37°C and 5% (v/v) CO_2.

Statistical analysis

Statistical analyses were performed using GraphPad Prism 9.0. All statistical results were presented as mean + standard error of the mean (SEM). The normality tests were conducted where appropriate, and all tested data confirmed to Kolmogorov–Smirnov normal distribution. The significance of difference was determined by one-way ANOVA and Student's t-test. A significant difference was indicated when $P<0.05$.

Chapter 4 Results

4.1 The involvement of cholinergic system in OA pathogenesis

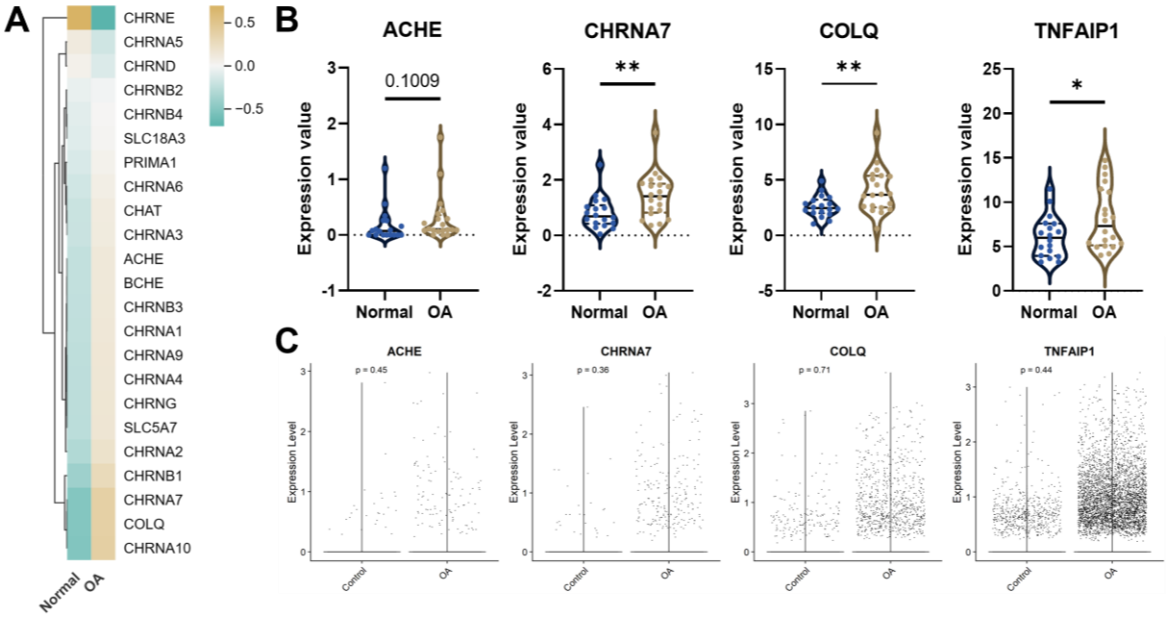

Figure 4-1 Analysis of publicly available RNA sequencing datasets. A. Heatmap showing the expression profiles of selected cholinergic signaling-related genes in bulk RNA-seq dataset (GSE114007). **B.** Individual expression plots of selected genes in bulk RNA-seq dataset (GSE114007). **C.** Individual expression plots of selected genes in single-cell RNA-seq dataset (GSE255460). Unpaired two-tailed Student's t-test were performed. * $p<0.05$; ** $p<0.005$; *** $p<0.001$; **** $p<0.0001$.

To explore the potential role of cholinergic signaling in osteoarthritis (OA) pathogenesis and to test our research hypothesis, we first performed a comparative transcriptomic analysis of human articular cartilage samples from OA and non-OA donors using two publicly available RNA sequencing datasets (GSE114007 and GSE255460). In GSE114007, differential expression analysis revealed a significant upregulation of CHRNA7 (encoding the α7 nicotinic acetylcholine receptor, α7nAChR) and CHRNA10 (encoding the α10nAChR subunit), along with a downregulation of CHRNE (encoding the ε subunit of nAChR) in OA cartilage (Figure 4-1A and 4-1B).

These alterations suggest the involvement of cholinergic signaling in OA pathogenesis. In parallel, several genes involved in acetylcholine metabolism exhibited altered expression, including COLQ (encoding the collagen like tail subunit of asymmetric acetylcholinesterase) and AChE itself, which showed a numerical but statistically non-significant increase in OA cartilage compared with controls ($p = 0.1009$) (Figure 4-1, A-B). BChE expression remained unchanged. Importantly, genes related to inflammatory signaling, such as TNFAIP1 and MMP-13 were upregulated (Figure 4-1B). These findings suggest the involvement of inflammatory cytokines in inflamed chondrocytes and OA. Single-cell RNA-seq analysis from dataset GSE255460 further supported these observations, showing similar upward trends in cholinergic signaling components and inflammatory mediators in OA compared to normal controls (Figure 4-1C). Collectively, these transcriptomic changes indicate a coordinated dysregulation of cholinergic homeostasis and inflammation in OA pathophysiology.

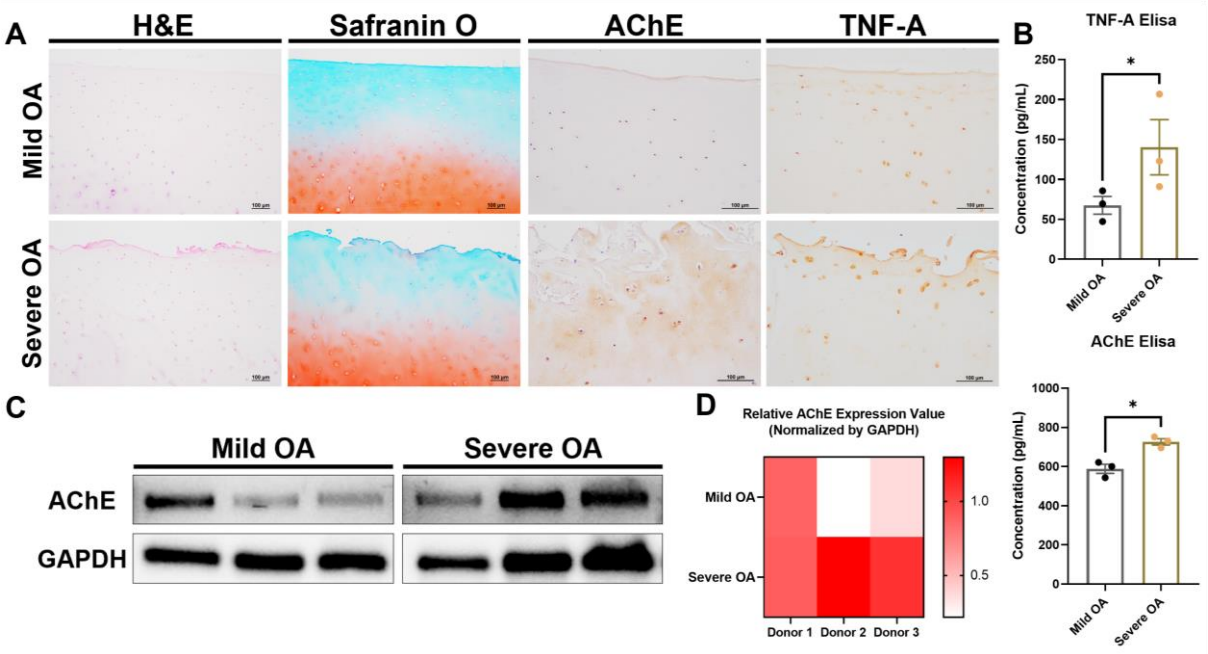

Figure 4-2 Characterization of clinical human OA specimens. A. Representative histochemical staining image of human osteoarthritic tibial plateau specimens. Scale bars = 100 μm. **B.** ELISA quantification of TNF-A and AChE protein levels in lysates from human OA chondrocytes (n=3). **C.** Western blot analysis of AChE concentration in human OA chondrocyte lysates from three different human donors. **D.** Heatmap showing the relative AChE expression value of western blot image, normalized by GAPDH (n=3). All data are expressed as means ± SEM. Paired two-tailed Student's t-test were performed. * $p<0.05$.

Characterization of clinical human OA specimens

To validate the bioinformatic predictions in a clinical context, we examined articular cartilage specimens collected from patients undergoing total knee arthroplasty (TKA). Samples from the medial compartment (severe OA) and the lateral compartment (mild OA) of the same joint were analyzed using Western blotting, ELISA, and immunohistochemistry (Figure 4-2, A-D). Medial compartment cartilage with severe OA exhibited higher expression of AChE and TNF-α compared with mild OA samples, mirroring the severity of histological cartilage degeneration. This directionality of change aligns with our transcriptomic data and supports an association between

cholinergic dysregulation and OA progression.

4.2 Genetical knockdown of Acetylcholinesterase

To elucidate the functional role of AChE in chondrocyte homeostasis and OA, we employed an in vitro model using the C28/I2 chondrocyte cell line. Cells were pre-seeded 24 hours prior to experimentation and subsequently exposed to 10 ng/mL interleukin-1β (IL-1β) for 24 hours, effectively simulating OA-like inflammatory conditions (Figure 4-3A). The induction of inflammation was confirmed by PCR analysis, which demonstrated robust upregulation of inflammatory markers (Figure 4-3D).

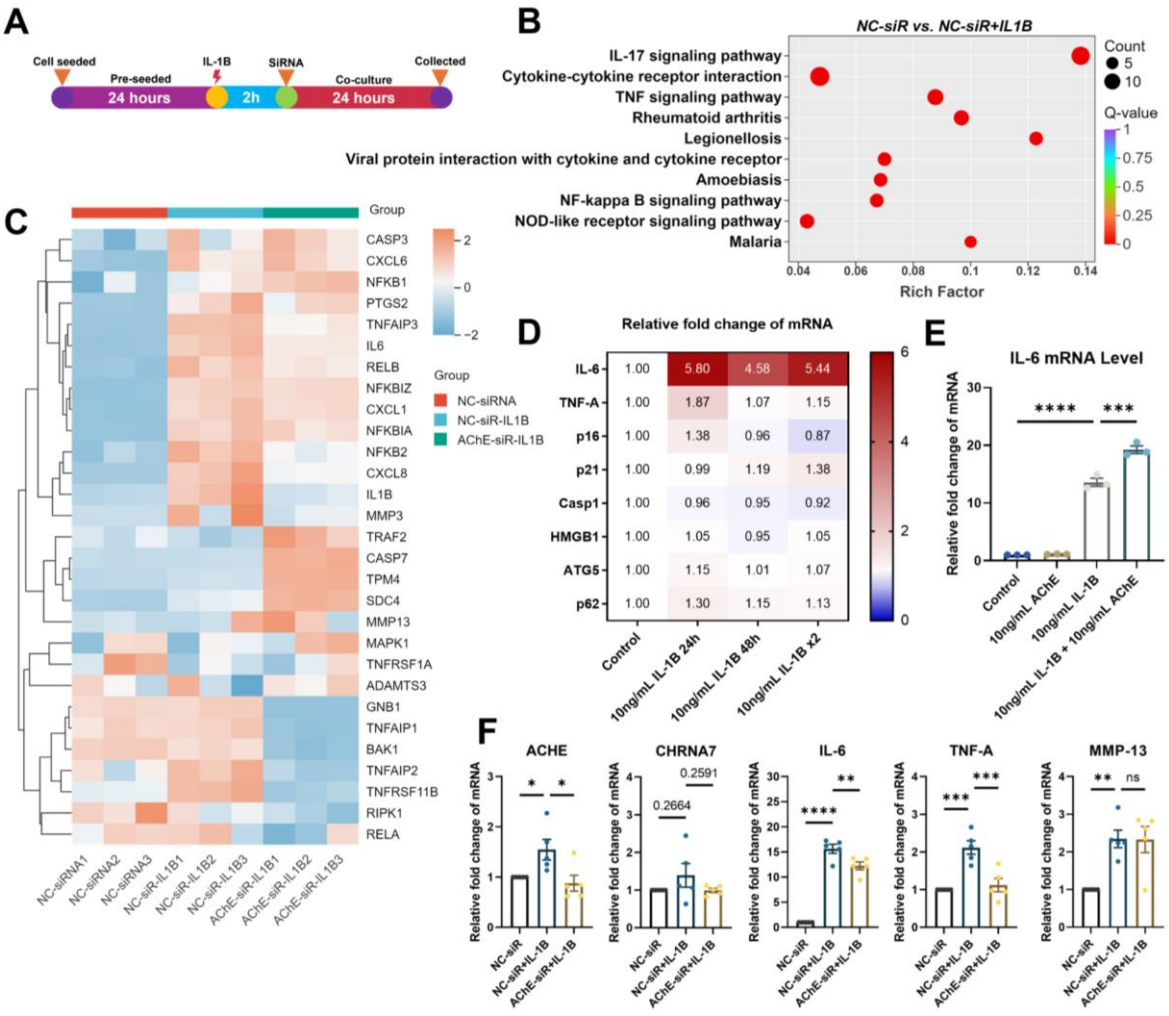

Figure 4-3 The anti-inflammation and chondral protective effects of knockdown in vitro. A. Schematic diagram of the *in vitro* experiments. **B.** KEGG pathway analysis of the inflammatory cell culture model. **C.** Heatmap showing the expression of selected inflammatory genes in bulk RNA-sequencing data. **D.** Characterization of interleukin-1β (IL-1β) stimulation in vitro. **E**. AChE enhances interleukin-6 (IL-6) expression in the presence of IL-1β. **F.** PCR validation of the anti-inflammatory effects following siRNA-mediated AChE knockdown. One-way ANOVA with Post-hoc tests were performed. * $p<0.05$; ** $p<0.005$; *** $p<0.001$; **** $p<0.0001$.

Comprehensive RNA sequencing revealed significant elevation of inflammation signaling pathways such as IL-17, TNF and NF-kappa B signaling, and upregulation inflammation-related genes, including TNFAIP2, IL-1B, IL-6, and NFKB2, further validating the activation of inflammatory signaling pathways (Figure 4-3B-C). Notably, siRNA-mediated knockdown of AChE resulted in a marked reduction in the expression

of these pro-inflammatory cytokines (Figure 4-3C). Quantitative PCR analyses corroborated these findings, showing that AChE knockdown significantly attenuated the IL-1β induced upregulation of TNF-α and IL-6 (Figure 4-3F), in agreement with the transcriptomic data. Moreover, co-culture experiments revealed that the presence of AChE exacerbated IL-6 expression in the context of IL-1β stimulation, underscoring the pro-inflammatory role of AChE in chondrocytes. Collectively, these results indicate that suppression of AChE dampens inflammatory signaling and contributes to the preservation of cartilage matrix homeostasis under conditions of inflammatory stress.

The anti-inflammation and chondral protective effects of knockdown *in vivo*: osteoblast-specific AChE knock out mice with posttraumatic OA

To further validate the anti-inflammatory and chondroprotective effects of AChE knockdown observed in vitro, we extended our investigation to in vivo models by generating conditional knockout (cKO) mice with tissue-specific deletion of AChE in osteoblasts (Osteocalcin-Cre; $AChE^{flox/flox}$) and chondrocytes (Col2a1-Cre; $AChE^{flox/flox}$). OA was surgically induced in these mice via anterior cruciate ligament transection (ACLT), a well-established model for post-traumatic OA. In the osteoblast-specific AChE knockout cohort, mice were sacrificed two months post-OA induction for comprehensive analysis. Importantly, conditional deletion of AChE did not adversely affect the overall growth or development of the mice, as evidenced by normal body size and weight (Figure 4-4A). The efficiency of AChE knockout was confirmed by immunohistochemical staining, which demonstrated a dramatic reduction in AChE protein levels in joint (Figure 4-12).

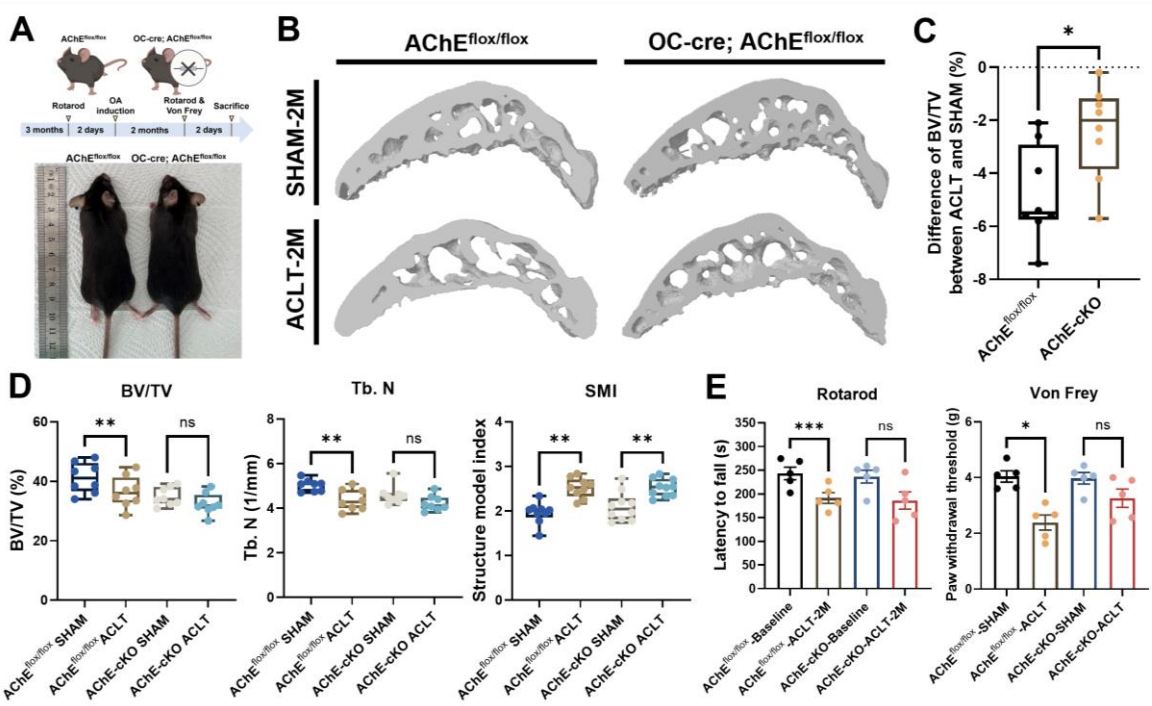

Figure 4-4 Osteoblast-specific AChE knockout mice in posttraumatic OA – bone volume analysis and behavioral tests. A. Schematic diagram of animal experiments and the body size of animals. **B.** Representative micro-CT images of medial subchondral bone. **C.** Quantitative analysis of BV/TV differences between ACLT and SHAM legs in each group (n=8). **D.** Quantitative analysis of BV/TV, Tb. N and structure model index in each group (n=8). **E.** Behavioral assessments of animals using the Rotarod and von Frey tests (n=8). All data are expressed as means ± SEM. One-way ANOVA with Post-hoc tests or unpaired two-tailed Student's t-test were performed. * $p<0.05$; ** $p<0.005$; *** $p<0.001$; **** $p<0.0001$.

Micro-computed tomography (micro-CT) analysis further showed that subchondral bone loss in the medial compartment was markedly attenuated in cKO mice (Figure 4-4B-D), suggesting a protective effect against OA-associated bone degeneration. Functional assessments of joint health and pain sensitivity were performed using the Rotarod and von Frey tests (Figure 4-4E). $AChE^{flox/flox}$ control mice exhibited a decline in mobility following OA induction, as measured by decreased latency to fall in the Rotarod test (Figure 4-4E). In the von Frey test, flox/flox control mice displayed significantly heightened pain sensitivity, whereas cKO mice maintained a higher pain

threshold, indicative of improved pain tolerance and reduced OA-associated discomfort (Figure 4-4E). Histological examination of joint tissues revealed significant preservation of cartilage and synovial integrity in cKO mice compared to flox/flox controls, as indicated by lower OARSI scores and synovial lining thickness (Figure 4-5A). These findings strongly support the anti-inflammatory and chondroprotective effects of AChE knockdown *in vivo*. Interestingly, analysis of serum levels revealed an increasing trend of ACh level in serum (not statistically significant, $p = 0.1860$) between cKO and control mice, suggesting that conditional AChE knockout in peripheral may alter the cholinergic signaling (Figure 4-5C). This also highlights the importance of tissue-specific modulation of cholinergic signaling in the context of OA. These results demonstrate that AChE/α7nAChR signaling within osteoblasts plays a critical role in the pathogenesis of OA, likely through the regulation of bone-cartilage crosstalk and local inflammatory responses.

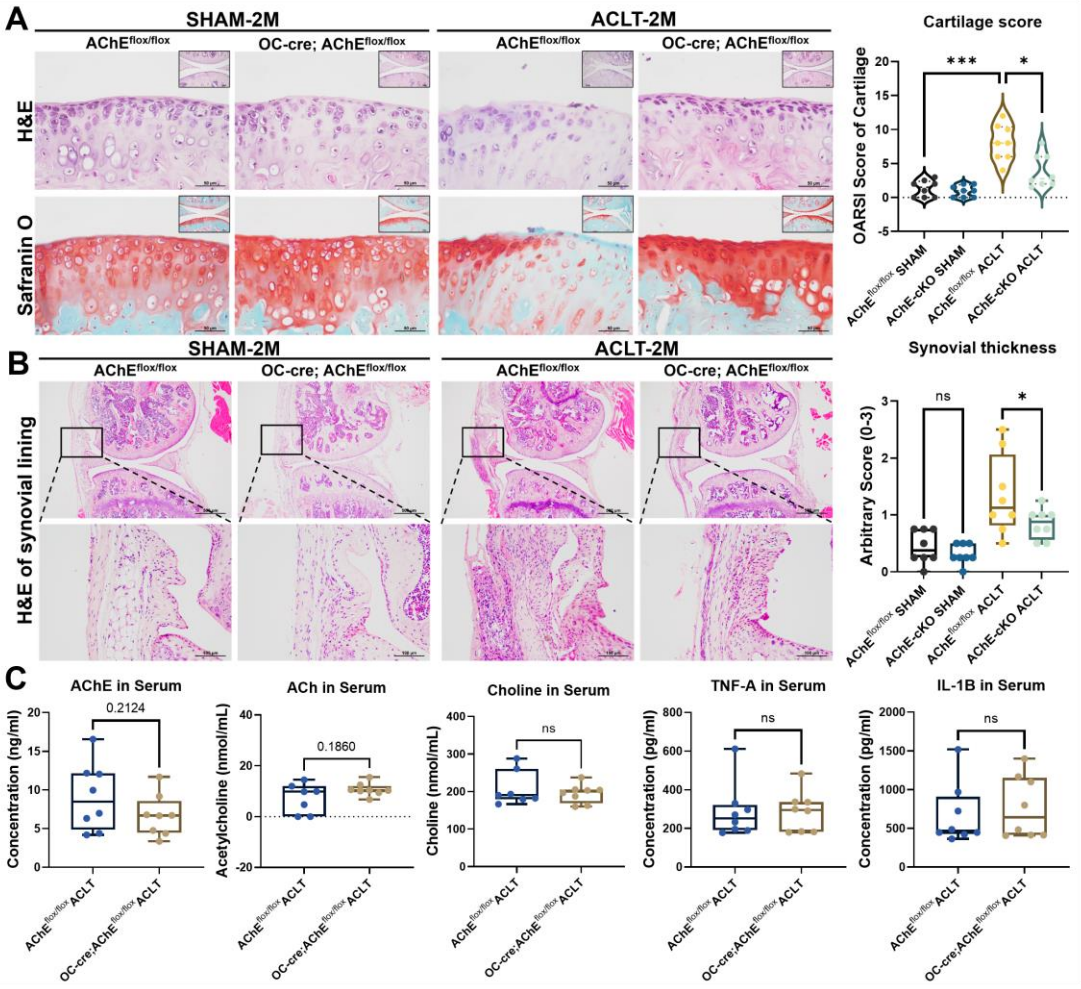

Figure 4-5 Osteochondral-specific AChE knockout mice in posttraumatic OA – histological staining and analysis of cartilage and synovium. A. Representative histological images of tibial articular cartilage with OARSI scoring in joint morphology and cartilage integrity (n=8). Scale bars = 50 μm. **B.** Representative images and quantitative analysis of synovial lining thickness using an arbitrary scoring system ranging from 0-3 (n=8). Scale bars = 100 μm & 500 μm. **C.** Serum AChE, ACh, choline, TNF-α, and IL-1β were measured at the end point. All data are expressed as means ± SEM. One-way ANOVA with Post-hoc tests or unpaired two-tailed Student's t-test were performed. * $p<0.05$; ** $p<0.005$.

The anti-inflammation and chondral protective effects of knockdown *in vivo*: chondrocyte-specific AChE knock out mice with posttraumatic OA

In parallel with our findings in osteoblast-specific knockout models, we investigated the effects of conditional deletion of AChE specifically in chondrocytes (Col2a1-Cre; $AChE^{flox/flox}$) to further delineate the tissues-specific contributions of AChE to OA

pathogenesis. Notably, chondrocyte-specific AChE knockout did not negatively impact the overall growth or general health of the mice, as evidenced by normal body size and weight throughout the experimental period (Figure 4-6A). Micro-CT assessments corroborated findings in the last chapter, showing that subchondral bone volume was better preserved in the cKO mice compared to controls (Figure 4-6B-D). This suggests that AChE deletion in chondrocytes not only protects cartilage but also mitigates OA-associated subchondral bone loss.

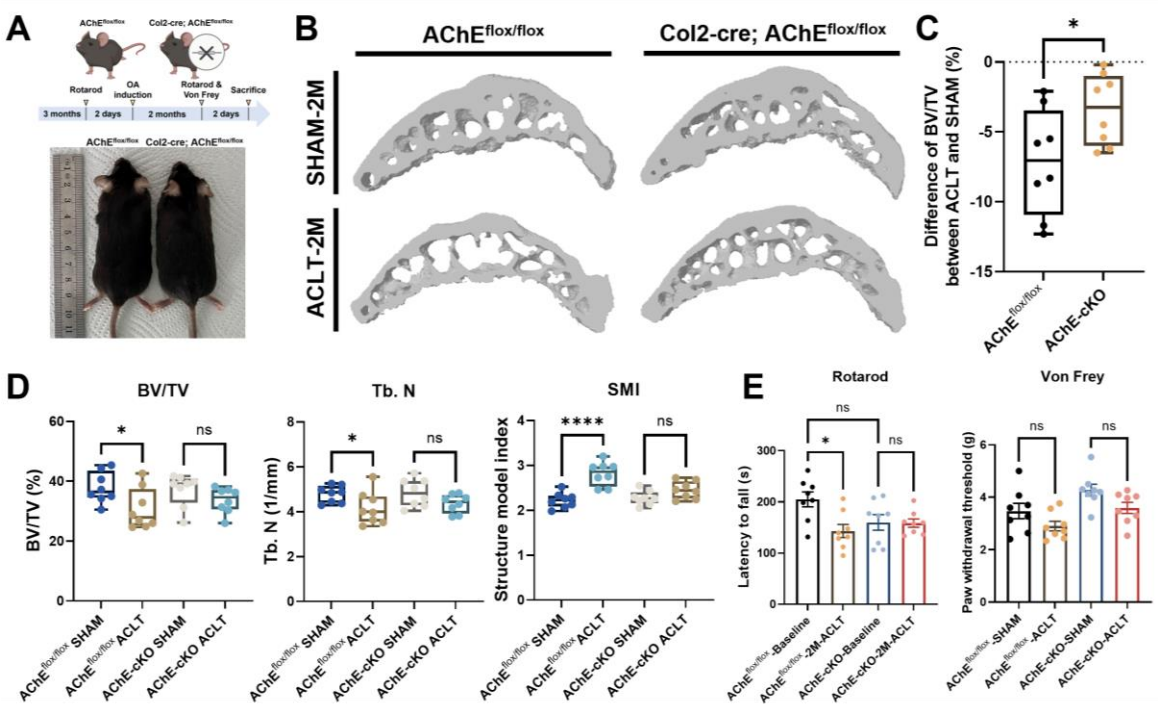

Figure 4-6 Chondrocyte-specific AChE knockout mice in posttraumatic OA – bone volume analysis and behavioral tests. A. Schematic diagram of animal experiments and the body size of animals. **B.** Representative micro-CT images of medial subchondral bone. **C.** Quantitative analysis of BV/TV differences between ACLT and SHAM legs in each group (n=8). **D.** Quantitative analysis of BV/TV, Tb. N and structure model index in each group (n=8). **E.** Behavioral assessments of animals using the Rotarod and von Frey tests (n=8). All data are expressed as means ± SEM. One-way ANOVA with Post-hoc tests or unpaired two-tailed Student's t-test were performed. * $p<0.05$; ** $p<0.005$; *** $p<0.001$; **** $p<0.0001$.

Consistent with what we observed in osteochondral AChE deletion model, analysis of serum levels revealed an increase of ACh level in serum (marginally significant, p = 0.0715) between cKO and control mice, suggesting the activation of cholinergic signaling (Figure 4-7C). Behavioral analyses provided additional functional insights. While both groups underwent OA induction, chondrocyte-specific cKO mice maintained stable locomotor activity, as measured by the Rotarod test, whereas flox/flox controls exhibited a significant decline in mobility (Figure 4-6E). Interestingly, pain sensitivity, as assessed by the von Frey test, did not differ significantly between the two groups, indicating that the primary benefit of chondrocyte-specific AChE knockout may lie in the preservation of joint function rather than direct modulation of pain perception.

Upon induction of posttraumatic OA via ACLT, chondrocyte-specific AChE knockout mice exhibited remarkable resistance to cartilage degeneration and synovial inflammation compared to their flox/flox littermate controls (Figure 4-7A-B). Underscoring the broad anti-inflammatory effects of AChE inhibition within the joint microenvironment. These results highlight the protective role of AChE deletion in chondrocytes under posttraumatic OA conditions. The data support the notion that targeted inhibition of AChE in chondrocytes confers significant anti-inflammatory and chondroprotective effects, preserving both cartilage and subchondral bone integrity and maintaining joint function following injury.

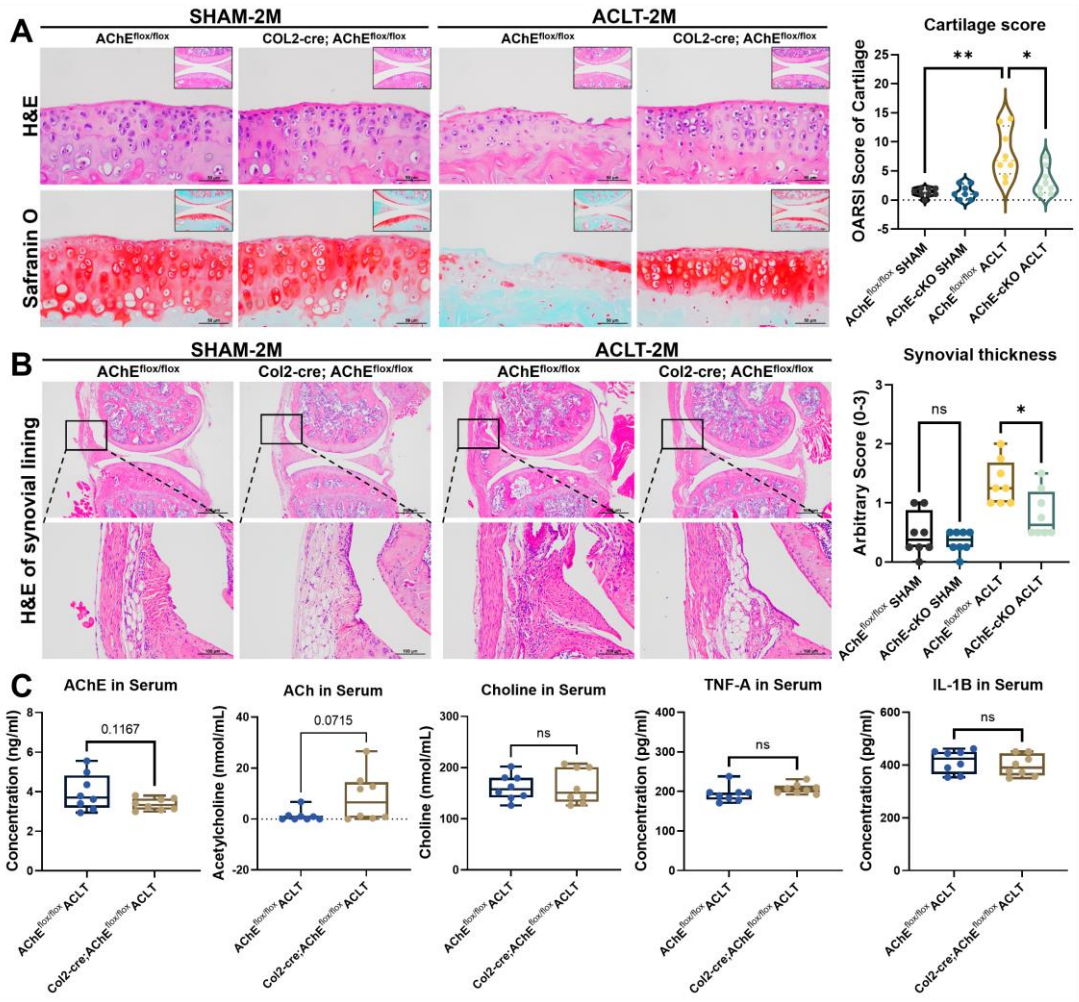

Figure 4-7 Chondrocyte-specific AChE knockout mice in posttraumatic OA – histological staining and analysis of cartilage and synovium. A. Representative histological images of tibial articular cartilage with OARSI scoring in joint morphology and cartilage integrity (n=8). Scale bars = 50 μm. **B.** Representative images and quantitative analysis of synovial lining thickness using an arbitrary scoring system ranging from 0-3 (n=8). Scale bars = 100 μm & 500 μm. **C.** Serum AChE, ACh, choline, TNF-α, and IL-1β were measured at the end point. All data are expressed as means ± SEM. One-way ANOVA with Post-hoc tests or unpaired two-tailed Student's t-test were performed. * $p<0.05$; ** $p<0.005$.

The anti-inflammation and chondral protective effects of knockdown *in vivo*: chondrocyte-specific AChE knock out mice with collagenase-induced OA

To further investigate the role of AChE in inflammatory OA, we employed a collagenase-induced OA (CIOA) model by administering intra-articular injections of collagenase type 1a in chondrocyte-specific AChE knockout mice (Figure 4-8A). This

model is widely recognized for mimicking the inflammatory features of OA. Micro-CT analysis revealed the deletion of AChE mitigated bone loss in cKO mice (Figure 4-8B-D). Specifically, there is no significant differences in bone volume fraction (BV/TV) and trabecular number (Tb.N) between the ACLT-operated leg and the SHAM leg in cKO groups, but dramatically decreased in the control group (Figure 4-8B-D), suggesting that AChE deletion in chondrocytes may confer some degree of protection against subchondral bone deterioration in the context of inflammatory OA. After CIOA induction, Rotarod performance did not differ significantly between cKO and flox/flox mice, whereas the pain threshold was modestly improved in the cKO group (Figure 4-8E).

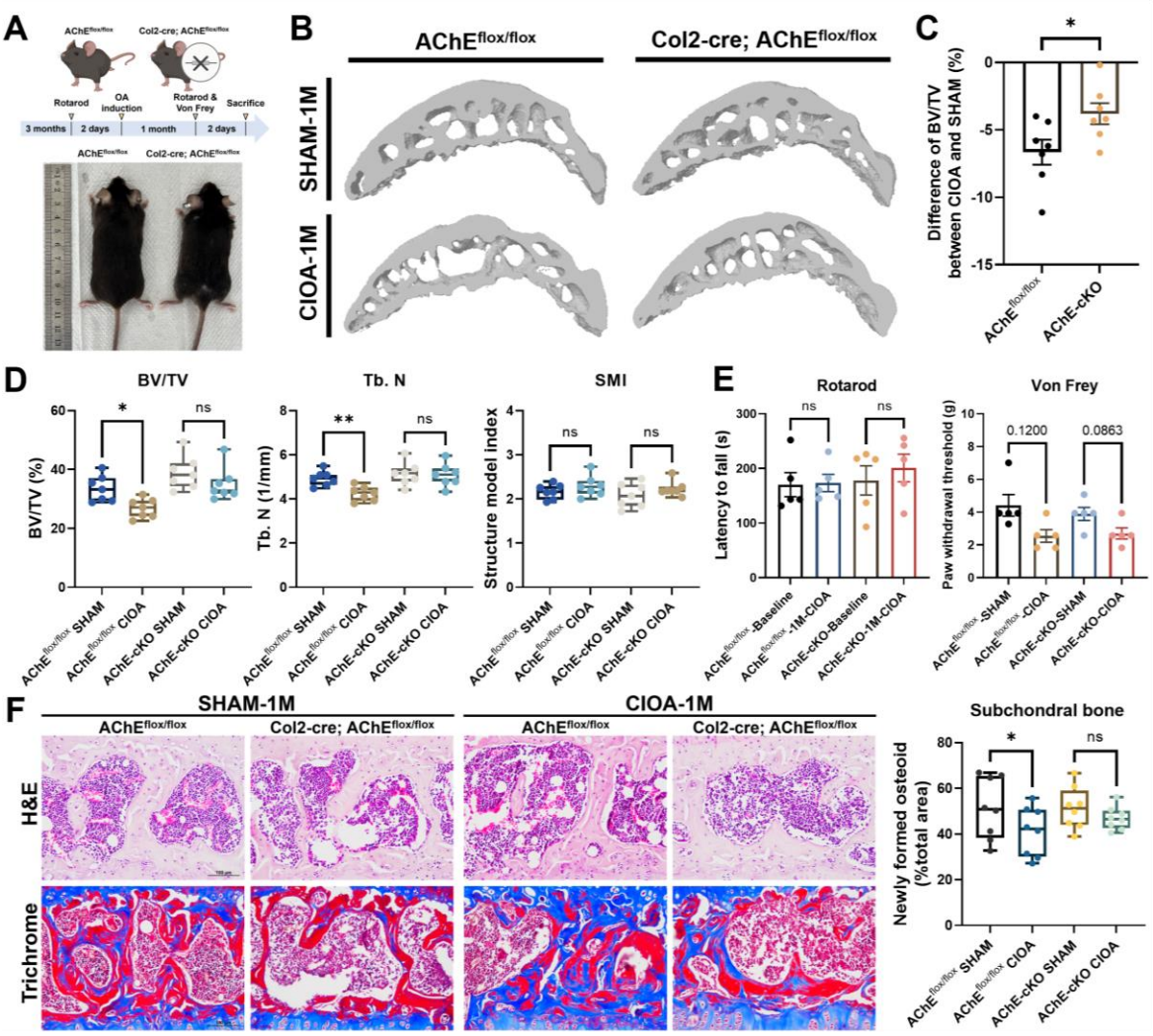

Figure 4-8 Chondrocyte-specific AChE knockout mice in inflammatory OA. A. Schematic diagram of animal experiments and the body size of animals. **B.** Representative micro-CT images of medial subchondral bone. **C.** Quantitative analysis of BV/TV differences between ACLT and SHAM legs in each group (n=8). **D.** Quantitative analysis of BV/TV, Tb. N and structure model index in each group (n=8). **E.** Behavioral assessments of animals using the Rotarod and von Frey tests (n=8). **F.** Representative histological images of subchondral bone and quantitative analysis of newly formed osteoid (n=8). Scale bars = 100 μm. All data are expressed as means ± SEM. One-way ANOVA with Post-hoc tests or unpaired two-tailed Student's t-test were performed. * $p<0.05$; ** $p<0.005$.

Relative to sham-operated controls, CIOA mice showed the expected increase in cartilage degeneration and synovial inflammation (Figure 4-7A–B). However, no statistically significant differences in these histopathological measures were detected

between flox/flox controls and cKO mice, this likely reflects model specific features and differences.

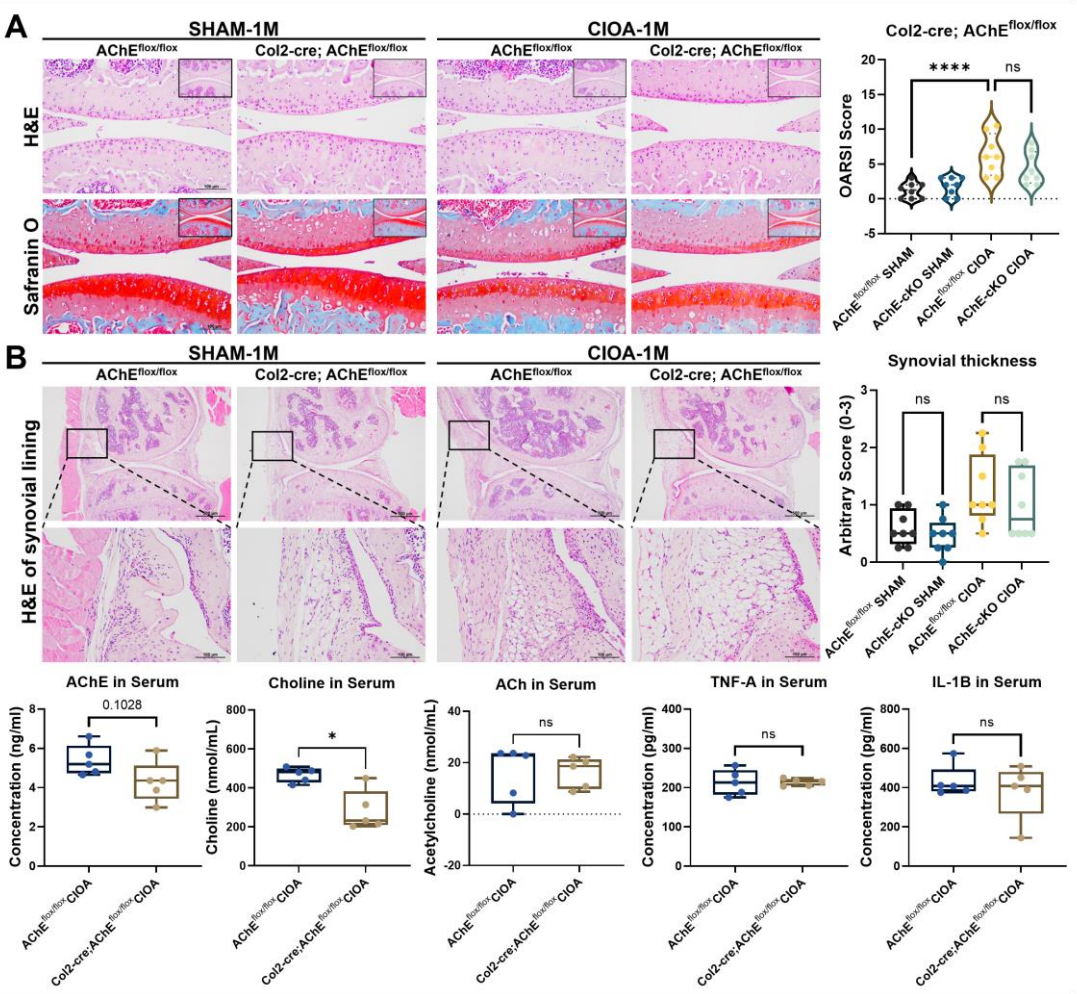

Figure 4-9 Histological staining of chondrocyte-specific AChE knockout mice in inflammatory. A. Representative histological images of tibial articular cartilage with OARSI scoring in joint morphology and cartilage integrity (n=8). Scale bars = 50 μm. **B.** Representative images and quantitative analysis of synovial lining thickness using an arbitrary scoring system ranging from 0-3 (n=8). Scale bars = 100 μm & 500 μm. All data are expressed as means ± SEM. One-way ANOVA with Post-hoc tests or unpaired two-tailed Student's t-test were performed. **** $p<0.0001$.

Overall, these results suggest that targeted inhibition of AChE in chondrocytes may also offer certain protective effects against bone loss and inflammation in inflammatory OA models. Larger studies are warranted to confirm these trends and further elucidate the

therapeutic potential of AChE modulation in diverse OA contexts.

4.3 Pharmaceutical inhibition of Acetylcholinesterase

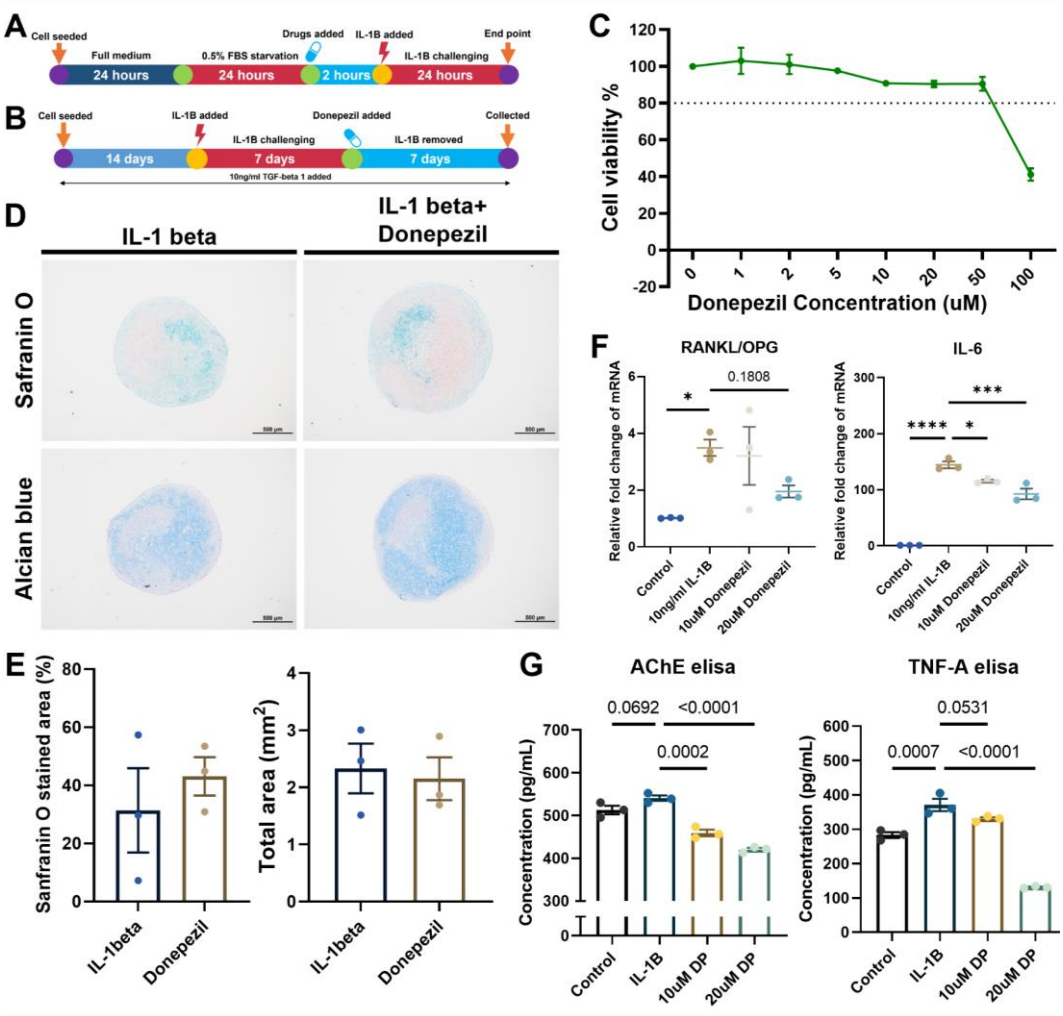

Figure 4-10 The anti-inflammation and chondral protective effects of donepezil *in vitro*. A. Schematic diagram of the experimental design for C28/I2 cell culture assays. **B.** Schematic diagram of the MSC-derived chondrocytic cell pellet model experiments. **C.** Cell viability analysis under increasing concentrations of donepezil. **D.** Representative histological images of chondrocytic cell pellets. Scale bars = 500 μm. **E.** Quantitative analysis of cell pellet morphology and size. **F.** Transcriptional expression levels of inflammatory cytokines. **G.** Protein levels of AChE and TNF-α. All data are expressed as means ± SEM. One-way ANOVA with Post-hoc tests or unpaired two-tailed Student's t-test were performed. * $p<0.05$; ** $p<0.005$; *** $p<0.001$; **** $p<0.0001$.

Building on our genetic studies, we explored the therapeutic potential of pharmacological AChE inhibition using donepezil, an FDA approved AChE inhibitor

for clinical use. In primary human OA chondrocyte cultures, treatment with donepezil significantly reduced the production of inflammatory cytokine IL-6 in mRNA and TNF-α in protein level in response to IL-1β stimulation (Figure 4-10A, F & G). Additionally, donepezil treatment did not affect the MSC pellet formation indicating AChE inhibition did not inhibit chondrogenesis (Figure 4-10B & E).

To further evaluate the therapeutic potential of AChE inhibition beyond tissue-specific genetic knockout, we investigated the systemic effects of pharmacological AChE inhibition using donepezil in a spontaneous hypertensive rat model of OA. Rats subjected to ACLT-induced OA received intraperitoneal injections of donepezil at a dosage of 3 mg/kg (Figure 4-11A), as established in previous studies (Pellegrini et al., 2021). This approach allowed us to assess both the efficacy of donepezil *in vivo* and its impact on whole-body inflammation and knee OA. Micro-CT results demonstrate that donepezil administration mitigated subchondral bone loss at two months post-OA induction (Figure 4-11B-C). Additionally, donepezil treatment improved the structural model index (SMI) of subchondral bone at both one and two months, suggesting enhanced preservation of bone architecture and quality over time (Figure 4-11C).

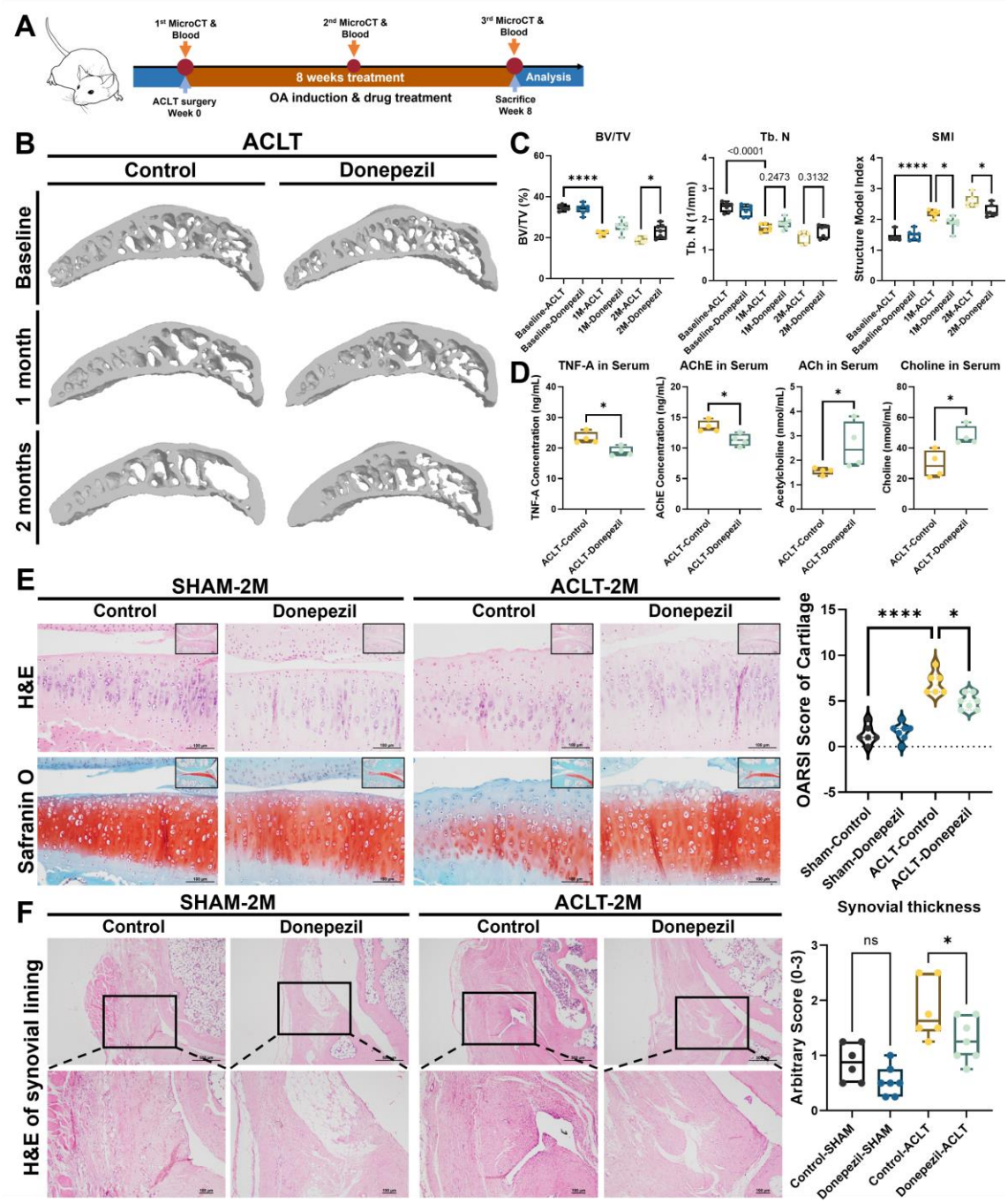

Figure 4-11 The anti-inflammation and chondral protective effects of donepezil *in vivo*. A. Schematic diagram of the animal experiments. **B.** Representative micro-CT images of medial subchondral bone, with quantitative analysis of BV/TV, Tb. N and structural model index. **D.** Serum levels of TNF-A, AChE, ACh and Choline measured at the end point. **E.** Representative histological images of rat articular cartilage. Scale bars = 100 μm. **F.** Representative histological images of rat articular cartilage. Scale bars = 100 μm or 500μm. All data are expressed as means ± SEM. One-way ANOVA with Post-hoc tests were performed. * $p<0.05$; ** $p<0.005$; *** $p<0.001$; **** $p<0.0001$.

At the molecular level, two months of donepezil treatment decreased the expression of both AChE and the pro-inflammatory cytokine TNF-α, while increasing ACh levels in serum, indicating effective suppression of inflammatory through cholinergic signaling pathways (Figure 4-11D). Histological analysis of knee joint sections revealed that donepezil treated hypertensive rats exhibited significantly less cartilage degeneration compared to vehicle-treated controls, as evidenced by improved cartilage integrity and lower synovial lining thickness (Figure 4-11E-F). These findings indicate a robust chondroprotective effect of systemic AChE inhibition in spontaneous hypertensive rat OA model.

These results demonstrate that pharmacological inhibition of AChE with donepezil not only confers significant protection against cartilage and bone degeneration in OA but also attenuates systemic inflammation.

4.4 Exploration of the mechanisms of acetylcholinesterase and alpha7 acetylcholine receptor signaling in inflammation regulation

Immunohistochemical staining of mouse joints revealed that AChE knockout exerts anti-inflammatory effects

Following OA induction, expression of TNF-α, NF-κB, and AChE increased, indicating an association between AChE and inflammatory signaling. Deletion of AChE attenuated these inflammatory responses (Figure 4-12). Notably, α7nAChR protein abundance remained unchanged across conditions (baseline, post-OA induction, and after AChE deletion). This suggests that the anti-inflammatory effect of AChE knockout

may mediated via modulation of α7nAChR activity rather than changes in receptor expression. Given that α7nAChR is a $Ca2^{+}$ permeable ligand gated ion channel (Habibi, 2010), we next assessed membrane potential and intracellular ion dynamics (Figure 4-14). Interestingly, analysis of serum levels of TNF-α, and IL-1β revealed no significant changes between cKO and control mice, suggesting that the anti-inflammation effects of conditional AChE knockout are localized to the joint microenvironment rather than systemic.

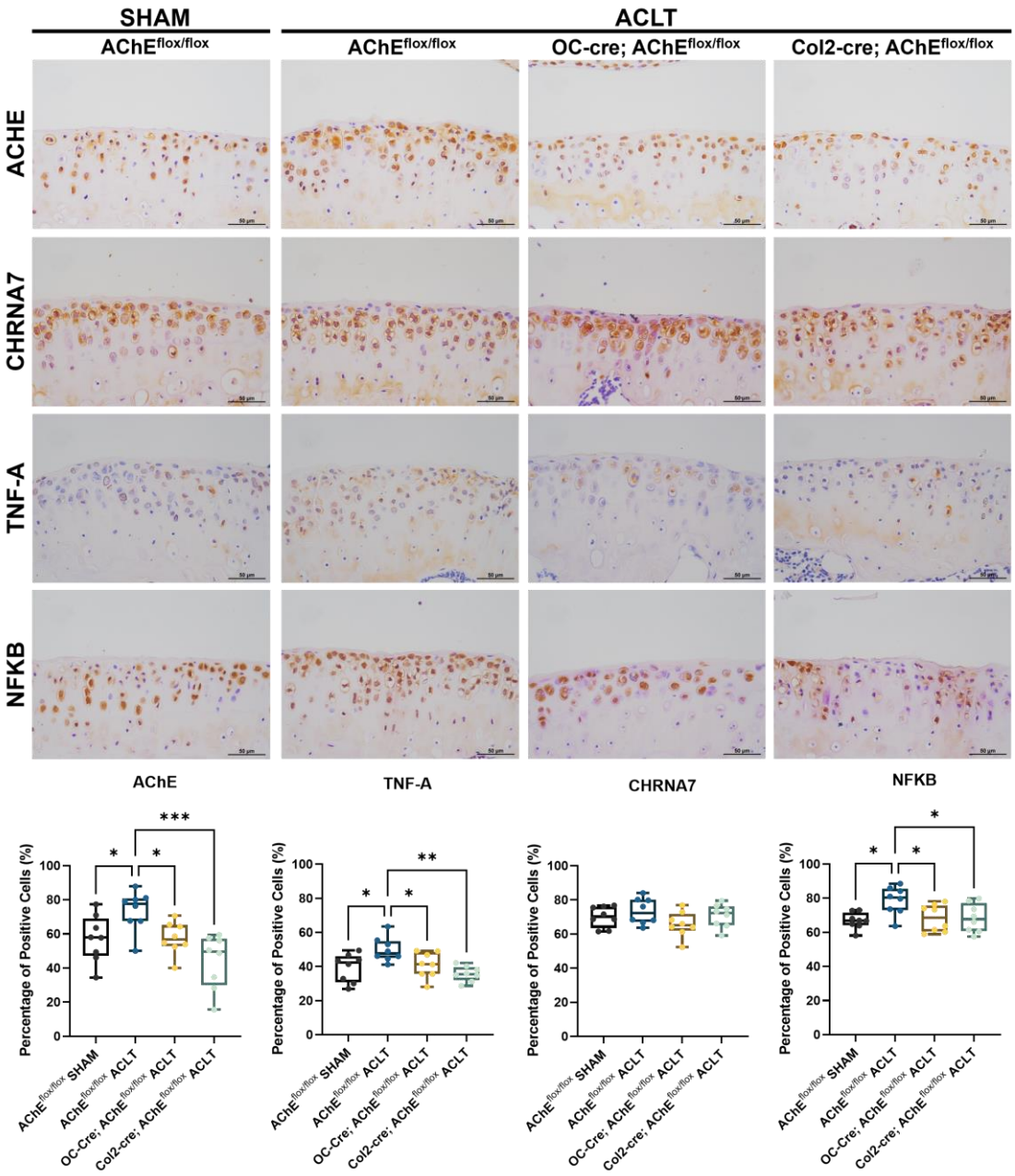

Figure 4-12 Immunohistochemical staining of mouse joints showed that AChE knockout reduced inflammatory cytokine expression in cartilage, without significant altering α7nAChR expression. Representative histological images of mice joint with quantitively analysis (n=8). Scale bars = 50 μm. All data are expressed as means ± SEM. One-way ANOVA with Post-hoc tests were performed. * $p<0.05$; ** $p<0.005$; *** $p<0.001$.

Investigation of AChE/α7nAChR signaling in inflammation and osteoarthritis

To elucidate the molecular mechanisms underlying the interplay between AChE and the α7nAChR in chondrocytes, we conducted a series of immunofluorescence staining

experiments on both human OA articular cartilage tissue sections and cultured human OA chondrocyte cells. Confocal microscopy analysis revealed substantial co-localization of AChE and α7nAChR at the cell membrane as well as in perinuclear regions (Figure 4-13A-B). This spatial proximity strongly suggests a potential physical or functional interaction between these two proteins within chondrocytes, which may facilitate the coordinated regulation of cholinergic signaling pathways in cartilage tissue.

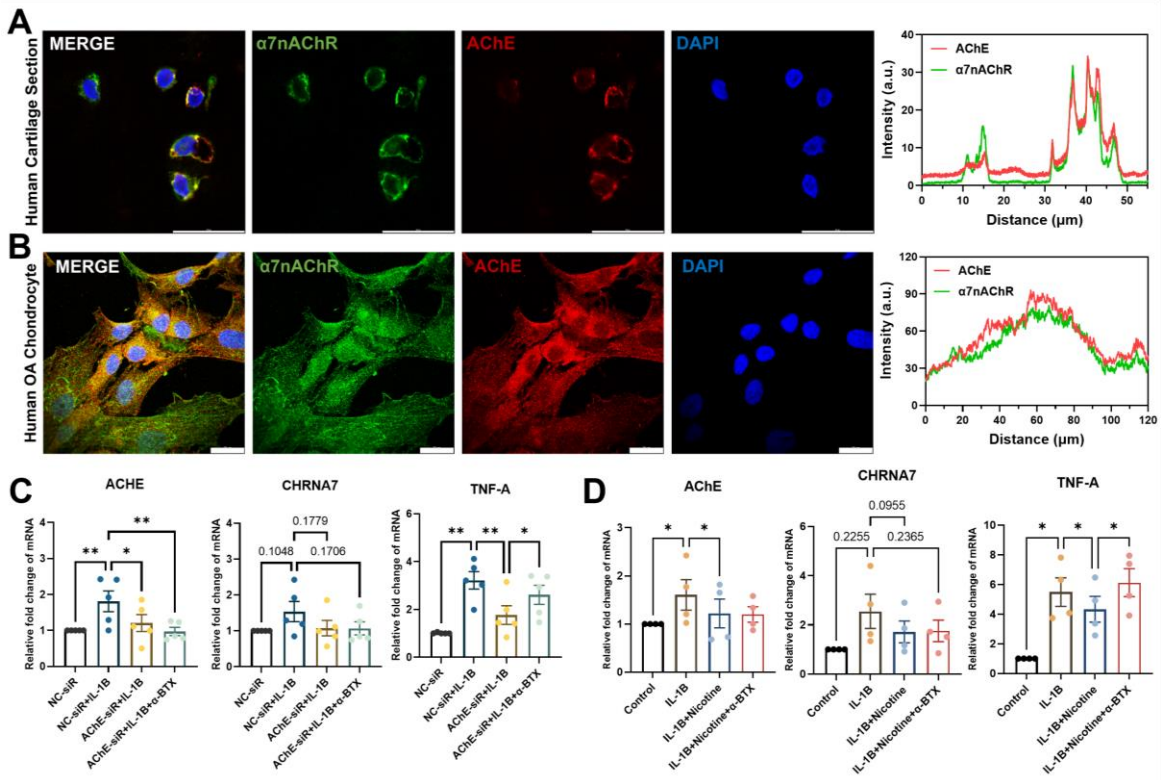

Figure 4-13 Investigation the regulation of AChE/α7nAChR in inflammation. A. Immunofluorescent co-localization staining of AChE and α7nAChR in human OA cartilage sections and the mapping of fluorescence intensity. Scale bars = 20 μm. **B.** Immunofluorescent co-localization staining of AChE and α7nAChR in cultured human OA chondrocytes and the mapping of fluorescence intensity. Scale bars = 20 μm. **C.** PCR validation of AChE/α7nAChR signaling with AChE knockdown and α7nAChR antagonist (n=5). **D. C.** PCR validation of AChE/α7nAChR signaling with α7nAChR agonist and antagonist (n=4). All data are expressed as means ± SEM. One-way ANOVA with Post-hoc tests. * $p<0.05$; ** $p<0.005$.

To further explore the functional significance of this interaction, we performed a range of *in vitro* assays. Notably, under inflammatory conditions, the anti-inflammatory benefits conferred by AChE knockdown and α7nAChR agonist (nicotine) were significantly reversed upon treatment with the α7nAChR antagonist α-bungarotoxin (α-BTX) (Figure 4-13C-D). This finding indicates that the anti-inflammatory effects of AChE inhibition are dependent on α7nAChR activation. Calcium imaging experiments further demonstrated that both ACh-treated and AChE-knockdown chondrocytes displayed increased calcium channel activation relative to untreated cells, reinforcing the notion that α7nAChR functions as a critical ligand-gated ion channel that can be activated by ACh or knockdown of AChE in chondrocyte (Figure 4-14A). Complementary electrophysiological studies using patch-clamp techniques provided additional mechanistic insights. In the presence of α7nAChR antagonism (α-BTX) and acetylcholine (ACh), AChE knockdown cells exhibited higher membrane currents at -100 mV compared to negative control cells (Figure 4-14B-F). These results suggest that AChE knockdown could counteract the inhibitory effects of α7nAChR antagonism, thereby enhancing ion channel activity and supporting the role of α7nAChR as a key mediator of cholinergic anti-inflammation signaling in chondrocytes.

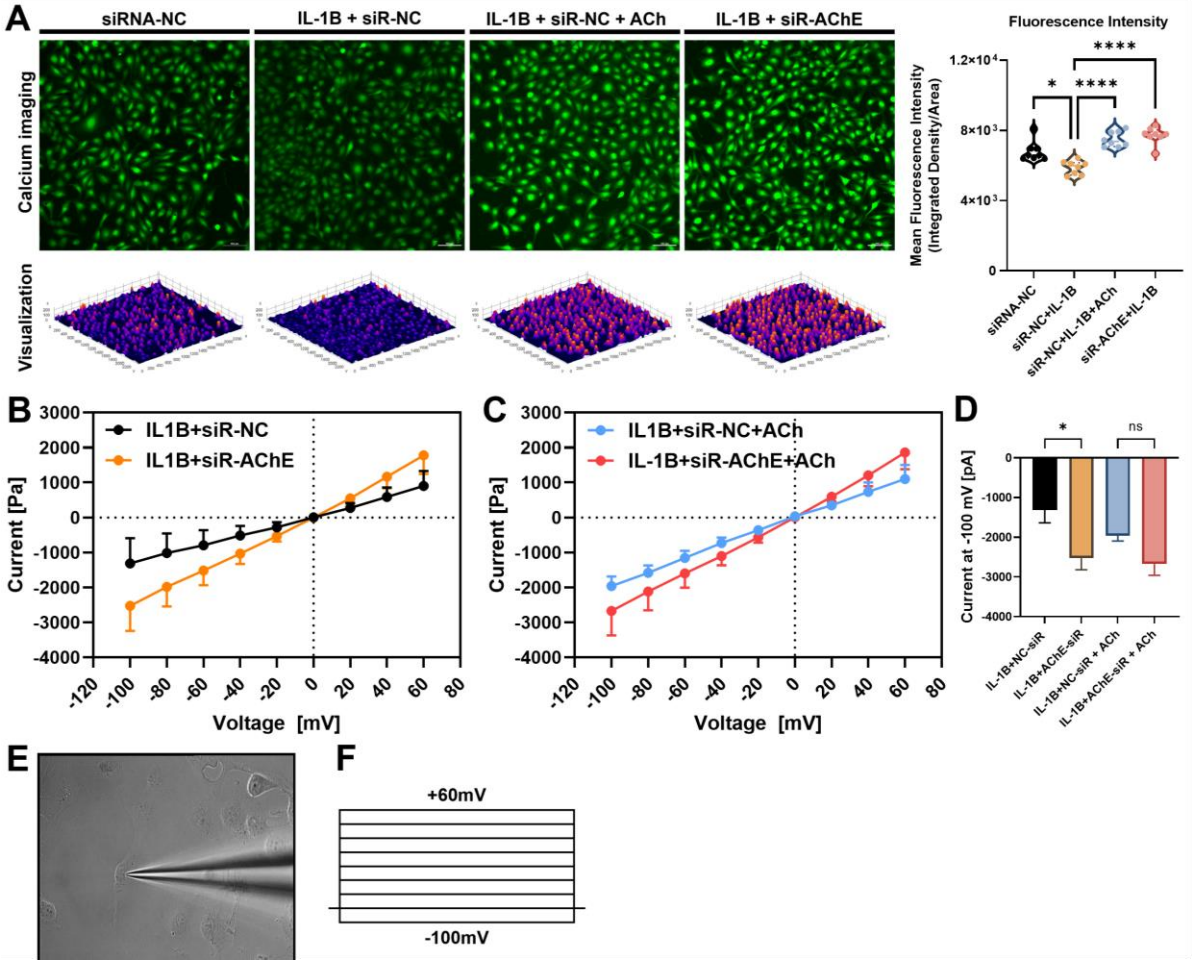

Figure 4-14 Investigation of AChE/α7nAChR signaling. A. Calcium imaging of cultured chondrocyte cells, with visualization and quantitively analysis of mean fluorescence intensity (n=8). Scale bar = 100 μm. **B.** Cell membrane current changes under voltage steps in negative control siRNA groups (n=4). **C.** Cell membrane current changes under voltage steps in AChE knockdown groups (n=4). **D.** Current difference at -100mV between AChE knockdown and negative control, with or without ACh added (n=4)**. E.** Real image of needle attached to the cell membrane. **F.** Experimental design of voltage steps. All data are expressed as means ± SEM. One-way ANOVA with Post-hoc tests or unpaired two-tailed Student's t-test were performed. * $p<0.05$; ** $p<0.005$; *** $p<0.001$; **** $p<0.0001$.

In summary, our findings provide evidence for the role of AChE/α7nAChR signaling in maintaining cartilage integrity and regulating inflammatory responses in OA pathogenesis. The observed co-localization and functional interplay between AChE and α7nAChR highlight a novel mechanistic axis that integrates cholinergic signaling and inflammatory pathways in chondrocytes. However, further studies with larger sample

sizes and more detailed experimental approaches, including additional replicates in patch-clamp, and functional assays are warranted to fully validate and expand upon these observations.

Chapter 5 Discussion and Conclusion

5.1 Discussion

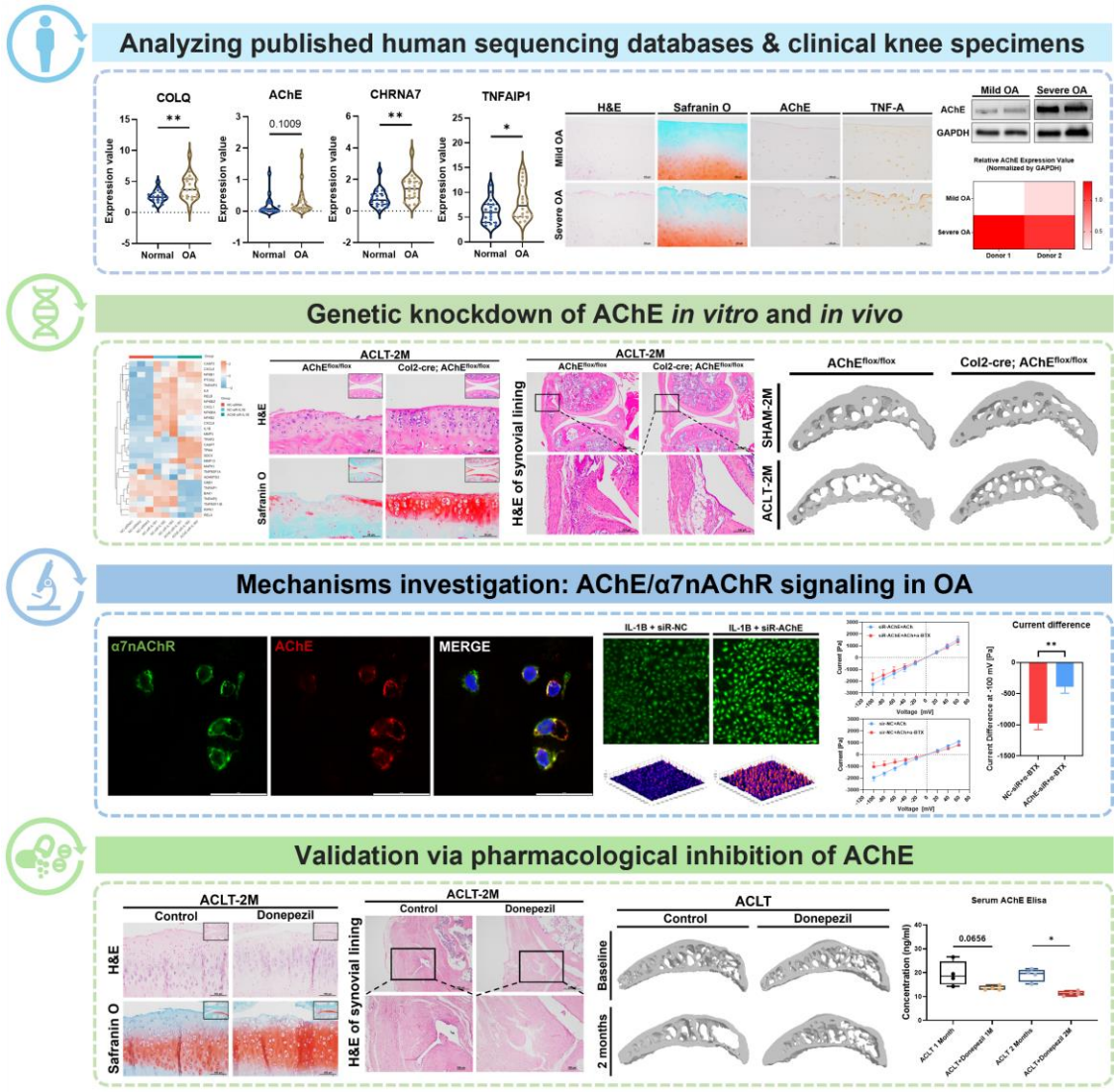

Figure 5-1 Overall framework of the study. The research progresses from the analysis of human sequencing databases and clinical knee specimens to genetic knockdown and pharmacological inhibition of AChE, and ultimately to mechanistic investigations of AChE/α7nAChR signaling in osteoarthritis.

This thesis systematically investigates the role of chondrocytic acetylcholinesterase (AChE) and α7 nicotinic acetylcholine receptor (α7nAChR) signaling in cartilage homeostasis and osteoarthritis (OA) pathogenesis, providing new insights into the

peripheral branch of "brain-joint axis" and the cholinergic regulation of skeletal tissues. We characterized AChE/ACh/α7nAChR expression in different models and OA progression and evaluated its potential as a regulatory target axis for OA management.

In the initial phase of the study, analysis of publicly available RNA sequencing datasets revealed that the cholinergic system and inflammatory pathways are implicated in OA pathogenesis. Specifically, the expression of AChE (not statistically significant, $p = 0.1001$), COLQ, CHRNA7, CHRNA10, MMP-13, and TNFAIP1 exhibited increased in human OA chondrocytes compared with non-OA controls. These findings suggest a potential link between cholinergic dysregulation and inflammation in OA, highlighting the need for further mechanistic studies. To further explore the involvement of cholinergic signaling in OA, we collected human OA joint specimens from patients underwent total knee arthroplasty, with patients' consent. An upregulation of TNF-α and AChE expression was observed in the severe OA compartment compared with the mild OA compartment. However, the sample size is (n = 3 for joint specimens) and absence of normal control samples, future studies with larger sample sizes and inclusion of non-OA control samples are required to enhance the conclusions and confirm the association between AChE expression and OA severity.

Previous studies have shown that AChE contributes to the progression of inflammation in neurons and osteoclasts, extending beyond its cholinergic hydrolytic functions (Liu et al., 2020; Xia et al., 2025). Our findings corroborate these findings and uniquely identified AChE as an inflammation modulator in chondrocytes and OA.

Subsequent *in vitro* experiments demonstrated that siRNA-mediated knockdown of AChE in IL-1β stimulated C28/I2 chondrocyte cell lines led to reduced expression of inflammatory mediators, including TNF-α and IL-6. This supports the hypothesis that cholinergic dysregulation may play a pro-inflammatory role in chondrocytes under inflammatory conditions. However, these findings are limited by the use of a single cell line and the absence of primary human chondrocyte validation at this stage. Future studies should include additional cell models and quantitative analyses to strengthen these observations.

In vivo, both chondrocyte-specific (Col2a1-Cre; $AChE^{flox/flox}$) and osteoblast-specific (Osteocalcin-Cre; $AChE^{flox/flox}$) AChE knockout mice exhibited less cartilage degeneration, improved synovial morphology, reduced subchondral bone loss and joint inflammation following posttraumatic OA compared to $AChE^{flox/flox}$ controls, as assessed by OARSI scoring of articular cartilage, synovial thickness, BV/TV of subchondral bone and immunohistochemical staining. In behavioral testing, two months after OA induction, the locomotion ability in $AChE^{flox/flox}$ mice declined markedly, whereas chondrocyte specific knockout mice have no significant difference, as characterized by the Rotarod test. For pain sensitivity, assessed using the von Frey test, osteoblast-specific knockout mice exhibited a higher pain threshold than $AChE^{flox/flox}$ mice two months after OA induction, in both cases relative to the sham leg. Histochemical staining revealed lower expression of AChE, Nf-kB, and TNF-α in cartilage and synovium of knockout mice, confirming the anti-inflammatory and

chondroprotective effects of AChE deficiency. Additionally, in a collagenase type 1a–induced inflammatory OA model (CIOA), chondrocyte-specific knockout mice showed reduced subchondral bone loss. However, no statistically significant differences in cartilage morphology and synovial lining thickness were detected between AChE-flox/flox controls and AChE-cKO mice, this may reflect model specific features and differences. Unlike the ACLT-induced OA, which is primarily mechanically driven with chronic inflammation, CIOA involves direct intra-articular injection into the joint capsule and elicits more pronounced synovitis, potentially masking the protective effects of AChE deletion in cartilage.

Serum samples from all animal groups were collected and analyzed by ELISA and a choline assay kit to measure AChE, TNF-α, IL-1β, ACh, and choline. Conditional AChE knockout led to a marginally significantly increased the ACh levels in serum of AChE knockout mice after 2 months of ACLT, which is encouraging given that this is a local rather than a global deletion of AChE. However, there were no statistically significant changes in TNF-α or IL-1β levels compared with flox/flox control mice, suggesting that tissue-specific knockout may be insufficient to alleviate systemic inflammation.

While these results provide evidence for the involvement of AChE in cartilage homeostasis and OA pathogenesis, their translational relevance is constrained by species differences and the infeasibility of gene knockout in humans. Future studies

should incorporate more human tissue samples and bioinformatics analyses to validate these findings in clinically relevant contexts.

To further validate our findings from genetic inhibition experiments, employed pharmacological inhibition of AChE using donepezil in primary human OA chondrocytes. Primary human OA chondrocytes were challenged with IL-1β to simulate inflammation, following 24- or 48-hour donepezil treatment, the expression of inflammatory cytokines such as TNF-α was reduced at both the transcriptional and protein levels. Similarly, in a post-traumatic OA hypertensive rat model, pharmacological AChE inhibition via intraperitoneal donepezil administration for two months led to attenuated cartilage degeneration, synovial inflammation and subchondral bone loss compared with the non-treatment group, as evidenced by OARSI cartilage score, synovial lining thickness and BV/TV from micro-CT analyses.

In the *in vitro* experiments, sample size was limited, and *in vivo* findings are restricted to a murine model. Further studies with larger cohorts are necessary to confirm these effects and assess safety profiles. Additional clinical evidence is also required, as the osteoprotective effects of donepezil are currently being prospectively evaluated in a randomized, double-blind, placebo-controlled trial (NCT06041789) in older adults with AD (North et al., 2025). In summary, these results suggest that the AChE inhibitor donepezil has potential as a therapeutic drug in combination with existing non-steroidal anti-inflammatory drugs (NSAIDs) for OA management, particularly in patients with OA and AD co-existing. Clinical observations have reported that donepezil may provide

additional analgesia in neuropathic pain (Basnet et al., 2014; Nicolodi et al., 2002), and some case reports have documented its use in patients with both OA and AD (Basnet et al., 2014). Nevertheless, further clinical trials are required to substantiate these potential benefits in inflammation and OA.

Finally, we investigated the mechanisms by which AChE regulates inflammation. Immunofluorescence analyses demonstrated co-localization of AChE and α7-nAChR in primary human OA chondrocytes and in OA cartilage sections, suggesting a potential direct or indirect interactions between these proteins. In C28/I2 chondrocyte cell-line, the anti-inflammatory effects of AChE inhibition were at least partially mediated through the activation of α7-nAChR and cholinergic anti-inflammatory signaling. Under inflammatory conditions, these effects were attenuated by the α7-nAChR antagonist α-bungarotoxin (α-BTX), as indicated by increased TNF-α transcript levels. Patch-clamp electrophysiology showed that AChE knockdown activated the ion channels and significantly counteracted the inhibitory effects of α-BTX by increasing membrane currents, indicating greater ion channel activity relative to the control group. Given that α7-nAChR is a ligand-gated cation channel with high Ca^{2+} permeability, these findings are consistent with a mechanism in which AChE knockdown acts, at least in part, through α7-nAChR dependent signaling. Building on this evidence, we monitored calcium dynamics in C28/I2 chondrocyte cell line using the fluorescent indicator Calbryte 520 AM and live-cell imaging. Time-lapse imaging revealed fluctuations in fluorescence intensity, indicating altered ion channel activity.

Collectively, these data identify AChE/α7-nAChR signaling as a modifiable target in OA progression and delineate a mechanistic axis linking cholinergic signaling and inflammation regulation in cartilage homeostasis. However, further investigation is warranted, for patch-clamp experiments, the current sample size is limited, and future studies should employ larger cohorts. Complementary approaches are necessary to validate direct interactions between AChE and α7-nAChR, such as co-immunoprecipitation (Co-IP) performed under varied experimental conditions would provide new insights into this aspect. Although prior studies have suggested protein–protein interactions of AChE/α7-nAChR in murine macrophages (Liu et al., 2020), to our knowledge this interaction has not been demonstrated in chondrocytes.

5.2 Conclusion

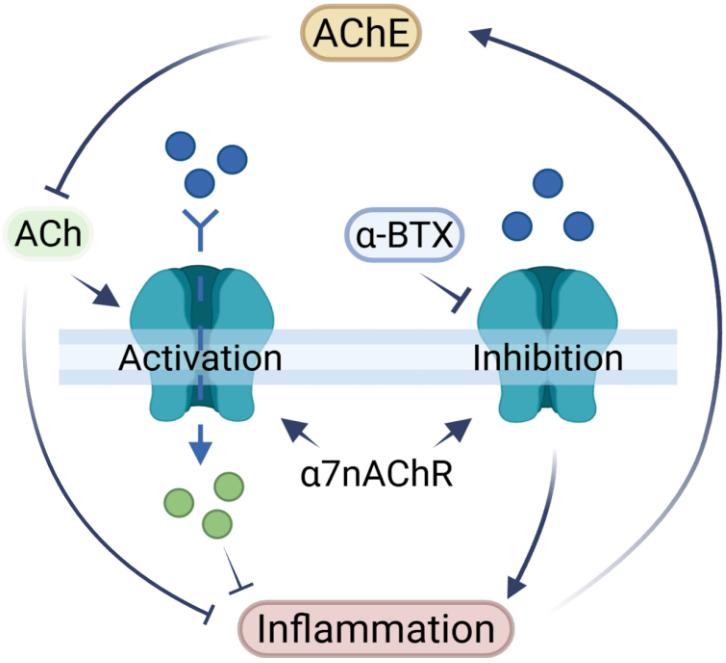

Figure 5-2 Schematic of the AChE/α7-nAChR signaling in inflammation regulation.

This thesis demonstrates that local AChE/ACh/α7nAChR signaling is a critical regulator of joint inflammation, cartilage integrity and subchondral bone remodeling in osteoarthritis. By integrating transcriptomic analysis with functional experiments, we observed that disruption of cholinergic signaling is closely associated with heightened inflammatory responses in OA cartilage. Notably, both genetic and pharmacological suppression of AChE resulted in reduced inflammatory mediator production and conferred protection against cartilage and bone degeneration in experimental models. These results extend previous observations of AChE's involvement in inflammatory processes beyond neural tissues (Liu et al., 2020; Xia et al., 2025), and for the first time, implicate AChE as a key modulator of inflammatory signaling in chondrocytes. While our findings suggest that targeting AChE/ACh/α7nAChR signaling could be a promising therapeutic avenue, further validation in diverse cell types and more physiologically relevant models will be essential to fully elucidate its role in OA pathogenesis.

Our findings demonstrate that AChE critically modulates joint inflammation and tissue integrity through its interaction with α7nAChR in OA. Conditional knockout of AChE in chondrocytes (AChEflox/flox; Col2a1-Cre) or osteoblasts (AChEflox/flox; Osteocalcin-Cre) protected against cartilage degeneration, synovial deterioration, subchondral bone loss, and inflammation progression after OA induction, consistent with previous studies showing α7nAChR activation is chondroprotective (Liu et al., 2015; Liu et al., 2021; Teng et al., 2019), while its deficiency worsens cartilage

damage and OA progression (Courties, Do, et al., 2020; Courties, Petit, et al., 2022).

OA induction increased AChE expression and decreased after deletion, but not α7nAChR, suggesting AChE mainly affects receptor function through the activation of ACh. As α7nAChR is a functional ligand-gated ion channel (Noviello et al., 2021), the upregulation and deletion of AChE may not exert much influence on the expression of α7nAChR but its functions (Liu et al., 2020). Immunofluorescence revealed co-localization of AChE and α7nAChR in human OA cartilage tissue sections and human OA chondrocyte cells, and both AChE inhibition and α7nAChR agonist treatment reduced inflammatory cytokines via α7nAChR activation in vitro, as confirmed by antagonist studies, calcium imaging and electrophysiological data. These results highlight the functional interplay between AChE and α7nAChR in regulating inflammation and cartilage homeostasis in OA.

Without nerve stimulation, these anti-inflammatory effects were achieved locally, and did not significantly alter systemic inflammatory markers, highlighting the accessibility and importance of local cholinergic modulation (Simon et al., 2023). Furthermore, treatment with the AChE inhibitor donepezil increased ACh level in serum of rats and reduced inflammatory cytokines and OA symptoms in both human OA chondrocytes and animal models, supporting its potential as a therapeutic option. Clinical observations have reported that donepezil may provide additional analgesia in neuropathic pain (Basnet et al., 2014; Nicolodi et al., 2002), and some case reports have documented its use in patients with both OA and Alzheimer's disease (Basnet et

al., 2014). However, further clinical studies are needed to confirm the efficacy of AChE-targeted therapies in broader OA populations, as the osteoprotective effects of donepezil are currently being clinically evaluated (NCT06041789) in patients with Alzheimer's disease (North et al., 2025).

Previous studies have established the presence of cholinergic innervation in the bone matrix (Gadomski et al., 2022), synovium (Forsgren, 2012), and at the cartilage–subchondral bone interface (Courties, Belle, et al., 2020), with recent murine research showing that cholinergic nerve fibers closely interact with osteocytes to influence bone adaptation (Gadomski et al., 2022; Mora-Antoinette et al., 2025). Our data further confirm the existence of cholinergic components such as AChE and α7nAChR at the bone–cartilage interface and their involvement in inflammatory signaling and cartilage homeostasis. Given the increasing burden of OA and the lack of disease modifying therapies, targeting the cholinergic system through agents such as the AChE inhibitor donepezil or α7nAChR activation strategies, represents a promising approach to reduce joint inflammation and protect cartilage. However, successful clinical translation will require a deeper understanding of cholinergic signaling within joint tissues and its relationship to pain pathways. Our findings advance the concept of a local AChE/α7nAChR axis in OA, supporting the broader "brain–joint cholinergic axis" framework and highlighting its potential as a disease-modifying strategy. Future research should focus on clinical validation and large-scale bioinformatics analyses to confirm the therapeutic relevance of targeting AChE/ACh/α7nAChR signaling in OA.

In conclusion, this study identifies novel roles for AChE/ACh/α7nAChR signaling in cartilage homeostasis and OA progression. Both genetic knockdown and pharmacological inhibition of AChE produced concordant chondroprotective and osteoprotective effects *in vitro* and *in vivo*, supporting the therapeutic potential of targeting AChE/ACh/α7nAChR signaling in OA. Furthermore, we identified AChE inhibition can increase the level of ACh and lead to the activation of anti-inflammation signaling pathways, providing new mechanistic insight into cholinergic regulation of joint homeostasis. Together, these findings advance current understanding of the cholinergic signaling and lay a foundation for developing AChE/α7nAChR targeted strategies for OA and related skeletal disorders.

Chapter 6 Limitations and future Plan

This research advances understanding of acetylcholinesterase (AChE) in joint homeostasis and its interaction with the α7 nicotinic acetylcholine receptor (α7nAChR) in osteoarthritis (OA). Our findings demonstrated that AChE/ACh/α7nAChR signaling contributes to OA pathogenesis by modulating inflammation, bone resorption, synovial deterioration and cartilage degradation, and that both genetic and pharmacological inhibition of AChE exerts protective effects in inflammatory and OA models. Together, these findings position AChE as a potential therapeutic target and widen insight into systemic and local mechanisms of OA progression. However, several limitations exist in this study. Some experiments are ongoing, and additional data is needed to further substantiate the conclusion. Analysis of public single-cell RNA-sequencing datasets revealed a relatively small cluster of cells expressing cholinergic signaling related genes compared with bulk RNA-sequencing, highlighting cellular heterogeneity within cartilage and suggesting that cholinergic signaling may be restricted to specific cell subsets rather than uniformly distributed across the entire tissue. In clinical human OA specimens, a larger, well-phenotyped cohorts are warranted to rigorously test associations between OA severity and AChE expression.

In the section of genetic inhibition, the anti-inflammatory effects of genetic AChE inhibition are required to be further verified in primary human chondrocytes, integrating transcript and protein measurements of AChE and key inflammatory cytokines to confirm the engagement of ACh/α7nAChR signaling and downstream

effects. *In vivo* functional interpretation would be strengthened by additional behavioral assays, such as CatWalk gait analysis, to link molecular and histological findings to joint function and pain-related outcomes.

Pharmacological studies also have constraints. The *in vitro* evaluation of the AChE inhibitor donepezil was limited by sample size despite the use of primary human OA chondrocytes. Future experiments should increase the sample size and include various cell types. In animal models, deeper characterization of AChE/α7nAChR signaling and other cholinergic components at transcript, protein, and functional levels is needed to connect pathway modulation with cartilage and subchondral bone phenotypes.

Meanwhile, animals experiments of this study were conducted exclusively in male mice and rat, whereas sex differences in cholinergic signaling and OA susceptibility have been reported (Kliemann et al., 2012; Lips et al., 2015; Mora-Antoinette et al., 2025). Future research should address potential sex-specific effects of AChE modulation. Additionally, the use of constitutive rather than inducible knockout models raise the possibility of developmental adaptations influencing our results. Employing tamoxifen-inducible systems will be important to distinguish the effects of AChE deletion during OA progression from those arising during development. For mechanism focused experiments, co-immunoprecipitation (Co-IP) could directly probe potential protein–protein interactions between AChE and α7nAChR in chondrocytes.

Finally, species and genetic differences between murine models and humans limit translational generalizability. Future research should prioritize clinical validation and bioinformatics analysis using large, well-annotated human datasets to confirm the clinical relevance of these findings and application of human joint-on-a-chip or co-cultured system to mimic human joint environment and ACh monitoring in the future to further refine the therapeutic potential of targeting AChE/ACh/α7nAChR signaling in inflammation and OA.

Reference

Abdel Shaheed, C., Ferreira, G. E., Dmitritchenko, A., McLachlan, A. J., Day, R. O., Saragiotto, B., Lin, C., Langendyk, V., Stanaway, F., Latimer, J., Kamper, S., McLachlan, H., Ahedi, H., & Maher, C. G. (2021). The efficacy and safety of paracetamol for pain relief: an overview of systematic reviews. *Med J Aust*, *214*(7), 324-331. https://doi.org/10.5694/mja2.50992

Albuquerque, E. X., Pereira, E. F., Alkondon, M., & Rogers, S. W. (2009). Mammalian nicotinic acetylcholine receptors: from structure to function. *Physiol Rev*, *89*(1), 73-120. https://doi.org/10.1152/physrev.00015.2008

Aoyagi, K., LaValley, M., Edwards, R., Lechuga, J., Rivas, E., Wagler, A., & Neogi, T. (2024). PRELIMINARY EFFECTS OF TRANSCUTANEOUS AURICULAR VAGUS NERVE STIMULATION ON CHRONIC PAIN IN PEOPLE WITH KNEE OSTEOARTHRITIS. *Osteoarthritis and Cartilage*, *32*, S569-S570. https://doi.org/10.1016/j.joca.2024.02.842

Aoyagi, K., Rivas, E., Shababi, R., Edwards, R., LaValley, M., Lechuga, J., Napadow, V., & Neogi, T. (2025). Safety and preliminary efficacy of transcutaneous auricular vagus nerve stimulation on chronic knee pain: A pilot trial. *Osteoarthr Cartil Open*, *7*(1), 100545. https://doi.org/10.1016/j.ocarto.2024.100545

Basnet, A., Butler, S., HonorÉ, P. H., Butler, M., Gordh, T. E., Kristensen, K., & Bjerrum, O. J. (2014). Donepezil provides positive effects to patients treated with gabapentin for neuropathic pain: an exploratory study. *Acta anaesthesiologica Scandinavica.*, *58*(1), 61-73. https://doi.org/10.1111/aas.12218

Bellocchi, C., Carandina, A., Della Torre, A., Turzi, M., Arosio, B., Marchini, M., Vigone, B., Scatà, C., Beretta, L., Rodrigues, G. D., Tobaldini, E., & Montano, N. (2023). Transcutaneous auricular branch vagal nerve stimulation as a non-invasive add-on therapeutic approach for pain in systemic sclerosis. *Rheumatic & musculoskeletal diseases open*, *9*(3), e003265. https://doi.org/10.1136/rmdopen-2023-003265

Berenbaum, F., & Meng, Q.-J. (2016). The brain–joint axis in osteoarthritis: nerves, circadian clocks and beyond. *Nature Reviews Rheumatology*, *12*(9), 508-516. https://doi.org/10.1038/nrrheum.2016.93

Birmingham, T. B., Marriott, K. A., Leitch, K. M., Moyer, R. F., Lorbergs, A. L., Walton, Dave M., Willits, K., Litchfield, R. B., Getgood, A., Fowler, P. J., & Giffin, J. R. (2019). Association Between Knee Load and Pain: Within-Patient, Between-Knees, Case–Control Study in Patients With Knee Osteoarthritis. *Arthritis care & research (2010)*, *71*(5), 647-650. https://doi.org/10.1002/acr.23704

Bonaz, B., Sinniger, V., & Pellissier, S. (2016). Anti-inflammatory properties of the vagus nerve: potential therapeutic implications of vagus nerve stimulation. *J Physiol*, *594*(20), 5781-5790. https://doi.org/10.1113/jp271539

Bonin, R. P., Bories, C., & De Koninck, Y. (2014). A simplified up-down method

(SUDO) for measuring mechanical nociception in rodents using von Frey filaments. *Mol Pain*, *10*, 26. https://doi.org/10.1186/1744-8069-10-26

Bouzat, C., Gumilar, F., Spitzmaul, G., Wang, H.-L., Rayes, D., Hansen, S. B., Taylor, P., & Sine, S. M. (2004). Coupling of agonist binding to channel gating in an ACh-binding protein linked to an ion channel. *Nature*, *430*(7002), 896-900. https://doi.org/10.1038/nature02753

Chang, S. H., Mori, D., Kobayashi, H., Mori, Y., Nakamoto, H., Okada, K., Taniguchi, Y., Sugita, S., Yano, F., Chung, U.-i., Kim-Kaneyama, J.-r., Yanagita, M., Economides, A., Canalis, E., Chen, D., Tanaka, S., & Saito, T. (2019). Excessive mechanical loading promotes osteoarthritis through the gremlin-1–NF-κB pathway. *Nature communications*, *10*(1), 1442-1442. https://doi.org/10.1038/s41467-019-09491-5

Chen, T., Weng, W., Liu, Y., Aspera-Werz, R. H., Nüssler, A. K., & Xu, J. (2021). Update on Novel Non-Operative Treatment for Osteoarthritis: Current Status and Future Trends. *Frontiers in pharmacology*, *12*, 755230-755230. https://doi.org/10.3389/fphar.2021.755230

Chen, Y. H., & Lo, R. Y. (2017). Alzheimer's disease and osteoporosis. *Ci Ji Yi Xue Za Zhi*, *29*(3), 138-142. https://doi.org/10.4103/tcmj.tcmj_54_17

Courties, A., Belle, M., Senay, S., Cambon-Binder, A., Sautet, A., Chédotal, A., Berenbaum, F., & Sellam, J. (2020). Clearing method for 3-dimensional immunofluorescence of osteoarthritic subchondral human bone reveals peripheral cholinergic nerves. *Scientific Reports*, *10*(1), 8852. https://doi.org/10.1038/s41598-020-65873-6

Courties, A., Deprouw, C., Maheu, E., Gibert, E., Gottenberg, J. E., Champey, J., Banneville, B., Chesnel, C., Amarenco, G., Rousseau, A., Berenbaum, F., & Sellam, J. (2022). Effect of Transcutaneous Vagus Nerve Stimulation in Erosive Hand Osteoarthritis: Results from a Pilot Trial. *J Clin Med*, *11*(4). https://doi.org/10.3390/jcm11041087

Courties, A., Deprouw, C., Rousseau, A., Berard, L., Touati, A., Kalsch, J., Villevieille, M., Maheu, E., Miquel, A., Simon, T., Berenbaum, F., & Sellam, J. (2022). Transcutaneous vagus nerve stimulation in erosive hand osteoarthritis: protocol for the randomised, double-blind, sham-controlled ESTIVAL trial. *BMJ Open*, *12*(3), e056169. https://doi.org/10.1136/bmjopen-2021-056169

Courties, A., Do, A., Leite, S., Legris, M., Sudre, L., Pigenet, A., Petit, J., Nourissat, G., Cambon-Binder, A., Maskos, U., Berenbaum, F., & Sellam, J. (2020). The Role of the Non-neuronal Cholinergic System in Inflammation and Degradation Processes in Osteoarthritis. *Arthritis & rheumatology.*, *72*(12), 2072-2082. https://doi.org/10.1002/art.41429

Courties, A., Petit, J., Do, A., Legris, M., Kouki, I., Pigenet, A., Sacitharan, P. K., Ehkirch, F. P., Berenbaum, F., & Sellam, J. (2022). Alpha-7 Nicotinic Receptor Dampens Murine Osteoblastic Response to Inflammation and Age-Related Osteoarthritis. *Front Immunol*, *13*, 842538.

https://doi.org/10.3389/fimmu.2022.842538

Courties, A., Tuffet, S., Cormier, G., Roux, C., Ornetti, P., Pers, Y.-M., Gottenberg, J.-E., Lespessailles, E., Chapurlat, R., Arniaud, D., Rannou, F., Wendling, D., Eymard, F., Mathieu, S., Richette, P., Saraux, A., Marotte, H., Poursac, N., rat, A.-C., . . . Sellam, J. (2024). 002 - TRANSCUTANEOUS AURICULAR VAGUS NERVE STIMULATION IN EROSIVE HAND OSTEOARTHRITIS: RESULTS OF THE ESTIVAL MULTICENTER RANDOMIZED SHAM-CONTROLLED TRIAL. *Osteoarthritis and Cartilage*, *32*, S6. https://doi.org/https://doi.org/10.1016/j.joca.2024.02.013

Cruz, C. J., Yeater, T. D., Griffith, J. L., & Allen, K. D. (2024). Vagotomy accelerates the onset of symptoms during early disease progression and worsens joint-level pathogenesis in a male rat model of chronic knee osteoarthritis. *Osteoarthr Cartil Open*, *6*(2), 100467. https://doi.org/10.1016/j.ocarto.2024.100467

D'Haens, G., Eberhardson, M., Cabrijan, Z., Danese, S., van den Berg, R., Löwenberg, M., Fiorino, G., Schuurman, P. R., Lind, G., Almqvist, P., Olofsson, P. S., Tracey, K. J., Hanauer, S. B., Zitnik, R., Chernoff, D., & Levine, Y. A. (2023). Neuroimmune Modulation Through Vagus Nerve Stimulation Reduces Inflammatory Activity in Crohn's Disease Patients: A Prospective Open-label Study. *Journal of Crohn's and Colitis*, *17*(12), 1897-1909. https://doi.org/10.1093/ecco-jcc/jjad151

Demircioğlu, G., Özden, A. V., & Genç, H. (2024). Comparison of the efficacy of auricular vagus nerve stimulation and conventional low back rehabilitation in patients with chronic low back pain. *Complementary Therapies in Clinical Practice*, *56*, 101862. https://doi.org/https://doi.org/10.1016/j.ctcp.2024.101862

Dong, H., Yuede, C. M., Coughlan, C. A., Murphy, K. M., & Csernansky, J. G. (2009). Effects of donepezil on amyloid-β and synapse density in the Tg2576 mouse model of Alzheimer's disease. *Brain Research*, *1303*, 169-178. https://doi.org/https://doi.org/10.1016/j.brainres.2009.09.097

Drewes, A. M., Brock, C., Rasmussen, S. E., Møller, H. J., Brock, B., Deleuran, B. W., Farmer, A. D., & Pfeiffer-Jensen, M. (2021). Short-term transcutaneous non-invasive vagus nerve stimulation may reduce disease activity and pro-inflammatory cytokines in rheumatoid arthritis: results of a pilot study. *Scandinavian Journal of Rheumatology*, *50*(1), 20-27. https://doi.org/10.1080/03009742.2020.1764617

Elsehrawy, G. G., Ibrahim, M. E., A.moneim, N. H., Hefny, M. A., & El Shaarawy, N. K. (2025). Transcutaneous vagus nerve stimulation as a pain modulator in knee osteoarthritis: a randomized controlled clinical trial. *BMC musculoskeletal disorders*, *26*(1), 68. https://doi.org/10.1186/s12891-025-08288-6

Fisher, A. A., Davis, M. W., Srikusalanukul, W., & Budge, M. M. (2006). Six-fold increased risk of hip fracture in older Australians (≥60 years) with dementia [journal article]. *Archives of Osteoporosis*, *1*(1), 13-19.

https://doi.org/10.1007/s11657-006-0003-4

Forsgren, S. (2012). Presence of ChAT mRNA and a very marked α7nAChR immunoreaction in the synovial lining layer of the knee joint. *Life Sci*, *91*(21-22), 1043-1047. https://doi.org/10.1016/j.lfs.2012.03.028

Gadomski, S., Fielding, C., García-García, A., Korn, C., Kapeni, C., Ashraf, S., Villadiego, J., Toro, R. D., Domingues, O., Skepper, J. N., Michel, T., Zimmer, J., Sendtner, R., Dillon, S., Poole, K. E. S., Holdsworth, G., Sendtner, M., Toledo-Aral, J. J., De Bari, C., . . . Robey, P. G. (2022). A cholinergic neuroskeletal interface promotes bone formation during postnatal growth and exercise. *Cell stem cell.*, *29*(4), 528-544.e529. https://doi.org/10.1016/j.stem.2022.02.008

Genovese, M. C., Gaylis, N. B., Sikes, D., Kivitz, A., Lewis Horowitz, D., Peterfy, C., Glass, E. V., Levine, Y. A., & Chernoff, D. (2020). Safety and efficacy of neurostimulation with a miniaturised vagus nerve stimulation device in patients with multidrug-refractory rheumatoid arthritis: a two-stage multicentre, randomised pilot study. *The Lancet Rheumatology*, *2*(9), e527-e538. https://doi.org/10.1016/S2665-9913(20)30172-7

Glasson, S. S., Blanchet, T. J., & Morris, E. A. (2007). The surgical destabilization of the medial meniscus (DMM) model of osteoarthritis in the 129/SvEv mouse. *Osteoarthritis and Cartilage*, *15*(9), 1061-1069. https://doi.org/https://doi.org/10.1016/j.joca.2007.03.006

Glyn-Jones, S., Palmer, A. J. R., Agricola, R., Price, A. J., Vincent, T. L., Weinans, H., & Carr, A. J. (2015). Osteoarthritis. *The Lancet*, *386*(9991), 376-387. https://doi.org/https://doi.org/10.1016/S0140-6736(14)60802-3

Gnatek, Y., Zimmerman, G., Goll, Y., Najami, N., Soreq, H., & Friedman, A. (2012). Acetylcholinesterase loosens the brain's cholinergic anti-inflammatory response and promotes epileptogenesis. *Frontiers in molecular neuroscience*, *5*(2012), 66. https://doi.org/10.3389/fnmol.2012.00066

Grässel, S., & Muschter, D. (2020). Recent advances in the treatment of osteoarthritis. *F1000Res*, *9*. https://doi.org/10.12688/f1000research.22115.1

Guo, J., Wang, L., Xu, H., & Che, X. (2014). Expression of non-neuronal cholinergic system in maxilla of rat in vivo. *Biological Research*, *47*(1), 72. https://doi.org/10.1186/0717-6287-47-72

Gupta, D. P., Lee, Y.-S., Choe, Y., Kim, K.-T., Song, G. J., & Hwang, S.-C. (2023). Knee osteoarthritis accelerates amyloid beta deposition and neurodegeneration in a mouse model of Alzheimer's disease. *Molecular Brain*, *16*(1), 1. https://doi.org/10.1186/s13041-022-00986-9

Ha, Z. Y., Mathew, S., & Yeong, K. Y. (2020). Butyrylcholinesterase: A Multifaceted Pharmacological Target and Tool. *Curr Protein Pept Sci*, *21*(1), 99-109. https://doi.org/10.2174/1389203720666191107094949

Habibi, M. (2010). Acetylcholine. In K. Kompoliti & L. V. Metman (Eds.), *Encyclopedia of Movement Disorders* (pp. 11-14). Academic Press.

https://doi.org/https://doi.org/10.1016/B978-0-12-374105-9.00146-5
Halder, N., & Lal, G. (2021). Cholinergic System and Its Therapeutic Importance in Inflammation and Autoimmunity. *Frontiers in immunology*, *12*, 660342-660342. https://doi.org/10.3389/fimmu.2021.660342
Hogg, R. C., Raggenbass, M., & Bertrand, D. (2003). Nicotinic acetylcholine receptors: from structure to brain function. In *Reviews of Physiology, Biochemistry and Pharmacology* (pp. 1-46). Springer Berlin Heidelberg. https://doi.org/10.1007/s10254-003-0005-1
Hoover, D. B. (2017). Cholinergic modulation of the immune system presents new approaches for treating inflammation. *Pharmacol Ther*, *179*, 1-16. https://doi.org/10.1016/j.pharmthera.2017.05.002
Huang, S.-W., Wang, W.-T., Chou, L.-C., Liao, C.-D., Liou, T.-H., & Lin, H.-W. (2015). Osteoarthritis Increases the Risk of Dementia: A Nationwide Cohort Study in Taiwan. *Scientific Reports*, *5*(1), 10145. https://doi.org/10.1038/srep10145
Hunter, D. J., & Bierma-Zeinstra, S. (2019). Osteoarthritis. *The Lancet*, *393*(10182), 1745-1759. https://doi.org/https://doi.org/10.1016/S0140-6736(19)30417-9
Inkson, C. A., Brabbs, A. C., Grewal, T. S., Skerry, T. M., & Genever, P. G. (2004). Characterization of acetylcholinesterase expression and secretion during osteoblast differentiation. *Bone*, *35*(4), 819-827. https://doi.org/10.1016/j.bone.2004.05.026
Issa, S. N., & Sharma, L. (2006). Epidemiology of osteoarthritis: An update. *Current Rheumatology Reports*, *8*(1), 7-15. https://doi.org/10.1007/s11926-006-0019-1
Jeon, O. H., Kim, C., Laberge, R.-M., Demaria, M., Rathod, S., Vasserot, A. P., Chung, J. W., Kim, D. H., Poon, Y., David, N., Baker, D. J., van Deursen, J. M., Campisi, J., & Elisseeff, J. H. (2017). Local clearance of senescent cells attenuates the development of post-traumatic osteoarthritis and creates a pro-regenerative environment. *Nature Medicine*, *23*(6), 775-781. https://doi.org/10.1038/nm.4324
Jin, H., Li, M., Jeong, E., Castro-Martinez, F., & Zuker, C. S. (2024). A body–brain circuit that regulates body inflammatory responses. *Nature*, *630*(8017), 695-703. https://doi.org/10.1038/s41586-024-07469-y
Johnson, G., & Moore, S. W. (2012). Why has butyrylcholinesterase been retained? Structural and functional diversification in a duplicated gene. *Neurochemistry International*, *61*(5), 783-797. https://doi.org/https://doi.org/10.1016/j.neuint.2012.06.016
Keever, K. R., Yakubenko, V. P., & Hoover, D. B. (2023). Neuroimmune nexus in the pathophysiology and therapy of inflammatory disorders: Role of α7 nicotinic acetylcholine receptors. *Pharmacological Research*, *191*, 106758. https://doi.org/https://doi.org/10.1016/j.phrs.2023.106758
Kelly, M. J., Breathnach, C., Tracey, K. J., & Donnelly, S. C. (2022). Manipulation of the inflammatory reflex as a therapeutic strategy. *Cell Reports Medicine*, *3*(7), 100696. https://doi.org/https://doi.org/10.1016/j.xcrm.2022.100696

Kim, J., Lee, H. J., Park, S. K., Park, J. H., Jeong, H. R., Lee, S., Lee, H., Seol, E., & Hoe, H. S. (2021). Donepezil Regulates LPS and Aβ-Stimulated Neuroinflammation through MAPK/NLRP3 Inflammasome/STAT3 Signaling. *Int J Mol Sci*, *22*(19). https://doi.org/10.3390/ijms221910637

Kliemann, K., Kneffel, M., Bergen, I., Kampschulte, M., Langheinrich, A. C., Dürselen, L., Ignatius, A., Kilian, O., Schnettler, R., & Lips, K. S. (2012). Quantitative analyses of bone composition in acetylcholine receptor M3R and alpha7 knockout mice. *Life Sciences*, *91*(21), 997-1002. https://doi.org/https://doi.org/10.1016/j.lfs.2012.07.024

Koopman, F. A., Chavan, S. S., Miljko, S., Grazio, S., Sokolovic, S., Schuurman, P. R., Mehta, A. D., Levine, Y. A., Faltys, M., Zitnik, R., Tracey, K. J., & Tak, P. P. (2016). Vagus nerve stimulation inhibits cytokine production and attenuates disease severity in rheumatoid arthritis. *Proceedings of the National Academy of Sciences - PNAS*, *113*(29), 8284-8289. https://doi.org/10.1073/pnas.1605635113

Kyrkanides, S., Tallents, R. H., Miller, J.-N. H., Olschowka, M. E., Johnson, R., Yang, M., Olschowka, J. A., Brouxhon, S. M., & O'Banion, M. K. (2011). Osteoarthritis accelerates and exacerbates Alzheimer's disease pathology in mice. *Journal of neuroinflammation*, *8*(1), 112-112. https://doi.org/10.1186/1742-2094-8-112

Lauwers, M., Courties, A., Sellam, J., & Wen, C. (2021). The cholinergic system in joint health and osteoarthritis: a narrative-review. *Osteoarthritis and Cartilage*, *29*(5), 643-653. https://doi.org/10.1016/j.joca.2021.02.005

Lee, S. E. (2013). Choline, an alpha7 nicotinic acetylcholine receptor agonist, alleviates hyperalgesia in a rat osteoarthritis model. *Neuroscience Letters*, *548*, 291-295. https://doi.org/https://doi.org/10.1016/j.neulet.2013.05.073

Li, A., Zhang, J., Chen, K., Wang, J., Xu, A., & Wang, Z. (2023). Donepezil attenuates inflammation and apoptosis in ulcerative colitis via regulating LRP1/AMPK/NF-κB signaling. *Pathol Int*, *73*(11), 549-559. https://doi.org/10.1111/pin.13380

Li, S., Teguh, D., Wu, D., Liu, L., Hu, C., Yuan, J., Inderjeeth, C. A., & Xu, J. (2023). Antidementia medication acetylcholinesterase inhibitors have therapeutic benefits on osteoporotic bone by attenuating osteoclastogenesis and bone resorption. *Journal of cellular physiology*, *238*(8), 1823-1835. https://doi.org/10.1002/jcp.31057

Lips, K. S., Yanko, Ö., Kneffel, M., Panzer, I., Kauschke, V., Madzharova, M., Henss, A., Schmitz, P., Rohnke, M., Bäuerle, T., Liu, Y., Kampschulte, M., Langheinrich, A. C., Dürselen, L., Ignatius, A., Heiss, C., Schnettler, R., & Kilian, O. (2015). Small changes in bone structure of female α7 nicotinic acetylcholine receptor knockout mice. *BMC musculoskeletal disorders*, *16*(1), 5. https://doi.org/10.1186/s12891-015-0459-8

Liu, E. Y. L., Xia, Y., Kong, X., Guo, M. S. S., Yu, A. X. D., Zheng, B. Z. Y., Mak, S.,

Xu, M. L., & Tsim, K. W. K. (2020). Interacting with α 7 nAChR is a new mechanism for AChE to enhance the inflammatory response in macrophages. *Acta Pharm Sin B*, *10*(10), 1926-1942. https://doi.org/10.1016/j.apsb.2020.05.005

Liu, Y., Wu, D., Song, F., Zhu, C., Hui, Y., Zhu, Q., Wu, J., Fan, W., & Hu, J. (2015). Activation of a7 Nicotinic Acetylcholine Receptors Prevents Monosodium Iodoacetate-Induced Osteoarthritis in Rats. *Cellular physiology and biochemistry*, *35*(2), 627-638. https://doi.org/10.1159/000369724

Liu, Y., Xu, S., Zhang, H., Qian, K., Huang, J., Gu, X., Li, Y., Fan, Y., & Hu, J. (2021). Stimulation of α7-nAChRs coordinates autophagy and apoptosis signaling in experimental knee osteoarthritis. *Cell Death & Disease*, *12*(5), 448. https://doi.org/10.1038/s41419-021-03726-4

Long, H., Liu, Q., Yin, H., Wang, K., Diao, N., Zhang, Y., Lin, J., & Guo, A. (2022). Prevalence trends of site-specific osteoarthritis from 1990 to 2019: findings from the Global Burden of Disease Study 2019. *Arthritis Rheumatol*. https://doi.org/10.1002/art.42089

Loskutova, N., Honea, R. A., Vidoni, E. D., Brooks, W. M., & Burns, J. M. (2009). Bone density and brain atrophy in early Alzheimer's disease. *J Alzheimers Dis*, *18*(4), 777-785. https://doi.org/10.3233/jad-2009-1185

Luo, X., Lauwers, M., Layer, P. G., & Wen, C. (2020). Non-neuronal Role of Acetylcholinesterase in Bone Development and Degeneration. *Front Cell Dev Biol*, *8*, 620543. https://doi.org/10.3389/fcell.2020.620543

Marsal, S., Corominas, H., de Agustín, J. J., Pérez-García, C., López-Lasanta, M., Borrell, H., Reina, D., Sanmartí, R., Narváez, J., Franco-Jarava, C., Peterfy, C., Narváez, J. A., Sharma, V., Alataris, K., Genovese, M. C., & Baker, M. C. (2021). Non-invasive vagus nerve stimulation for rheumatoid arthritis: a proof-of-concept study. *The Lancet Rheumatology*, *3*(4), e262-e269. https://doi.org/10.1016/S2665-9913(20)30425-2

Matsumoto, S., Yakabe, M., Hosoi, T., Fujimori, K., Tamaki, J., Nakatoh, S., Ishii, S., Okimoto, N., Akishita, M., Iki, M., & Ogawa, S. (2024). Relationship between donepezil and fracture risk in patients with dementia with Lewy bodies. *Geriatrics & gerontology international*, *24*(8), 782-788. https://doi.org/10.1111/ggi.14929

Meriney, S. D., & Fanselow, E. E. (2019). Chapter 16 - Acetylcholine. In S. D. Meriney & E. E. Fanselow (Eds.), *Synaptic Transmission* (pp. 345-367). Academic Press. https://doi.org/https://doi.org/10.1016/B978-0-12-815320-8.00016-8

Mora-Antoinette, M., Garcia-Ortiz, A., Obaji, M., Saffari, A., Matthews, M. D., Wasi, M., & Lewis, K. J. (2025). Cholinergic regulation of osteocyte mechanobiology: A paradigm for bone adaptation. *Science advances*, *11*(34), eads9720. https://doi.org/10.1126/sciadv.ads9720

Muhammad, S. A., Nordin, N., Hussin, P., Mehat, M. Z., Tan, S. W., & Fakurazi, S. (2021). Optimization of Protocol for Isolation of Chondrocytes from Human

Articular Cartilage. *Cartilage*, *13*(2_suppl), 872S-884S. https://doi.org/10.1177/1947603519876333

Neogi, T., Guermazi, A., Roemer, F., Nevitt, M. C., Scholz, J., Arendt-Nielsen, L., Woolf, C., Niu, J., Bradley, L. A., Quinn, E., & Frey Law, L. (2016). Association of Joint Inflammation With Pain Sensitization in Knee Osteoarthritis: The Multicenter Osteoarthritis Study. *Arthritis & rheumatology (Hoboken, N.J.)*, *68*(3), 654-661. https://doi.org/10.1002/art.39488

Nicolodi, M., Galeotti, N., Ghelardini, C., Bartolini, A., & Sicuteri, F. (2002). Central Cholinergic Challenging of Migraine by Testing Second-Generation Anticholinesterase Drugs. *Headache : the journal of head and face pain.*, *42*(7), 596-602. https://doi.org/10.1046/j.1526-4610.2002.02146.x

North, R., Liu, A. J., Pieper, C., Danus, S., Thacker, C. R., Ashner, M., Colón-Emeric, C., & Lee, R. H. (2025). Effect of donepezil on bone metabolism among older adults with Alzheimer's disease. *Contemporary Clinical Trials*, *148*, 107748. https://doi.org/https://doi.org/10.1016/j.cct.2024.107748

Noviello, C. M., Gharpure, A., Mukhtasimova, N., Cabuco, R., Baxter, L., Borek, D., Sine, S. M., & Hibbs, R. E. (2021). Structure and gating mechanism of the α7 nicotinic acetylcholine receptor. *Cell*, *184*(8), 2121-2134.e2113. https://doi.org/10.1016/j.cell.2021.02.049

Ogunwale, A. N., Colon-Emeric, C. S., Sloane, R., Adler, R. A., Lyles, K. W., & Lee, R. H. (2020). Acetylcholinesterase inhibitors are associated with reduced fracture risk among older Veterans with dementia. *Journal of bone and mineral research*, *35*(3), 440-445.

Oo, W. M., & Hunter, D. J. (2022). Repurposed and investigational disease-modifying drugs in osteoarthritis (DMOADs). *Therapeutic Advances in Musculoskeletal Disease*, *14*, 1759720X221090297. https://doi.org/10.1177/1759720X221090297

Ordovas-Montanes, J., Rakoff-Nahoum, S., Huang, S., Riol-Blanco, L., Barreiro, O., & von Andrian, U. H. (2015). The Regulation of Immunological Processes by Peripheral Neurons in Homeostasis and Disease. *Trends Immunol*, *36*(10), 578-604. https://doi.org/10.1016/j.it.2015.08.007

Park, J.-E., Leem, Y.-H., Park, J.-S., Kim, D.-Y., Kang, J. L., & Kim, H.-S. (2022). Anti-Inflammatory and Neuroprotective Mechanisms of GTS-21, an α7 Nicotinic Acetylcholine Receptor Agonist, in Neuroinflammation and Parkinson's Disease Mouse Models. *International journal of molecular sciences*, *23*(8), 4420. https://doi.org/10.3390/ijms23084420

Park, S., & Shin, B. K. (2022). Intermittent fasting with a high-protein diet mitigated osteoarthritis symptoms by increasing lean body mass and reducing inflammation in osteoarthritic rats with Alzheimer's disease-like dementia. *British Journal of Nutrition*, *127*(1), 55-67. https://doi.org/10.1017/S0007114521000829

Patel, H., McIntire, J., Ryan, S., Dunah, A., & Loring, R. (2017). Anti-inflammatory

effects of astroglial α7 nicotinic acetylcholine receptors are mediated by inhibition of the NF-KB pathway and activation of the Nrf2 pathway. *Journal of neuroinflammation*, *14*(1), 192-192. https://doi.org/10.1186/s12974-017-0967-6

Pavlov, V. A., Parrish, W. R., Rosas-Ballina, M., Ochani, M., Puerta, M., Ochani, K., Chavan, S., Al-Abed, Y., & Tracey, K. J. (2009). Brain acetylcholinesterase activity controls systemic cytokine levels through the cholinergic anti-inflammatory pathway. *Brain, Behavior, and Immunity*, *23*(1), 41-45. https://doi.org/https://doi.org/10.1016/j.bbi.2008.06.011

Pellegrini, C., D'Antongiovanni, V., Fornai, M., Duranti, E., Baldacci, F., Bernardini, N., Taddei, S., Virdis, A., Blandizzi, C., Masi, S., & Antonioli, L. (2021). Donepezil improves vascular function in a mouse model of Alzheimer's disease. *Pharmacol Res Perspect*, *9*(6), e00871. https://doi.org/10.1002/prp2.871

Prieto-Alhambra, D., Judge, A., Javaid, M. K., Cooper, C., Diez-Perez, A., & Arden, N. K. (2014). Incidence and risk factors for clinically diagnosed knee, hip and hand osteoarthritis: influences of age, gender and osteoarthritis affecting other joints. *Ann Rheum Dis*, *73*(9), 1659-1664. https://doi.org/10.1136/annrheumdis-2013-203355

Pritzker, K. P. H., Gay, S., Jimenez, S. A., Ostergaard, K., Pelletier, J. P., Revell, P. A., Salter, D., & van den Berg, W. B. (2006). Osteoarthritis cartilage histopathology: grading and staging. *Osteoarthritis and Cartilage*, *14*(1), 13-29. https://doi.org/10.1016/j.joca.2005.07.014

Rice, S. J., Cheung, K., Reynard, L. N., & Loughlin, J. (2019). Discovery and analysis of methylation quantitative trait loci (mQTLs) mapping to novel osteoarthritis genetic risk signals. *Osteoarthritis and Cartilage*, *27*(10), 1545-1556. https://doi.org/https://doi.org/10.1016/j.joca.2019.05.017

Ringdahl, E. M. D., & Pandit, S. M. D. (2011). Treatment of Knee Osteoarthritis. *Am Fam Physician*, *83*(11), 1287-1292.

Rogers, S. L., Cooper, N. M., Sukovaty, R., Pederson, J. E., Lee, J. N., & Friedhoff, L. T. (1998). Pharmacokinetic and pharmacodynamic profile of donepezil HCl following multiple oral doses. *Br J Clin Pharmacol*, *46 Suppl 1*(Suppl 1), 7-12. https://doi.org/10.1046/j.1365-2125.1998.0460s1007.x

Rosas-Ballina, M., Olofsson, P. S., Ochani, M., Valdés-Ferrer, S. I., Levine, Y. A., Reardon, C., Tusche, M. W., Pavlov, V. A., Andersson, U., Chavan, S., Mak, T. W., & Tracey, K. J. (2011). Acetylcholine-Synthesizing T Cells Relay Neural Signals in a Vagus Nerve Circuit. *Science*, *334*(6052), 98-101. https://doi.org/doi:10.1126/science.1209985

Sam, C., & Bordoni, B. (2025). Physiology, Acetylcholine. In *StatPearls*. StatPearls Publishing

Sangsuwan, R., Yik, J. H. N., Owen, M., Liu, G.-Y., Haudenschild, D. R., & Lewis, J. S. (2022). Intra-articular injection of flavopiridol-loaded microparticles for

treatment of post-traumatic osteoarthritis. *Acta Biomaterialia*. https://doi.org/https://doi.org/10.1016/j.actbio.2022.06.042

Sato, T., Abe, T., Chida, D., Nakamoto, N., Hori, N., Kokabu, S., Sakata, Y., Tomaru, Y., Iwata, T., Usui, M., Aiko, K., & Yoda, T. (2010). Functional role of acetylcholine and the expression of cholinergic receptors and components in osteoblasts. *FEBS Lett*, *584*(4), 817-824. https://doi.org/10.1016/j.febslet.2010.01.001

Sato, T., Enoki, Y., Sakamoto, Y., Yokota, K., Okubo, M., Matsumoto, M., Hayashi, N., Usui, M., Kokabu, S., & Mimura, T. (2015). Donepezil prevents RANK-induced bone loss via inhibition of osteoclast differentiation by downregulating acetylcholinesterase. *Heliyon*, *1*(1), e00013.

Schubert, J., Beckmann, J., Hartmann, S., Morhenn, H.-G., Szalay, G., Heiss, C., Schnettler, R., & Lips, K. S. (2012). Expression of the non-neuronal cholinergic system in human knee synovial tissue from patients with rheumatoid arthritis and osteoarthritis. *Life Sciences*, *91*(21), 1048-1052. https://doi.org/https://doi.org/10.1016/j.lfs.2012.04.032

Simon, T., Kirk, J., Dolezalova, N., Guyot, M., Panzolini, C., Bondue, A., Lavergne, J., Hugues, S., Hypolite, N., Saeb-Parsy, K., Perkins, J., Macia, E., Sridhar, A., Vervoordeldonk, M. J., Glaichenhaus, N., Donegá, M., & Blancou, P. (2023). The cholinergic anti-inflammatory pathway inhibits inflammation without lymphocyte relay [Original Research]. *Frontiers in Neuroscience*, *Volume 17 - 2023*. https://doi.org/10.3389/fnins.2023.1125492

Spieker, J., Ackermann, A., Salfelder, A., Vogel-Höpker, A., & Layer, P. G. (2016). Acetylcholinesterase regulates skeletal in ovo development of chicken limbs by ACh-dependent and-independent mechanisms. *PloS one*, *11*(8), e0161675.

Spieker, J., Mudersbach, T., Vogel-Höpker, A., & Layer, P. G. (2017). Endochondral ossification is accelerated in cholinesterase-deficient mice and in avian mesenchymal micromass cultures. *PloS one*, *12*(1), e0170252-e0170252. https://doi.org/10.1371/journal.pone.0170252

Sprunks, T. E., McLeod, K. J., & Staelin, R. (2024). Pulsed shortwave electromagnetic field therapy increases quality of life in canines with symptoms of osteoarthritics. *Veterinary Medicine and Science*, *10*(3), e1408. https://doi.org/https://doi.org/10.1002/vms3.1408

Subramanian, N., Watson, B., Li, C.-Z., Moss, M., & Liu, C. (2023). Patterning amyloid-β aggregation under the effect of acetylcholinesterase using a biological nanopore - an in vitro study. *Sensors and Actuators Reports*, *6*, 100170. https://doi.org/https://doi.org/10.1016/j.snr.2023.100170

Suri, S., & Walsh, D. A. (2012). Osteochondral alterations in osteoarthritis. *Bone*, *51*(2), 204-211. https://doi.org/https://doi.org/10.1016/j.bone.2011.10.010

Tamimi, I., Nicolau, B., Eimar, H., Arekunnath Madathil, S., Kezouh, A., Karp, I., & Tamimi, F. (2018). Acetylcholinesterase inhibitors and the risk of osteoporotic fractures: nested case-control study. *Osteoporosis International*, *29*(4), 849-857.

Tamimi, I., Ojea, T., Sanchez-Siles, J. M., Rojas, F., Martin, I., Gormaz, I., Perez, A., Dawid-Milner, M. S., Mendez, L., & Tamimi, F. (2012). Acetylcholinesterase inhibitors and the risk of hip fracture in Alzheimer's disease patients: a case-control study. *J Bone Miner Res*, *27*(7), 1518-1527. https://doi.org/10.1002/jbmr.1616

Teng, P., Liu, Y., Dai, Y., Zhang, H., Liu, W. T., & Hu, J. (2019). Nicotine Attenuates Osteoarthritis Pain and Matrix Metalloproteinase-9 Expression via the α7 Nicotinic Acetylcholine Receptor. *J Immunol*, *203*(2), 485-492. https://doi.org/10.4049/jimmunol.1801513

Wang, H., Yu, M., Ochani, M., Amella, C. A., Tanovic, M., Susarla, S., Li, J. H., Wang, H., Yang, H., Ulloa, L., Al-Abed, Y., Czura, C. J., & Tracey, K. J. (2003). Nicotinic acetylcholine receptor α7 subunit is an essential regulator of inflammation. *Nature*, *421*(6921), 384-388. https://doi.org/10.1038/nature01339

Weber, A., Mak, S. H., Berenbaum, F., Sellam, J., Zheng, Y. P., Han, Y., & Wen, C. (2019). Association between osteoarthritis and increased risk of dementia: A systemic review and meta-analysis. *Medicine (Baltimore)*, *98*(10), e14355. https://doi.org/10.1097/md.0000000000014355

Wu, P. Y., Caceres, A. I., Chen, J., Sokoloff, J., Huang, M., Baht, G. S., Nackley, A. G., Jordt, S. E., & Terrando, N. (2023). Vagus nerve stimulation rescues persistent pain following orthopedic surgery in adult mice. *bioRxiv*. https://doi.org/10.1101/2023.05.16.540949

Xia, Y., Wang, X., Guo, M. S., Wu, J., Gao, J., Dong, T. T. X., & Tsim, K. W. K. (2025). The activation of inflammatory responses in the brain is potentiated by over-expressing acetylcholinesterase in myeloid lineage of transgenic mice. *Journal of neurochemistry*, *169*(2), e16251-n/a. https://doi.org/10.1111/jnc.16251

Yang, M., Su, Y., Xu, K., Wen, P., Xie, J., Wan, X., Jing, W., Yang, Z., Liu, L., & Xu, P. (2025). Viral infections of the central nervous system increase the risk of knee osteoarthritis: a two-sample mendelian randomization study. *Aging Clin Exp Res*, *37*(1), 30. https://doi.org/10.1007/s40520-025-02927-7

Zaagsma, J., & Meurs, H. (2006). ACETYLCHOLINE. In G. J. Laurent & S. D. Shapiro (Eds.), *Encyclopedia of Respiratory Medicine* (pp. 1-5). Academic Press. https://doi.org/https://doi.org/10.1016/B0-12-370879-6/00002-8

Zhang, D., & Zhou, Y. (2014). The protective effects of Donepezil (DP) against cartilage matrix destruction induced by TNF-α. *Biochemical and Biophysical Research Communications*, *454*(1), 115-118. https://doi.org/https://doi.org/10.1016/j.bbrc.2014.10.046

Zhao, Y., Shen, L., & Ji, H. F. (2012). Alzheimer's disease and risk of hip fracture: a meta-analysis study. *ScientificWorldJournal*, *2012*, 872173. https://doi.org/10.1100/2012/872173

Zhiyang, W., Xin, Z., Tiantian, C., Yankun, L., Xi, G., Xiangyang, Z., Dawei, W., Zhi, L., & Luyao, Z. (2023). Transcutaneous auricular vagus nerve stimulation

reduces cytokine production in sepsis: An open double-blind, sham-controlled, pilot study Transcutaneous auricular vagus nerve stimulation reduces cytokine production in sepsis: An open double-blind, sham-controlled, pilot study. *Brain stimulation*, *16*(2), 507-514.

Zhu, S., Huang, S., Xia, G., Wu, J., Shen, Y., Wang, Y., Ostrom, R. S., Du, A., Shen, C., & Xu, C. (2021). Anti-inflammatory effects of α7-nicotinic ACh receptors are exerted through interactions with adenylyl cyclase-6. *British journal of pharmacology*, *178*(11), 2324-2338. https://doi.org/10.1111/bph.15412

Zhu, X., Dai, S., Xia, B., Gong, J., & Ma, B. (2021). Activation of the alpha 7 nicotinic acetylcholine receptor mitigates osteoarthritis progression by inhibiting NF-κB/NLRP3 inflammasome activation and enhancing autophagy. *PloS one*, *16*(12), e0256507. https://doi.org/10.1371/journal.pone.0256507

Ziadlou, R., Barbero, A., Stoddart, M. J., Wirth, M., Li, Z., Martin, I., Wang, X.-L., Qin, L., Alini, M., & Grad, S. (2019). Regulation of inflammatory response in human osteoarthritic chondrocytes by novel herbal small molecules. *International journal of molecular sciences*, *20*(22), 5745. https://doi.org/10.3390/ijms20225745

Ziemian, S. N., Witkowski, A. M., Wright, T. M., Otero, M., & van der Meulen, M. C. H. (2021). Early inhibition of subchondral bone remodeling slows load-induced posttraumatic osteoarthritis development in mice. *Journal of bone and mineral research*, *36*(10), 2027-2038. https://doi.org/10.1002/jbmr.4397

Zivkovic, A. R., Paul, G. M., Hofer, S., Schmidt, K., Brenner, T., Weigand, M. A., & Decker, S. O. (2023). Increased Enzymatic Activity of Acetylcholinesterase Indicates the Severity of the Sterile Inflammation and Predicts Patient Outcome following Traumatic Injury. *Biomolecules (Basel, Switzerland)*, *13*(2), 267. https://doi.org/10.3390/biom13020267